NORSAR

NORSAR Scientific Report No. 2-2002

Semiannual Technical Summary

1 January - 30 June 2002

Frode Ringdal (ed.)

Kjeller, August 2002

SECURITY CLASSIFICATION OF THIS PAGE

REPORT DOCUMENTATION PAGE

Form Approved
OMB No. 0704-0188

1a. REPORT SECURITY CLASSIFICATION
Unclassified

1b. RESTRICTIVE MARKINGS
Not applicable

2a. SECURITY CLASSIFICATION AUTHORITY
Not Applicable

2b. DECLASSIFICATION / DOWNGRADING SCHEDULE

3. DISTRIBUTION / AVAILABILITY OF REPORT
Approved for public release; distribution unlimited

4. PERFORMING ORGANIZATION REPORT NUMBER(S)
Scientific Rep. 2-2002

5. MONITORING ORGANIZATION REPORT NUMBER(S)
Scientific Rep. 2-2002

6a. NAME OF PERFORMING ORGANIZATION
NORSAR

6b. OFFICE SYMBOL *(If applicable)*

7a. NAME OF MONITORING ORGANIZATION
HQ/AFTAC/TTS

6c. ADDRESS *(City, State, and ZIP Code)*
Post Box 53
NO-2027 Kjeller, Norway

7b. ADDRESS *(City, State, and ZIP Code)*
Patrick AFB, FL 32925-6001

8a. NAME OF FUNDING / SPONSORING ORGANIZATION
Defense Threat Reduction Agency/NTPO

8b. OFFICE SYMBOL *(If applicable)*
DTRA/NTPO

9. PROCUREMENT INSTRUMENT IDENTIFICATION NUMBER
Contract No. F08650-01-C-0055

8c. ADDRESS *(City, State, and ZIP Code)*
1515 Wilson Blvd., Suite 720
Arlington, VA 22209

10. SOURCE OF FUNDING NUMBERS

PROGRAM ELEMENT NO.	PROJECT NO.	TASK NO.	WORK UNIT ACCESSION NO.
R&D	NORSAR Phase 3	SOW Task 5.0	Sequence No. 004A2

11. TITLE *(Include Security Classification)*
Semiannual Technical Summary, 1 January - 30 June 2002 (Unclassified)

12. PERSONAL AUTHOR(S)

13a. TYPE OF REPORT	13b. TIME COVERED	14. DATE OF REPORT *(Year, Month, Day)*	15. PAGE COUNT
Scientific Summary	FROM 1 Jan 02 TO 30 Jun 02	2002 Aug	113

16. SUPPLEMENTARY NOTATION

17. COSATI CODES			18. SUBJECT TERMS *(Continue on reverse if necessary and identify by block number)*
FIELD	GROUP	SUB-GROUP	
8	11		NORSAR, Norwegian Seismic Array

19. ABSTRACT *(Continue on reverse if necessary and identify by block number)*

This report describes the research activities carried out at NORSAR under Contract No. F08650-01-C-0055 for the period 1 January - 30 June 2002. In addition, it provides summary information on operation and maintenance (O&M) activities at the Norwegian National Data Center (NDC) during the same period. Research activities described in this report, as well as transmission of selected data to the United States NDC, are funded by the United States Department of Defense. The O&M activities, including operation of transmission links within Norway and to Vienna, Austria, are being funded jointly by the CTBTO/PTS and the Norwegian Government, with the understanding that the funding of IMS-related activities will gradually be transferred to the CTBTO/PTS. The O&M statistics presented in this report are included for the purpose of completeness, and in order to maintain consistency with earlier reporting practice.

(cont.)

20. DISTRIBUTION / AVAILABILITY OF ABSTRACT
☐ UNCLASSIFIED/UNLIMITED ☐ SAME AS RPT. ☐ DTIC USERS

21. ABSTRACT SECURITY CLASSIFICATION

22a. NAME OF RESPONSIBLE INDIVIDUAL
Lt. Col. William S. Jones

22b. TELEPHONE *(Include Area Code)*
(407) 494-7985

22c. OFFICE SYMBOL
AFTAC/TTS

DD Form 1473, JUN 86 *Previous editions are obsolete.* SECURITY CLASSIFICATION OF THIS PAGE

Abstract (cont.)

The seismic arrays operated by the Norwegian NDC comprise the Norwegian Seismic Array (NOA), the Norwegian Regional Seismic Array (NORES), the Arctic Regional Seismic Array (ARCES) and the Spitsbergen Regional Array (SPITS). This report also presents statistics for additional seismic stations which through cooperative agreements with institutions in the host countries provide continuous data to the NORSAR Data Processing Center (NDPC). These stations comprise the Finnish Regional Seismic Array (FINES), the Hagfors array in Sweden and the regional seismic array in Apatity, Russia.

The NOA Detection Processing system has been operated throughout the period with an average uptime of 100.00%. A total of 1872 seismic events have been reported in the NOA monthly seismic bulletin from January through June 2002. On-line detection processing and data recording at the NDC of NORES, ARCES and FINES data have been conducted throughout the period. Data from two small-aperture arrays at sites in Spitsbergen and Apatity, Kola Peninsula, as well as the Hagfors array in Sweden, have also been recorded and processed. Processing statistics for the arrays for the reporting period are given.

A summary of the activities related to the GSETT-3 experiment and experience gained at the Norwegian NDC during the reporting period is provided in Section 4. Norway is now contributing primary station data from two seismic arrays: ARCES and NOA and one auxiliary array (SPITS). These data are being provided to the IDC via the global communications infrastructure (GCI). Continuous data from all three arrays are in addition being transmitted to the US NDC. The performance of the data transmission to the US NDC has been satisfactory during the reporting period.

The PrepCom has encouraged states that operate IMS-designated stations to continue to do so on a voluntary basis and in the framework of the GSETT-3 experiment until the stations have been certified for formal inclusion in IMS. So far among the Norwegian stations, the NOA and the ARCES array (PS27 and PS28 respectively) have been certified. We envisage continuing the provision of data from these and other Norwegian IMS-designated stations in accordance with current procedures.

Summaries of six scientific and technical contributions are presented in Chapter 6 of this report.

Section 6.1 contains a report from the meeting of the IDC Technical Experts Group on Seismic Event Location in Oslo, Norway on 22-26 April 2002. This was the fourth annual meeting of the Experts Group in support of Working Group B of the CTBTO Preparatory Commission. The meeting was held jointly with the IDC Technical Experts Group on Seismoacoustic Event Screening. The purpose of the meeting was to support the ongoing calibration and screening efforts of the IDC and in particular to review progress toward developing regionalized travel times to improve the quality of location estimates of seismic events reported in the IDC bulletins.

The meeting was attended by sixty-six technical experts, coming from twelve signatory countries and the Provisional Technical Secretariat. Dr. Frode Ringdal of Norway chaired the meeting, which was organized into four sessions, and included Working Group discussions to address the technical issues in detail. Recommendations from the meeting have been presented to Working Group B in Vienna during its June 2002 session (CTBT/WGB/TL-2/70).

Section 6.2 is entitled "Research in regional seismic monitoring" and contains a summary paper presented at the 24th Annual Seismic Research Review, describing a continued effort in regional monitoring research. We have used data from the regional networks operated by NORSAR and the Kola Regional Seismological Centre (KRSC) to assess the seismicity and characteristics of regional phases of the European Arctic. An especially interesting recent seismic event, which has been analyzed in detail, occurred on Novaya Zemlya on 23 February 2002. This small event (magnitude about 3.0) is the first seismic event detected in or near Novaya Zemlya since the two Kara Sea events of 16 August 1997. The event was recorded with particularly high SNR by the International Monitoring System (IMS) arrays Spitsbergen and ARCES, and by the Amderma station (operated by KRSC) south of Novaya Zemlya. We have located the event at the eastern coast of Novaya Zemlya, approximately 100 km NE of the former nuclear test site. Our attempts to estimate the depth of this event proved inconclusive, and a depth of 0 could not be ruled out.

We have begun an effort to develop an optimized site-specific threshold monitoring system for the Lop Nor test site in China. Initial results show that, among the available stations, the IMS Makanchi array in Kazakhstan (at an epicentral distance of 6 degrees) is the most sensitive station for detecting events at Lop Nor, followed by some of the best teleseismic arrays, for example the NORES array in Norway. Combining the data by using the threshold monitoring technique, we have found that the Lop Nor site can be monitored down to a threshold close to m_b 3.2. This threshold is about 0.8 magnitude units higher than the corresponding capability for the Novaya Zemlya test site, for which the highly sensitive arrays ARCES and Spitsbergen are both at a distance of only 10 degrees. We note that no stations inside China were selected for the Lop Nor study.

Section 6.3 is a design study of a possible reconfiguration of the Spitsbergen array (SPITS). This array needs a technical refurbishment before it can be certified for inclusion in the IMS, and the motivation for the present study is to determine possible options for reconfiguring the array so as to improve its monitoring capabilities. The SPITS array is situated in a geological/tectonic environment that is very different from that of Fennoscandia. This results in a number of characteristic features that must be taken into account when processing SPITS data.

The SPITS array often reports a large number of detections, which can reach thousands per day. A detailed analysis shows that the majority of these detections are real seismic signals caused by small sources located at close distances. The numerous local events typically show P onsets, no well defined S onsets, and dominant Rg onsets. Investigating the mean backazimuths of these Rg phases, one can see a strong correlation with the direction to a nearby coal-mine area and to nearby glaciers. To avoid spatial aliasing of these signals a denser inner ring of seismometers would be helpful. To improve the separation between phase types based on apparent velocities, an increase in the array aperture is required. This would also provide improved resolution in the azimuth estimates.

At the SPITS array we observe a relatively large number of high SNR P detections from regional events without any corresponding detection of an S phase. The regional S-phases at SPITS in general have the largest amplitudes and SNR on the horizontal components. The current SPITS configuration has only one three-component instrument at site SPB4. With more three-component sites, the detection capability of S-phases can be improved by creating S-velocity beams from the rotated radial and transverse components, as now done for ARCES and NORES. In addition, the F-K analysis can be performed on the horizontal components.

The paper suggests specific extensions for the SPITS array to increase its detection and monitoring capabilities. These points will form the basis for our proposed Spitsbergen upgrade/refurbishment.

Section 6.4 is a study of seismic data from a series of underground cavity decoupled chemical explosions in the Älvdalen region of Sweden, with the aim of quantitatively predicting the decoupling effect of underground cavities of known dimensions and shape. A database of seismic waveform data has been compiled for seven such cavity explosions. Only three factors differentiate these events; the quantity of explosive, the composition and arrangement of the explosives, and the size and configuration of the explosion chamber. In addition, the Swedish Armed Forces regularly detonate outdated ammunition at ground level at a site approximately 15 km from the underground chambers. Seismic waveforms from 12 such events were added to the database to provide a comparison with the decoupled explosions.

In order to quantify the differences between these events, we examine the power density spectra of the signals recorded by NOA, NORES and HFS. The recordings from explosions in the cavities at Älvdalen are characterized by a large amount of high-frequency energy (8-16 Hz) compared with the energy at lower frequencies (2-5 Hz). Such spectral characteristics are not observed for the surface explosions. The effect is more pronounced for P than for S waves.

With regard to decoupling efficiency, three 10 ton explosions in a $1000m^3$ chamber appear to have been more efficiently decoupled than three 5 ton explosions in chambers of $200m^3$ and $300m^3$. The signals from the explosions in the smaller chambers were far stronger, in spite of significantly lower yields, and displayed a less pronounced high-to-low frequency energy ratio than the explosions in the larger chambers.

We plan to assemble NOA, HFS and NORES recordings of earthquakes located at distances similar to Älvdalen and Mossibränden, but at different azimuths, in order to make comparative studies of their spectral characteristics. Comparisons between records from decoupled explosions and ripple fired mining explosions are also recognized as an important future target.

Section 6.5 is a study of experimental Site-Specific Generalized Beamforming (SSGBF) applied to the Lop Nor test site in China. The SSGBF approach supplements the SSTM system described in the preceding NORSAR Semiannual Technical Summary. We also comment briefly on the relative merits of the two approaches (SSTM and SSGBF), and the extent to which they complement each other in this particular case study.

In the present study we have calibrated all available high-quality seismic stations within regional distance from Lop Nor and supplemented them with the best IMS arrays at teleseismic distances. As a calibration data base, we use several past nuclear explosions at the test site, combined with nearby, well-recorded earthquakes. We present some preliminary results in applying site-specific generalized beamforming to the Lop Nor test site, using two data sets for performance testing. The first data set covers one day (10 September 2001), and in these data the recordings of 4 explosions were scaled and embedded at some (but not all of) the stations. Secondly, a 10 day test period with data from August 2 through 11, 2001 has been used. Examples of the data analysis for these data sets are presented.

The paper concludes that the Site-Specific Generalized Beamforming performance tests for the Lop Nor test site were successful. The combination of the SSTM and the SSGBF techniques appears to be a very promising new development. Each of these two approaches has its specific

strengths. The SSTM technique has as its main strength the ability to display the real seismic field, without regard to "station detector performance". On the other hand, the SSGBF technique takes advantage of the individual station detector outputs, and uses this combined information to narrow down the number of possible candidates for events in the target area.

Section 6.6 is a study of seismic threshold monitoring applied to the Barents Sea region. A database comprising a total of 45 events, selected to provide the best possible ray path coverage of the Barents Sea and adjacent areas, was compiled and reanalyzed in a consistent manner. This resulted in new regional attenuation relations for Pn and Sn, together with a preferred average velocity model to be used for predicting the travel times of regional phases. We have now applied these attenuation relations to investigate a regional threshold monitoring scheme for the Barents Sea area.

A grid system with an approximately 100-km grid spacing was deployed for the Barents Sea region, and the observations at the arrays ARCES, SPITS, FINES and NORES were then used for calculating threshold magnitudes for each of the grid points. During an interval without seismic signals, the threshold magnitudes showed large variations over the region, and, in particular, in the vicinity of each array. However, for the region around the island of Novaya Zemlya the variations are modest, varying around a mean of magnitude 2.1-2.2.

We have studied the tradeoff between beam area coverage ("beam sharpness") and monitoring performance for the site-specific threshold monitoring of the Novaya Zemya test site. For this purpose, we have deployed a very dense grid system covering an area of 500 x 500 km around the test site, and calculated magnitude thresholds for each grid point for a two hour time interval, which included a seismic event in the region (23 February 2002, 01.12.21, magnitude 3). Using the arrays ARCES, SPITS, FINES and NORES, we find that even for a target region with radius as large as 100 km, the variations in threshold magnitudes are all within 0.2 magnitude units. This applies both for the time interval including the event and for background noise conditions. For the investigated station geometry, it will therefore be meaningful to represent the monitoring threshold of the entire Novaya Zemlya region using the values of a single target point, together with the *á priori* determined uncertainty bounds.

For areas with larger variations in threshold magnitudes, like in the vicinity of the arrays, a 100-km radius target region will obviously show larger differences between the maximum and minimum values. Examples illustrating this point are shown.

Frode Ringdal

This Page Intentionaly
Left Blank

AFTAC Project Authorization	:	T/0155/PKO
ARPA Order No.	:	4138 AMD # 53
Program Code No.	:	0F10
Name of Contractor	:	Stiftelsen NORSAR
Effective Date of Contract	:	1 Feb 2001 (T/0155/PKO)
Contract Expiration Date	:	31 December 2005
Project Manager	:	Frode Ringdal +47 63 80 59 00
Title of Work	:	The Norwegian Seismic Array (NORSAR) Phase 3
Amount of Contract	:	$ 3,383,445
Period Covered by Report	:	1 January - 30 June 2002

The views and conclusions contained in this document are those of the authors and should not be interpreted as necessarily representing the official policies, either expressed or implied, of the U.S. Government.

The research presented in this report was supported by the Defense Threat Reduction Agency and was monitored by AFTAC, Patrick AFB, FL32925, under contract no. F08650-01-C-0055.

The operational activities of the seismic field systems and the Norwegian National Data Center (NDC) are currently jointly funded by the Norwegian Government and the CTBTO/PTS, with the understanding that the funding of IMS-related activities will gradually be transferred to the CTBTO/PTS.

NORSAR Contribution No. 761

This Page Intentionaly
Left Blank

Table of Contents

1 Summary

This report describes the research activities carried out at NORSAR under Contract No. F08650-01-C-0055 for the period 1 January - 30 June 2002. In addition, it provides summary information on operation and maintenance (O&M) activities at the Norwegian National Data Center (NDC) during the same period. Research activities described in this report, as well as transmission of selected data to the United States NDC, are funded by the United States Department of Defense. The O&M activities, including operation of transmission links within Norway and to Vienna, Austria are being funded jointly by the CTBTO/PTS and the Norwegian Government, with the understanding that the funding of all IMS-related activities will gradually be transferred to the CTBTO/PTS. The O&M statistics presented in this report are included for the purpose of completeness, and in order to maintain consistency with earlier reporting practice.

The seismic arrays operated by the Norwegian NDC comprise the Norwegian Seismic Array (NOA), the Norwegian Regional Seismic Array (NORES), the Arctic Regional Seismic Array (ARCES) and the Spitsbergen Regional Array (SPITS). This report also presents statistics for additional seismic stations which through cooperative agreements with institutions in the host countries provide continuous data to the NORSAR Data Processing Center (NDPC). These stations comprise the Finnish Regional Seismic Array (FINES), the Hagfors array in Sweden and the regional seismic array in Apatity, Russia.

The NOA Detection Processing system has been operated throughout the period with an average uptime of 100.00%. A total of 1872 seismic events have been reported in the NOA monthly seismic bulletin from January through June 2002. On-line detection processing and data recording at the NDC of NORES, ARCES and FINES data have been conducted throughout the period. Data from two small-aperture arrays at sites in Spitsbergen and Apatity, Kola Peninsula, as well as the Hagfors array in Sweden, have also been recorded and processed. Processing statistics for the arrays for the reporting period are given.

A summary of the activities related to the GSETT-3 experiment and experience gained at the Norwegian NDC during the reporting period is provided in Section 4. Norway is now contributing primary station data from two seismic arrays: ARCES and NOA and one auxiliary array (SPITS). These data are being provided to the IDC via the global communications infrastructure (GCI). Continuous data from all three arrays are in addition being transmitted to the US NDC. The performance of the data transmission to the US NDC has been satisfactory during the reporting period.

The PrepCom has encouraged states that operate IMS-designated stations to continue to do so on a voluntary basis and in the framework of the GSETT-3 experiment until the stations have been certified for formal inclusion in IMS. So far among the Norwegian stations, the NOA and the ARCES array (PS27 and PS28 respectively) have been certified. We envisage continuing the provision of data from these and other Norwegian IMS-designated stations in accordance with current procedures.

Summaries of six scientific and technical contributions are presented in Chapter 6 of this report.

Section 6.1 contains a report from the meeting of the IDC Technical Experts Group on Seismic Event Location in Oslo, Norway on 22-26 April 2002. This was the fourth annual meeting of the Experts Group in support of Working Group B of the CTBTO Preparatory Commission. The meeting was held jointly with the IDC Technical Experts Group on Seismoacoustic Event

Screening. The purpose of the meeting was to support the ongoing calibration and screening efforts of the IDC and in particular to review progress toward developing regionalized travel times to improve the quality of location estimates of seismic events reported in the IDC bulletins.

The meeting was attended by sixty-six technical experts, coming from twelve signatory countries and the Provisional Technical Secretariat. Dr. Frode Ringdal of Norway chaired the meeting, which was organized into four sessions, and included Working Group discussions to address the technical issues in detail. Recommendations from the meeting have been presented to Working Group B in Vienna during its June 2002 session (CTBT/WGB/TL-2/70).

Section 6.2 is entitled "Research in regional seismic monitoring" and contains a summary paper presented at the 24th Annual Seismic Research Review, describing a continued effort in regional monitoring research. We have used data from the regional networks operated by NORSAR and the Kola Regional Seismological Centre (KRSC) to assess the seismicity and characteristics of regional phases of the European Arctic. An especially interesting recent seismic event, which has been analyzed in detail, occurred on Novaya Zemlya on 23 February 2002. This small event (magnitude about 3.0) is the first seismic event detected in or near Novaya Zemlya since the two Kara Sea events of 16 August 1997. The event was recorded with particularly high SNR by the International Monitoring System (IMS) arrays Spitsbergen and ARCES, and by the Amderma station (operated by KRSC) south of Novaya Zemlya. We have located the event at the eastern coast of Novaya Zemlya, approximately 100 km NE of the former nuclear test site. Our attempts to estimate the depth of this event proved inconclusive, and a depth of 0 could not be ruled out.

We have begun an effort to develop an optimized site-specific threshold monitoring system for the Lop Nor test site in China. Initial results show that, among the available stations, the IMS Makanchi array in Kazakhstan (at an epicentral distance of 6 degrees) is the most sensitive station for detecting events at Lop Nor, followed by some of the best teleseismic arrays, for example the NORES array in Norway. Combining the data by using the threshold monitoring technique, we have found that the Lop Nor site can be monitored down to a threshold close to m_b 3.2. This threshold is about 0.8 magnitude units higher than the corresponding capability for the Novaya Zemlya test site, for which the highly sensitive arrays ARCES and Spitsbergen are both at a distance of only 10 degrees. We note that no stations inside China were selected for the Lop Nor study.

Section 6.3 is a design study of a possible reconfiguration of the Spitsbergen array (SPITS). This array needs a technical refurbishment before it can be certified for inclusion in the IMS, and the motivation for the present study is to determine possible options for reconfiguring the array so as to improve its monitoring capabilities. The SPITS array is situated in a geological/tectonic environment that is very different from that of Fennoscandia. This results in a number of characteristic features that must be taken into account when processing SPITS data.

The SPITS array often reports a large number of detections, which can reach thousands per day. A detailed analysis shows that the majority of these detections are real seismic signals caused by small sources located at close distances. The numerous local events typically show P onsets, no well defined S onsets, and dominant Rg onsets. Investigating the mean backazimuths of these Rg phases, one can see a strong correlation with the direction to a nearby coal-mine area and to nearby glaciers. To avoid spatial aliasing of these signals a denser inner ring of seismometers would be helpful. To improve the separation between phase types based on apparent velocities, an

increase in the array aperture is required. This would also provide improved resolution in the azimuth estimates.

At the SPITS array we observe a relatively large number of high SNR P detections from regional events without any corresponding detection of an S phase. The regional S-phases at SPITS in general have the largest amplitudes and SNR on the horizontal components. The current SPITS configuration has only one three-component instrument at site SPB4. With more three-component sites, the detection capability of S-phases can be improved by creating S-velocity beams from the rotated radial and transverse components, as now done for ARCES and NORES. In addition, the F-K analysis can be performed on the horizontal components.

The paper suggests specific extensions for the SPITS array to increase its detection and monitoring capabilities. These points will form the basis for our proposed Spitsbergen upgrade/refurbishment.

Section 6.4 is a study of seismic data from a series of underground cavity decoupled chemical explosions in the Älvdalen region of Sweden, with the aim of quantitatively predicting the decoupling effect of underground cavities of known dimensions and shape. A database of seismic waveform data has been compiled for seven such cavity explosions. Only three factors differentiate these events; the quantity of explosive, the composition and arrangement of the explosives, and the size and configuration of the explosion chamber. In addition, the Swedish Armed Forces regularly detonate outdated ammunition at ground level at a site approximately 15 km from the underground chambers. Seismic waveforms from 12 such events were added to the database to provide a comparison with the decoupled explosions.

In order to quantify the differences between these events, we examine the power density spectra of the signals recorded by NOA, NORES and HFS. The recordings from explosions in the cavities at Älvdalen are characterized by a large amount of high-frequency energy (8-16 Hz) compared with the energy at lower frequencies (2-5 Hz). Such spectral characteristics are not observed for the surface explosions. The effect is more pronounced for P than for S waves.

With regard to decoupling efficiency, three 10 ton explosions in a $1000m^3$ chamber appear to have been more efficiently decoupled than three 5 ton explosions in chambers of $200m^3$ and $300m^3$. The signals from the explosions in the smaller chambers were far stronger, in spite of significantly lower yields, and displayed a less pronounced high-to-low frequency energy ratio than the explosions in the larger chambers.

We plan to assemble NOA, HFS and NORES recordings of earthquakes located at distances similar to Älvdalen and Mossibränden, but at different azimuths, in order to make comparative studies of their spectral characteristics. Comparisons between records from decoupled explosions and ripple fired mining explosions are also recognized as an important future target.

Section 6.5 is a study of experimental Site-Specific Generalized Beamforming (SSGBF) applied to the Lop Nor test site in China. The SSGBF approach supplements the SSTM system described in the preceding NORSAR Semiannual Technical Summary. We also comment briefly on the relative merits of the two approaches (SSTM and SSGBF), and the extent to which they complement each other in this particular case study.

In the present study we have calibrated all available high-quality seismic stations within regional distance from Lop Nor and supplemented them with the best IMS arrays at teleseismic distances. As a calibration data base, we use several past nuclear explosions at the test site, com-

bined with nearby, well-recorded earthquakes. We present some preliminary results in applying site-specific generalized beamforming to the Lop Nor test site, using two data sets for performance testing. The first data set covers one day (10 September 2001), and in these data the recordings of 4 explosions were scaled and embedded at some (but not all of) the stations. Secondly, a 10 day test period with data from August 2 through 11, 2001 has been used. Examples of the data analysis for these data sets are presented.

The paper concludes that the Site-Specific Generalized Beamforming performance tests for the Lop Nor test site were successful. The combination of the SSTM and the SSGBF techniques appears to be a very promising new development. Each of these two approaches has its specific strengths. The SSTM technique has as its main strength the ability to display the real seismic field, without regard to "station detector performance". On the other hand, the SSGBF technique takes advantage of the individual station detector outputs, and uses this combined information to narrow down the number of possible candidates for events in the target area.

Section 6.6 is a study of seismic threshold monitoring applied to the Barents Sea region. A database comprising a total of 45 events, selected to provide the best possible ray path coverage of the Barents Sea and adjacent areas, was compiled and reanalyzed in a consistent manner. This resulted in new regional attenuation relations for Pn and Sn, together with a preferred average velocity model to be used for predicting the travel times of regional phases. We have now applied these attenuation relations to investigate a regional threshold monitoring scheme for the Barents Sea area.

A grid system with an approximately 100-km grid spacing was deployed for the Barents Sea region, and the observations at the arrays ARCES, SPITS, FINES and NORES were then used for calculating threshold magnitudes for each of the grid points. During an interval without seismic signals, the threshold magnitudes showed large variations over the region, and, in particular, in the vicinity of each array. However, for the region around the island of Novaya Zemlya the variations are modest, varying around a mean of magnitude 2.1-2.2.

We have studied the tradeoff between beam area coverage ("beam sharpness") and monitoring performance for the site-specific threshold monitoring of the Novaya Zemya test site. For this purpose, we have deployed a very dense grid system covering an area of 500 x 500 km around the test site, and calculated magnitude thresholds for each grid point for a two hour time interval, which included a seismic event in the region (23 February 2002, 01.12.21, magnitude 3). Using the arrays ARCES, SPITS, FINES and NORES, we find that even for a target region with radius as large as 100 km, the variations in threshold magnitudes are all within 0.2 magnitude units. This applies both for the time interval including the event and for background noise conditions. For the investigated station geometry, it will therefore be meaningful to represent the monitoring threshold of the entire Novaya Zemlya region using the values of a single target point, together with the *á priori* determined uncertainty bounds.

For areas with larger variations in threshold magnitudes, like in the vicinity of the arrays, a 100-km radius target region will obviously show larger differences between the maximum and minimum values. Examples illustrating this point are shown.

Frode Ringdal

2 Operation of International Monitoring System (IMS) Stations in Norway

2.1 PS27 — Primary Seismic Station NOA

The average recording time was 100%, the same as for the previous reporting period.

Monthly uptimes for the NORSAR on-line data recording task, taking into account all factors (field installations, transmissions line, data center operation) affecting this task were as follows:

January	:	100%
February	:	100%
March	:	100%
April	:	100%
May	:	100%
June	:	100%

Fig. 2.1.1 shows the uptime for the data recording task, or equivalently, the availability of NORSAR data in our tape archive, on a day-by-day basis for the reporting period.

J. Torstveit

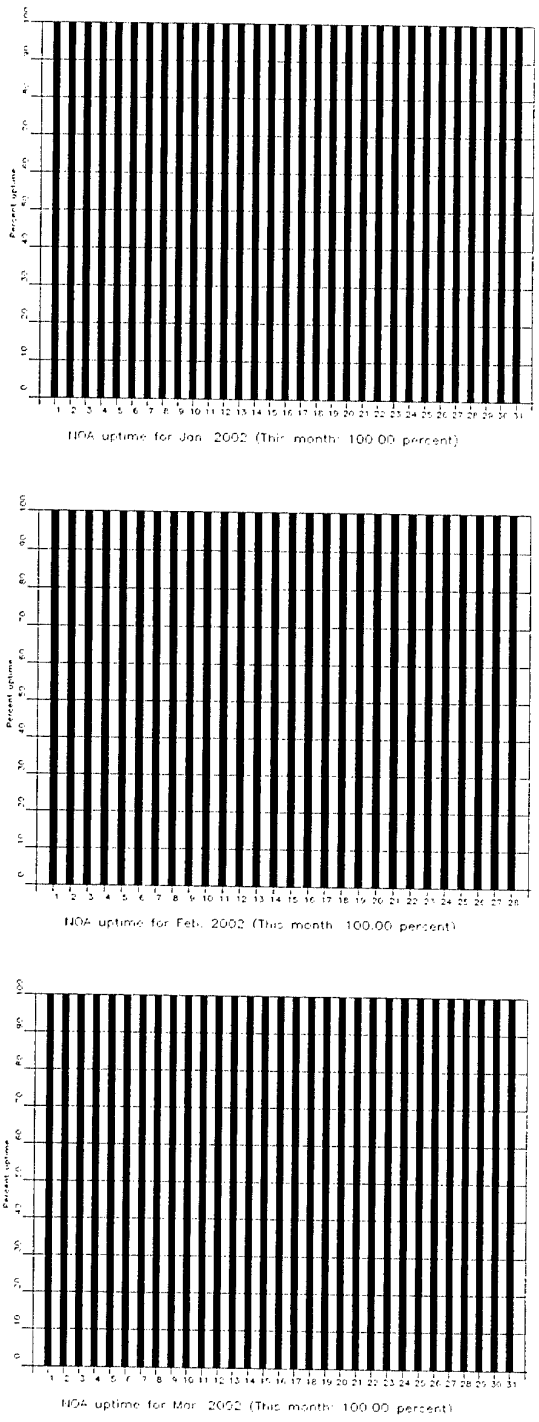

Fig. 2.1.1. *The figure shows the uptime for the data recording task or, equivalently, the availability of NOA data in our tape archive, on a day-by-day basis, for the reporting period. (Page 1 of 2, Jan-Mar 2002).*

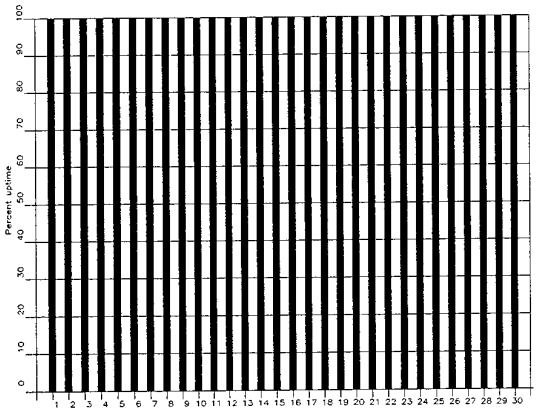

NOA uptime for Apr. 2002 (This month: 100.00 percent)

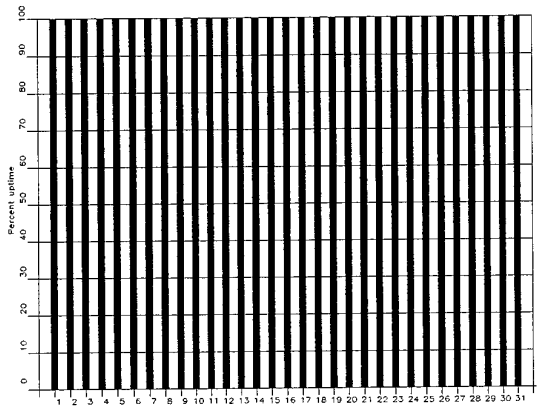

NOA uptime for May. 2002 (This month: 100.00 percent)

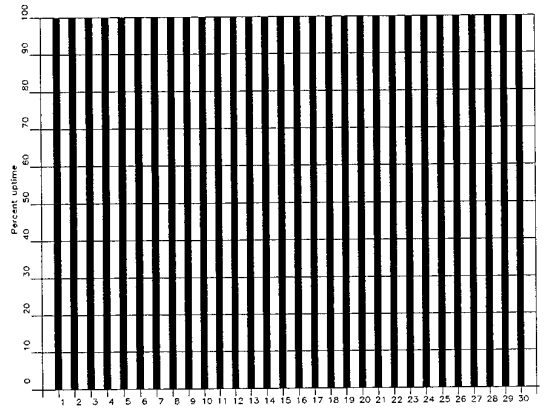

NOA uptime for Jun. 2002 (This month: 100.00 percent)

Fig. 2.1.1. *(cont.) (Page 2 of 2, Apr-Jun 2002).*

NOA Event Detection Operation

In Table 2.1.1 some monthly statistics of the Detection and Event Processor operation are given. The table lists the total number of detections (DPX) triggered by the on-line detector, the total number of detections processed by the automatic event processor (EPX) and the total number of events accepted after analyst review (teleseismic phases, core phases and total).

	Total DPX	Total EPX	Accepted Events		Sum	Daily
			P-phases	Core Phases		
Jan	12,660	870	184	67	251	8.1
Feb	11,032	721	162	48	210	7.5
Mar	12,508	918	266	82	348	11.2
Apr	7,919	853	295	67	362	12.1
May	5,144	699	286	53	339	10.9
Jun	6,352	830	293	69	362	12.1
	55,615	4,891	1,486	386	1,872	10.3

Table 2.1.1. *Detection and Event Processor statistics, 1 January - 30 June 2002.*

NOA detections

The number of detections (phases) reported by the NORSAR detector during day 001, 2002, through day 181, 2002, was 55,615, giving an average of 307 detections per processed day (181 days processed).

B. Paulsen
U. Baadshaug

2.2 PS28 — Primary Seismic Station ARCES

The average recording time was 99.19% as compared to 99.20% for the previous period. Table 2.2.1 lists the reasons for and time periods of the main downtimes in the reporting period.

Date	Time			Cause
02 Feb	0949	-		Power failure
03 Feb		-	1800	
24 Apr	1232	-	1301	Maintenance in array

Table 2.2.1. *The main interruptions in recording of ARCES data at NDPC, 1 January - 30 June 2002.*

Monthly uptimes for the ARCES on-line data recording task, taking into account all factors (field installations, transmission lines, data center operation) affecting this task were as follows:

January	:	99.99%
February	:	95.21%
March	:	100%
April	:	99.93%
May	:	100%
June	:	100%

J. Torstveit

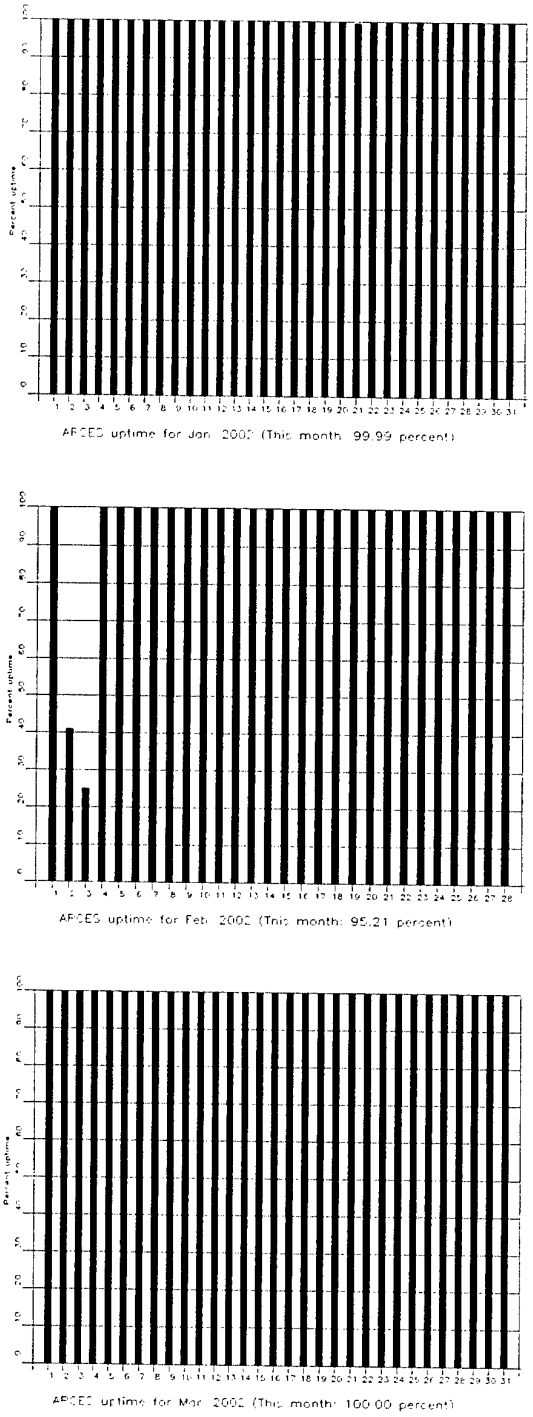

Fig. 2.2.1. *The figure shows the uptime for the data recording task or, equivalently, the availability of ARCES data in our tape archive, on a day-by-day basis, for the reporting period. (Page 1 of 2, Jan-Mar 2002)*

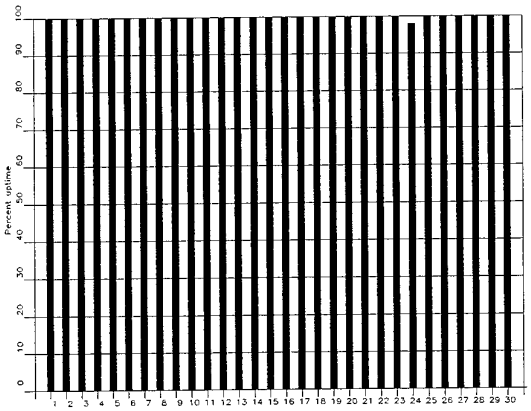

ARCES uptime for Apr. 2002 (This month: 99.93 percent)

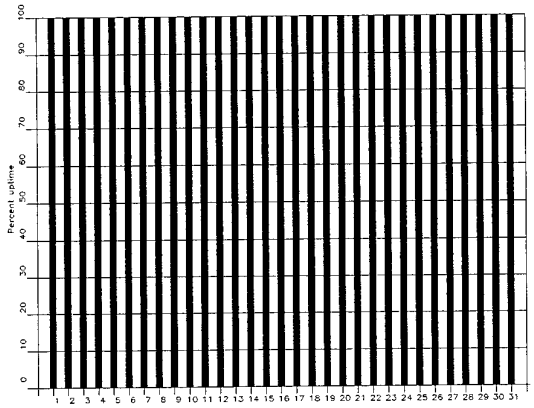

ARCES uptime for May. 2002 (This month: 100.00 percent)

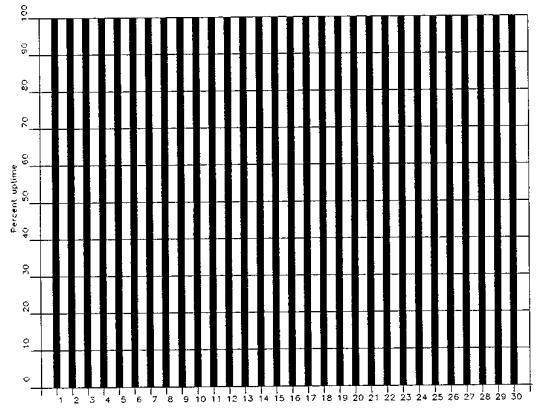

ARCES uptime for Jun. 2002 (This month: 100.00 percent)

Fig. 2.2.1 *(cont.) (Page 2 of 2, Apr-Jun 2002).*

Event Detection Operation

ARCES detections

The number of detections (phases) reported during day 001, 2002, through day 181, 2002, was 109,509, giving an average of 605 detections per processed day (181 days processed).

Events automatically located by ARCES

During days 001, 2002, through 181, 2002, 7,986 local and regional events were located by ARCES, based on automatic association of P- and S-type arrivals. This gives an average of 44.1 events per processed day (181 days processed). 62% of these events are within 300 km, and 85% of these events are within 1000 km.

U. Baadshaug

2.3 AS72 — Auxiliary Seismic Station Spitsbergen

The average recording time was 97.60% as compared to 99.99% for the previous reporting period.

Table 2.2.1 lists the reasons for and time periods of the main downtimes in the reporting period.

Date	Time			Cause
20 Jan	1801	-		Windmill broken
22 Jan		-	1226	Batteries charged by petrol aggregate
28 Jan	2113	-		Empty batteries
29 Jan			1335	Batteries charged by petrol aggregate
06 Feb	1155	-	1840	Empty batteries (charged again)
24 Feb	0116	-		Empty batteries
25 Feb			1304	Batteries charged by petrol aggregate
18 Mar				New windmill installed

Table 2.2.1. *The main interruptions in recording of Spitsbergen data at NDPC, 1 January - 30 June 2002.*

Monthly uptimes for the Spitsbergen on-line data recording task, taking into account all factors (field installations, transmissions line, data center operation) affecting this task were as follows:

January	:	92.07%
February	:	93.63%
March	:	99.98%
April	:	99.94%
May	:	100%
June	:	99.98%

J. Torstveit

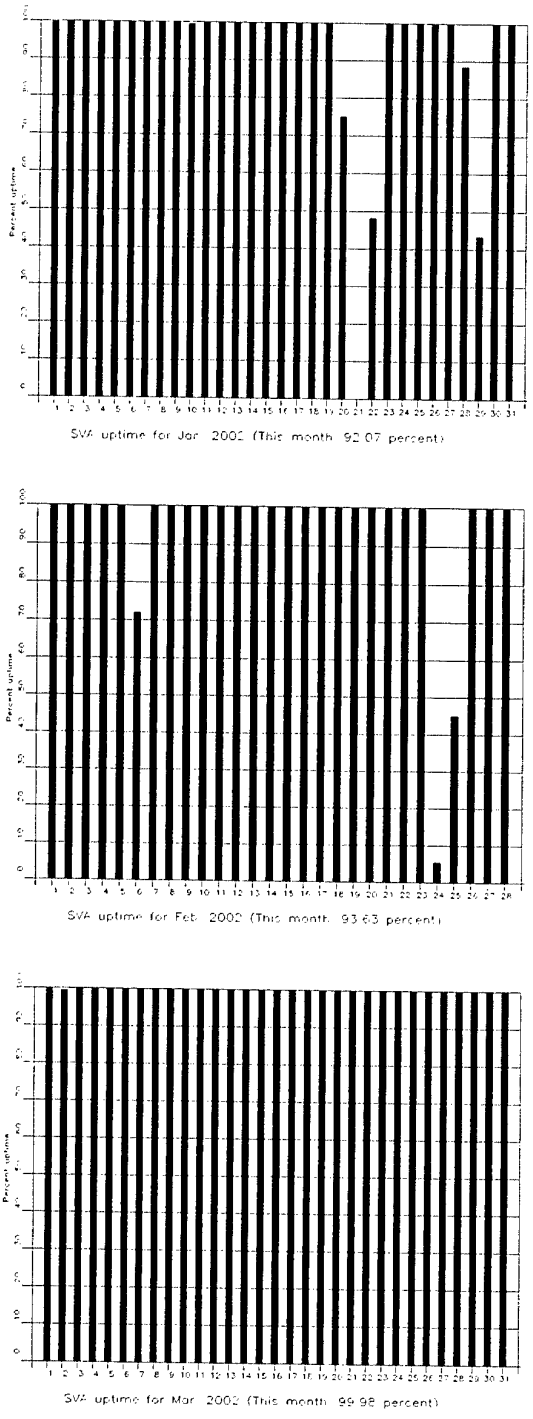

Fig. 2.3.1. *The figure shows the uptime for the data recording task or, equivalently, the availability of Spitsbergen data in our tape archive, on a day-by-day basis, for the reporting period. (Page 1 of 2, Jan-Mar 2002).*

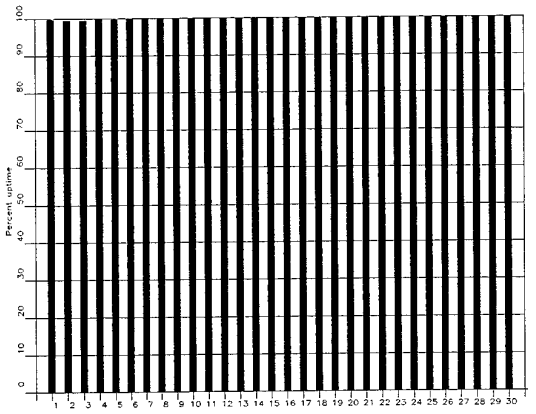

SVA uptime for Apr. 2002 (This month: 99.94 percent)

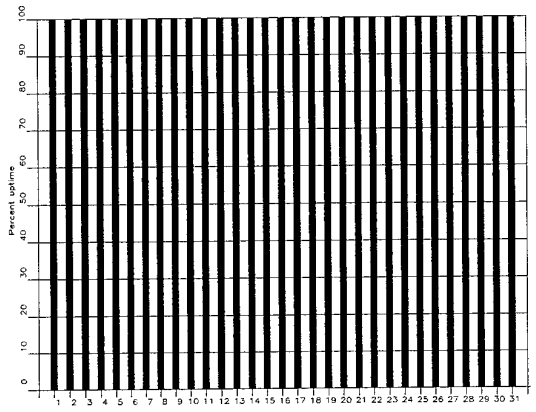

SVA uptime for May. 2002 (This month: 100.00 percent)

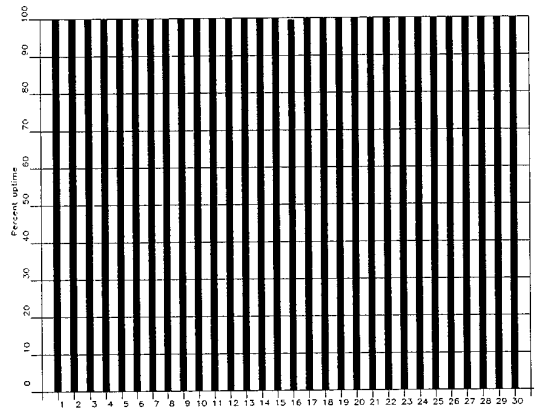

SVA uptime for Jun. 2002 (This month: 99.98 percent)

Fig. 2.3.1 *(cont.) (Page 2 of 2, Apr-Jun 2002).*

Event Detection Operation

Spitsbergen array detections

The number of detections (phases) reported from day 001, 2002, through day 181, 2002, was 295,419, giving an average of 1641 detections per processed day (180 days processed).

Events automatically located by the Spitsbergen array

During days 001, 2002, through 181, 2002, 36,467 local and regional events were located by the Spitsbergen array, based on automatic association of P- and S-type arrivals. This gives an average of 202.6 events per processed day (180 days processed). 68% of these events are within 300 km, and 84% of these events are within 1000 km.

U. Baadshaug

2.4 AS73 — Auxiliary Seismic Station at Jan Mayen

The IMS auxiliary seismic network will include a three-component station on the Norwegian island of Jan Mayen. The station location given in the protocol to the Comprehensive Nuclear-Test-Ban Treaty is 70.9°N, 8.7°W.

The University of Bergen has operated a seismic station at this location since 1970. An investment in the new station at Jan Mayen will be made in due course and in accordance with PrepCom program and budget decisions. A so-called Parent Network Station Assessment for AS73 was completed in April 2002. Work is now underway to prepare for the installation of a vault at a new location (71.0°N, 8.5°W) recently approved by the PrepCom. In the meantime, data from the existing seismic station on Jan Mayen are being transmitted to the NDC at Kjeller and to the University of Bergen via a VSAT link installed in April 2000.

J. Fyen

2.5 IS37 — Infrasound Station at Karasjok

The IMS infrasound network will include a station at Karasjok in northern Norway. The coordinates given for this station are 69.5°N, 25.5°E. These coordinates coincide with those of the primary seismic station PS28.

A site survey for this station was carried out during June/July 1998 as a cooperative effort between the Provisional Technical Secretariat of the CTBTO and NORSAR. Analysis of the data collected at several potential locations for this station in and around Karasjok has been completed. The results of this analysis have led to a recommendation on the exact location of the infrasound station. This location needs to be surveyed in detail. The next step will be to approach the local authorities to obtain the permission necessary to establish the station. Station installation is now expected to take place in the year 2003.

S. Mykkeltveit

2.6 RN49 — Radionuclide Station on Spitsbergen

The IMS radionuclide network will include a station at Longyearbyen on the island of Spitsbergen, with location 78.2°N, 16.4°E, as given in the protocol to the Comprehensive Nuclear-Test-Ban Treaty. These coordinates coincide with those of the auxiliary seismic station AS72. According to PrepCom decision, this station will also be among those IMS radionuclide stations that will have a capability of monitoring for the presence of relevant noble gases upon entry into force of the CTBT.

A site survey for this station was carried out in August of 1999 by NORSAR, in cooperation with the Norwegian Radiation Protection Authority. The site survey report to the PTS contained a recommendation to establish this station at Platåberget, some 20 km away from the Treaty location. The PrepCom approved the corresponding coordinate change in its meeting in May 2000. The station installation was part of PrepCom's work program and budget for the year 2000. The infrastructure for housing the station equipment has been established, and a noble gas detection system, based on the Swedish "SAUNA" design, was installed at this site in May 2001, as part of PrepCom's noble gas experiment. A particulate station ("ARAME" design) was installed at the same location in September 2001. Currently, the two systems are

undergoing testing and evaluation. It is expected that the particulate station will be certified by the end of 2002.

S. Mykkeltveit

3 Contributing Regional Seismic Arrays

3.1 NORES

Average recording time was 88.92% as compared to 70.32% for the previous period.

The outage that starts on 11 June 12.04 and continues throughout the month was due to a thunderstorm that caused major damage to the equipment.

Date	Time	Cause
10 Mar	1300 - 1630	UPS failure at HUB
15 Mar	0246 - 0950	UPS failure at HUB
11 Jun	1204 -	HUB damage due to thunderstorm

Table 3.1.1. *The main interruptions in recording of NORES data at the Norwegian NDC, 1 January - 30 June 2002.*

Monthly uptimes for the NORES on-line data recording task, taking into account all factors (field installations, transmissions line, data center operation) affecting this task were as follows:

January	:	100%
February	:	99.95%
March	:	98.58%
April	:	99.98%
May	:	99.99%
June	:	35.00%

Fig. 3.1.1 shows the uptime for the data recording task or, equivalently, the availability of NORES data in our tape archive on a day-by-day basis for the reporting period.

J. Torstveit

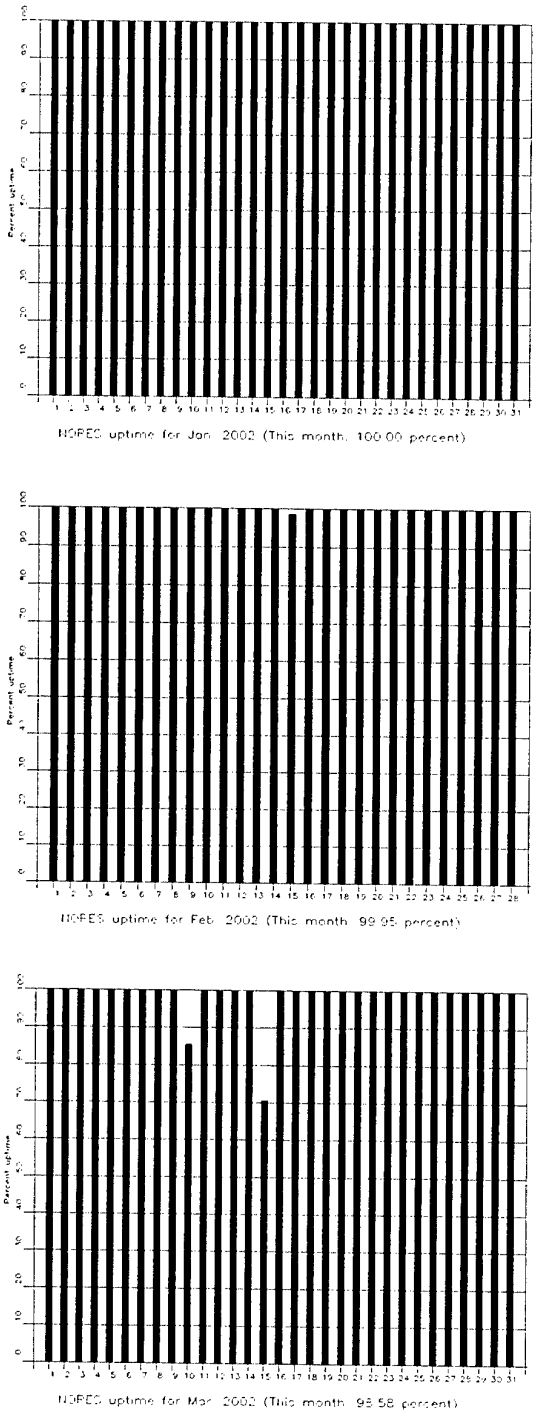

Fig. 3.1.1. *The figure shows the uptime for the data recording task or, equivalently, the availability of NORES data in our tape archive, on a day-by-day basis, for the reporting period (Page 1 of 2, Jan-Mar 2002).*

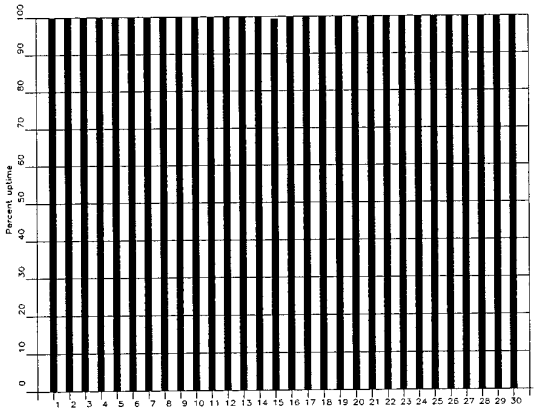

NORES uptime for Apr. 2002 (This month: 99.98 percent)

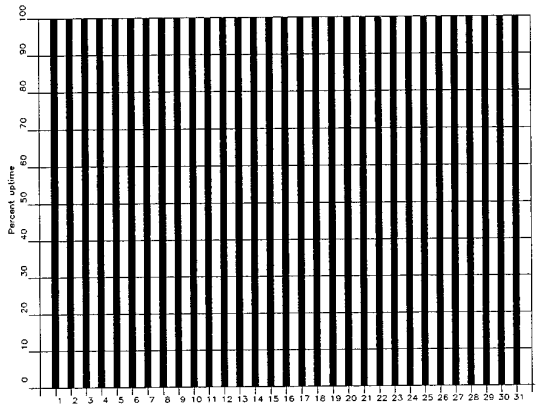

NORES uptime for May. 2002 (This month: 99.99 percent)

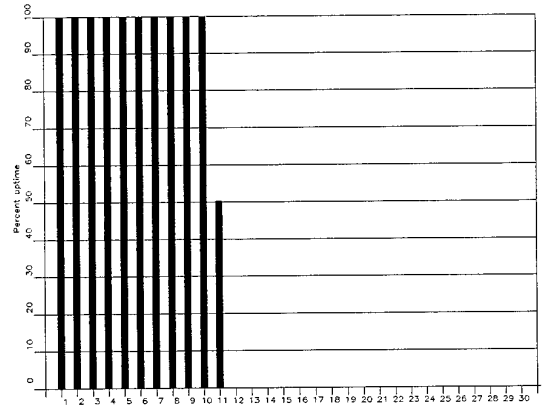

NORES uptime for Jun. 2002 (This month: 35.00 percent)

Fig. 3.1.1 *(cont.) (Page 2 of 2, Apr-Jun 2002).*

NORES Event Detection Operation

NORES detections

The number of detections (phases) reported from day 001, 2002, through day 181, 2002, was 139,063, giving an average of 858 detections per processed day (162 days processed).

Events automatically located by NORES

During days 001, 2002, through 181, 2002, 3,646 local and regional events were located by NORES, based on automatic association of P- and S-type arrivals. This gives an average of 22.5 events per processed day (162 days processed). 43% of these events are within 300 km, and 76% of these events are within 1000 km.

U. Baadshaug

3.2 Hagfors (IMS Station AS101)

The average recording time was 99.97% as compared to 99.91% for the previous reporting period.

Monthly uptimes for the Hagfors on-line data recording task, taking into account all factors (field installations, transmissions line, data center operation) affecting this task were as follows:

January	:	99.84%
February	:	100%
March	:	100%
April	:	99.99%
May	:	100%
June	:	100%

J. Torstveit

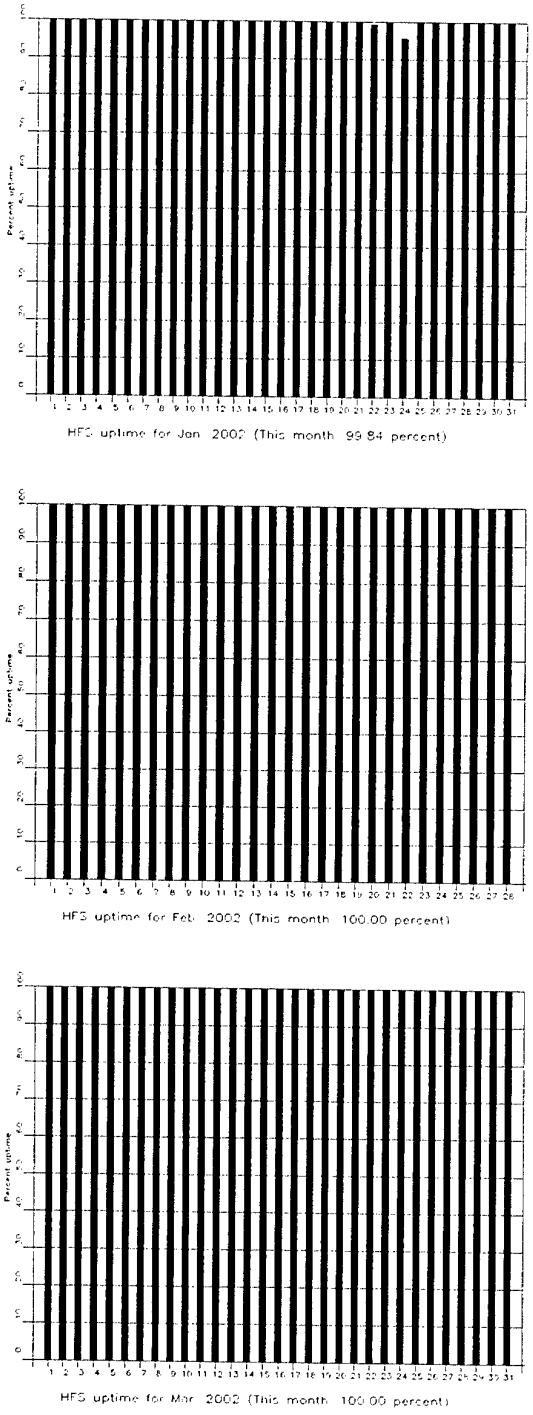

Fig. 3.2.1. *The figure shows the uptime for the data recording task or, equivalently, the availability of Hagfors data in our tape archive, on a day-by-day basis, for the reporting period (Page 1 of 2, Jan-Mar 2002).*

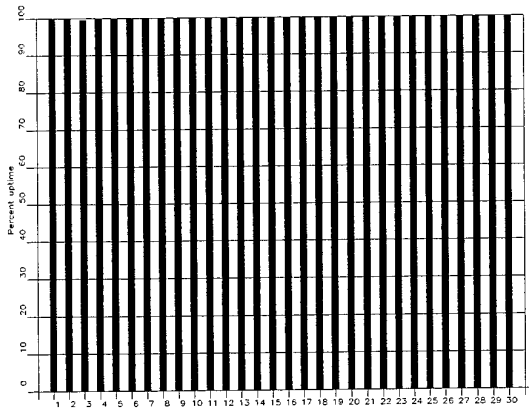

HFS uptime for Apr. 2002 (This month: 99.99 percent)

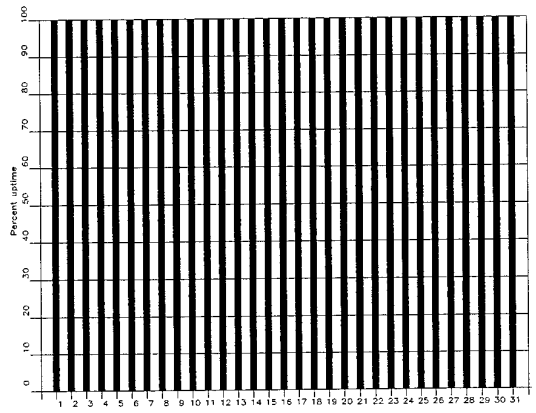

HFS uptime for May. 2002 (This month: 100.00 percent)

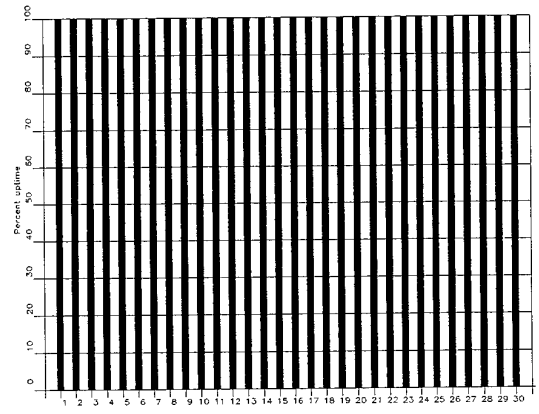

HFS uptime for Jun. 2002 (This month: 100.00 percent)

Fig. 3.2.1 *(cont.) (Page 2 of 2, Apr-Jun 2002).*

Hagfors Event Detection Operation

Hagfors array detections

The number of detections (phases) reported from day 001, 2002, through day 181, 2002, was 102,667, giving an average of 567 detections per processed day (181 days processed).

Events automatically located by the Hagfors array

During days 001, 2002, through 181, 2002, 3,016 local and regional events were located by the Hagfors array, based on automatic association of P- and S-type arrivals. This gives an average of 16.7 events per processed day (181 days processed). 56% of these events are within 300 km, and 83% of these events are within 1000 km.

U. Baadshaug

3.3 FINES (IMS station PS17)

The average recording time was 100% as compared to 99.99% for the previous reporting period.

Monthly uptimes for the FINES on-line data recording task, taking into account all factors (field installations, transmissions line, data center operation) affecting this task were as follows:

January	:	100%
February	:	100%
March	:	100%
April	:	100%
May	:	100%
June	:	100%

Fig. 3.3.1 shows the uptime for the data recording task, or equivalently, the availability of FINES data in our tape archive on a day-by-day basis for the reporting period.

J. Torstveit

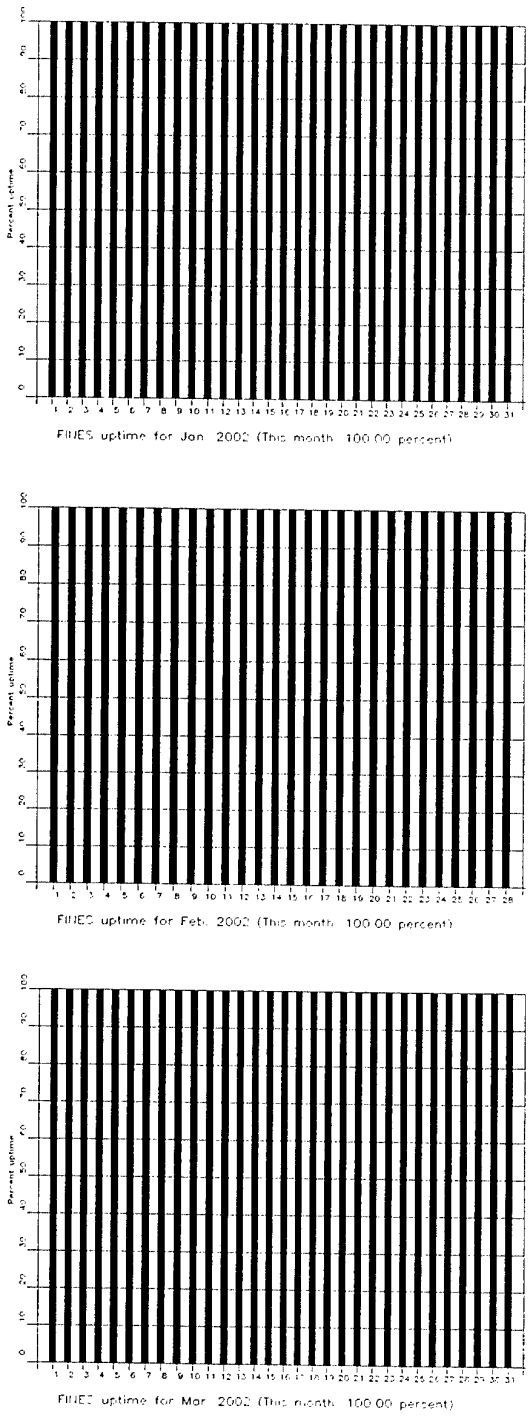

Fig. 3.3.1. *The figure shows the uptime for the data recording task or, equivalently, the availability of FINES data in our tape archive, on a day-by-day basis, for the reporting period (Page 1 of 2, Jan-Mar 2002).*

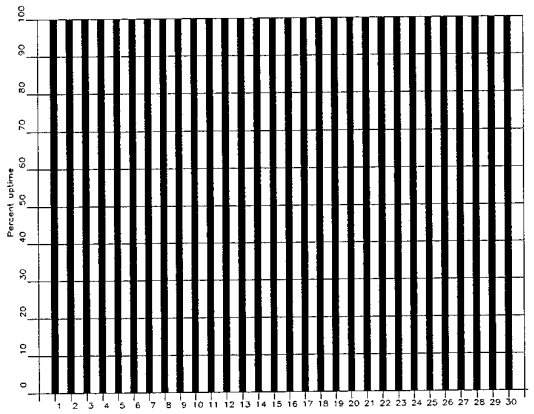

FINES uptime for Apr. 2002 (This month: 100.00 percent)

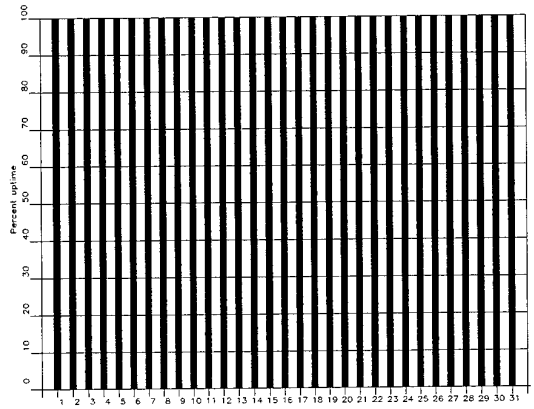

FINES uptime for May. 2002 (This month: 100.00 percent)

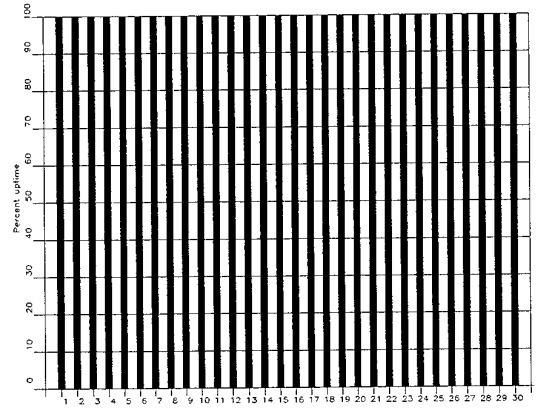

FINES uptime for Jun. 2002 (This month: 100.00 percent)

Fig. 3.3.1 *(cont.) (Page 2 of 2, Apr-Jun 2002)*

FINES Event Detection Operation

FINES detections

The number of detections (phases) reported during day 001, 2002, through day 181, 2002, was 44,060, giving an average of 243 detections per processed day (181 days processed).

Events automatically located by FINES

During days 001, 2002, through 181, 2002, 2,220 local and regional events were located by FINES, based on automatic association of P- and S-type arrivals. This gives an average of 12.9 events per processed day (181 days processed). 77% of these events are within 300 km, and 87% of these events are within 1000 km.

U. Baadshaug

3.4 Apatity

The average recording time was 99.94% in the reporting period compared to 98.31% during the previous period.

Monthly uptimes for the Apatity on-line data recording task, taking into account all factors (field installations, transmissions line, data center operation) affecting this task were as follows:

January	:	100%
February	:	99.98%
March	:	100%
April	:	99.64%
May	:	100%
June	:	100%

J. Torstveit

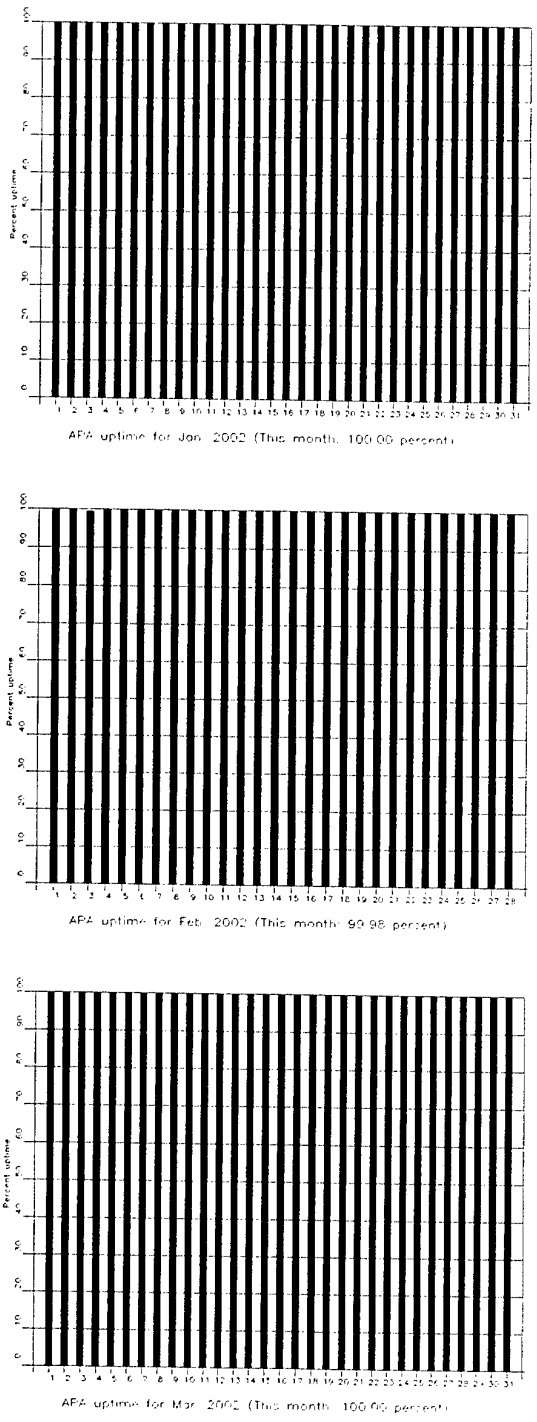

Fig. 3.4.1. *The figure shows the uptime for the data recording task, or equivalently, the availability of Apatity data in our tape archive, on a day-by-day basis, for the reporting period (Page 1 of 2, Jan-Mar 2002).*

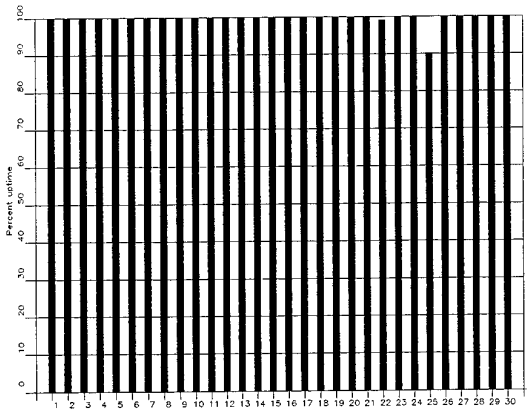

APA uptime for Apr. 2002 (This month: 99.64 percent)

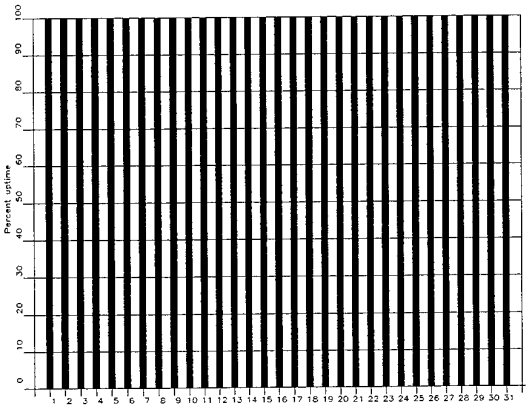

APA uptime for May. 2002 (This month. 100.00 percent)

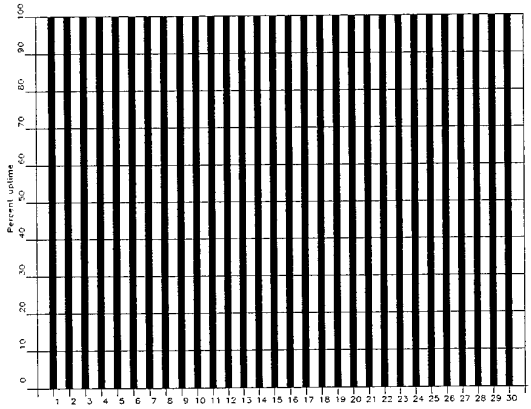

APA uptime for Jun. 2002 (This month: 100.00 percent)

Fig. 3.4.1 *(cont.) (Page 2 of 2, Apr-Jun 2002).*

Apatity Event Detection Operation

Apatity array detections

The number of detections (phases) reported from day 001, 2002, through day 181, 2002, was 164,442, giving an average of 904 detections per processed day (181 days processed).

As described in earlier reports, the data from the Apatity array is transferred by one-way (simplex) radio links to Apatity city. The transmission suffers from radio disturbances that occasionally result in a large number of small data gaps and spikes in the data. In order for the communication protocol to correct such errors by requesting retransmission of data, a two-way radio link would be needed (duplex radio). However, it should be noted that noise from cultural activities and from the nearby lakes cause most of the unwanted detections. These unwanted detections are "filtered" in the signal processing, as they give seismic velocities that are outside accepted limits for regional and teleseismic phase velocities.

Events automatically located by the Apatity array

During days 001, 2002, through 181, 2002, 1,872 local and regional events were located by the Apatity array, based on automatic association of P- and S-type arrivals. This gives an average of 10.3 events per processed day (181 days processed). 42% of these events are within 300 km, and 76% of these events are within 1000 km.

U. Baadshaug

3.5 Regional Monitoring System Operation and Analysis

The Regional Monitoring System (RMS) was installed at NORSAR in December 1989 and has been operated at NORSAR from 1 January 1990 for automatic processing of data from ARCES and NORES. A second version of RMS that accepts data from an arbitrary number of arrays and single 3-component stations was installed at NORSAR in October 1991, and regular operation of the system comprising analysis of data from the 4 arrays ARCES, NORES, FINES and GERES started on 15 October 1991. As opposed to the first version of RMS, the one in current operation also has the capability of locating events at teleseismic distances.

Data from the Apatity array was included on 14 December 1992, and from the Spitsbergen array on 12 January 1994. Detections from the Hagfors array were available to the analysts and could be added manually during analysis from 6 December 1994. After 2 February 1995, Hagfors detections were also used in the automatic phase association.

Since 24 April 1999, RMS has processed data from all the seven regional arrays ARCES, NORES, FINES, GERES (until January 2000), Apatity, Spitsbergen, and Hagfors. Starting 19 September 1999, waveforms and detections from the NORSAR array have also been available to the analyst.

Phase and event statistics

Table 3.5.1 gives a summary of phase detections and events declared by RMS. From top to bottom the table gives the total number of detections by the RMS, the number of detections that are associated with events automatically declared by the RMS, the number of detections that are not associated with any events, the number of events automatically declared by the RMS, and finally the total number of events worked on interactively (in accordance with criteria that vary over time; see below) and defined by the analyst.

New criteria for interactive event analysis were introduced from 1 January 1994. Since that date, only regional events in areas of special interest (e.g, Spitsbergen, since it is necessary to acquire new knowledge in this region) or other significant events (e.g, felt earthquakes and large industrial explosions) were thoroughly analyzed. Teleseismic events of special interest are also analyzed.

To further reduce the workload on the analysts and to focus on regional events in preparation for Gamma-data submission during GSETT-3, a new processing scheme was introduced on 2 February 1995. The GBF (Generalized Beamforming) program is used as a pre-processor to RMS, and only phases associated with selected events in northern Europe are considered in the automatic RMS phase association. All detections, however, are still available to the analysts and can be added manually during analysis.

	Jan 02	Feb 02	Mar 02	Apr 02	May 02	Jun 02	Total
Phase detections	115917	106190	160733	161223	215085	171119	930267
- Associated phases	4318	3513	6828	5245	6576	4226	30706
- Unassociated phases	111599	102677	153905	155978	208509	166893	899561
Events automatically declared by RMS	783	646	1388	976	1287	855	5935
No. of events defined by the analyst	76	76	82	68	66	66	434

Table 3.5.1. *RMS phase detections and event summary.*

U. Baadshaug
B. Paulsen

4 NDC and Field Activities

4.1 NDC Activitities

NORSAR functions as the Norwegian National Data Center (NDC) for CTBT verification. Six monitoring stations, comprising altogether 119 field instruments, will be located on Norwegian territory as part of the future IMS as described elsewhere in this report. The four seismic IMS stations are all in operation today, and three of them are currently providing data to the IDC. The radionuclide station at Spitsbergen is currently operating in a testing mode, whereas the infrasound station in northern Norway will need to be established within the next few years. Data recorded by the Norwegian stations is being transmitted in real time to the Norwegian NDC, and provided to the IDC through the Global Communications Infrastructure (GCI). Norway is connected to the GCI with a frame relay link to Vienna.

Operating the Norwegian IMS stations continues to require increased resources and additional personnel both at the NDC and in the field. The PTS has established new and strictly defined procedures as well as increased emphasis on regularity of data recording and timely data transmission to the IDC in Vienna. This has led to increased reporting activities and implementation of new procedures for the NDC operators. The NDC carries out all the technical tasks required in support of Norway's treaty obligations. NORSAR will also carry out assessments of events of special interest, and advise the Norwegian authorities in technical matters relating to treaty compliance.

Verification functions; information received from the IDC

After the CTBT enters into force, the IDC will provide data for a large number of events each day, but will not assess whether any of them are likely to be nuclear explosions. Such assessments will be the task of the States Parties, and it is important to develop the necessary national expertise in the participating countries. An important task for the Norwegian NDC will thus be to make independent assessments of events of particular interest to Norway, and to communicate the results of these analyses to the Norwegian Ministry of Foreign Affairs.

Monitoring the Arctic region

Norway will have monitoring stations of key importance for covering the Arctic, including Novaya Zemlya, and Norwegian experts have a unique competence in assessing events in this region. On several occasions in the past, seismic events near Novaya Zemlya have caused political concern, and NORSAR specialists have contributed to clarifying these issues.

International cooperation

After entry into force of the treaty, a number of countries are expected to establish national expertise to contribute to the treaty verification on a global basis. Norwegian experts have been in contact with experts from several countries with the aim of establishing bilateral or multilateral cooperation in this field. One interesting possibility for the future is to establish NORSAR as a regional center for European cooperation in the CTBT verification activities.

NORSAR event processing

The automatic routine processing of NORSAR events as described in NORSAR Sci. Rep. No. 2-93/94, has been running satisfactorily. The analyst tools for reviewing and updating the solutions have been continually modified to simplify operations and improve results. NORSAR is currently applying teleseismic detection and event processing using the large-aperture NORSAR array as well as regional monitoring using the network of small-aperture arrays in Fennoscandia and adjacent areas.

Certification of PS28

On 8 November 2001 the IMS station PS28-ARCES was formally certified. PTS personnel visited the station during the winter of 2000 and carried out a detailed technical evaluation. As a result of this inspection and subsequent discussions between NORSAR and the PTS, it was concluded that PS28 needed only one enhancement in order to be certified: to install a centralized authentication process at the central array recording facility. After this was done during the fall of 2001 and the subsequent verification by the PTS, station certification was granted.

Communication topology

Norway has implemented an independent subnetwork, which connects the IMS stations AS72, AS73, PS28, and RN49 operated by NORSAR to the GCI at NOR_NDC. A contract has been concluded and VSAT antennas have been installed at each station in the network. Under the same contract, VSAT antennas for 6 of the PS27 subarrays have been installed for intra-array communication. The seventh subarray is connected to the central recording facility via a leased land line. The central recording facility for PS27 is connected directly to the GCI (Basic Topology). All the VSAT communication is functioning satisfactorily.

The Norwegian NDC has been cooperating with institutions in other countries for transmission of IMS data to the Prototype IDC during GSETT-3. Details on this can be found in Section 4.2.

Jan Fyen

4.2 Status Report: Norway's Participation in GSETT-3

Introduction

This contribution is a report for the period January - June 2002 on activities associated with Norway's participation in the GSETT-3 experiment, which provides data to the International Data Centre (IDC) in Vienna on an experimental basis until the participating stations have been commissioned as part of the International Monitoring System (IMS) network defined in the protocol to the Comprehensive Nuclear-Test-Ban Treaty. This report represents an update of contributions that can be found in previous editions of NORSAR's Semiannual Technical Summary. It is noted that as of 30 June 2002, two out of the three Norwegian seismic stations providing data to the IDC have been formally certified and thus commissioned as part of the IMS network.

Norwegian GSETT-3 stations and communications arrangements

During the reporting interval 1 January - 30 June 2002, Norway has provided data to the GSETT-3 experiment from the three seismic stations shown in Fig. 4.2.1. The NORSAR array (PS27, station code NOA) is a 60 km aperture teleseismic array, comprised of 7 subarrays, each containing six vertical short period sensors and a three-component broadband instrument. ARCES is a 25-element regional array with an aperture of 3 km, whereas the Spitsbergen array (station code SPITS) has 9 elements within a 1-km aperture. ARCES and SPITS both have a broadband three-component seismometer at the array center.

The intra-array communication for NOA utilizes a land line for subarray NC6 and VSAT links based on TDMA technology for the other 6 subarrays. The central recording facility for NOA is at NOR_NDC.

Continuous ARCES data has been transmitted from the ARCES site to NOR_NDC using a 64 kbits/s VSAT satellite link, based on BOD technology.

Continuous SPITS data has been transmitted to NOR_NDC via a VSAT terminal located at Platåberget in Longyearbyen (which is the site of the IMS radionuclide monitoring station RN49 installed during 2001).

Seven-day station buffers have been established at the ARCES and SPITS sites and at all NOA subarray sites, as well as at NOR_NDC for ARCES, SPITS and NOA.

The NOA and ARCES arrays are primary stations in the GSETT-3 network and the IMS, which implies that data from these stations is transmitted continuously to the receiving international data center. Since October 1999, this data has been transmitted (from NOR_NDC) via the Global Communications Infrastructure (GCI) to the IDC in Vienna, whereas transmission of the same data to the Prototype International Data Center (IDC) in Arlington, VA, was discontinued on 7 February 2000. The SPITS array is an auxiliary station in GSETT-3 and the IMS, and the SPITS data have been available to both the IDC and the IDC throughout the reporting period on a request basis via use of the AutoDRM protocol (Kradolfer, 1993; Kradolfer, 1996). The Norwegian stations are thus participating in GSETT-3 with the same status (primary/auxiliary seismic stations) they have in the IMS defined in the protocol to the Comprehensive Nuclear-Test-Ban Treaty. In addition, continuous data from all three arrays is transmitted to the US NDC.

Starting with this report, data availabilities for primary stations and the number of requests made for auxiliary station data are reported with reference to the IDC, as opposed to the PIDC, as was done in previous reports.

Uptimes and data availability

Figs. 4.2.2 - 4.2.3 show the monthly uptimes for the Norwegian GSETT-3 primary stations ARCES and NOA, respectively, for the period 1 January - 30 June 2002, given as the hatched (taller) bars in these figures. These barplots reflect the percentage of the waveform data that are available in the NOR_NDC tape archives for these two arrays. The downtimes inferred from these figures thus represent the cumulative effect of field equipment outages, station site to NOR_NDC communication outage, and NOR_NDC data acquisition outages.

Figs. 4.2.2-4.2.3 also give the data availability for these two stations as reported by the IDC in the IDC Station Status reports. The main reason for the discrepancies between the NOR_NDC and IDC data availabilities as observed from these figures is the difference in the ways the two

data centers report data availability for arrays: Whereas NOR_NDC reports an array station to be up and available if at least one channel produces useful data, the IDC uses weights where the reported availability (capability) is based on the number of actually operating channels.

Use of the AutoDRM protocol

NOR_NDC's AutoDRM has been operational since November 1995 (Mykkeltveit & Baadshaug, 1996). The monthly number of requests by the IDC for SPITS data for the period January - June 2002 is shown in Fig. 4.2.4.

NDC automatic processing and data analysis

These tasks have proceeded in accordance with the descriptions given in Mykkeltveit and Baadshaug (1996). For the period January - June 2002, NOR_NDC derived information on 464 supplementary events in northern Europe and submitted this information to the Finnish NDC as the NOR_NDC contribution to the joint Nordic Supplementary (Gamma) Bulletin, which in turn is forwarded to the IDC. These events are plotted in Fig. 4.2.5.

Data forwarding for GSETT-3 stations in other countries

NOR_NDC continued to provide communications for the GSETT-3 auxiliary station at Nilore, Pakistan, through a VSAT satellite link between NOR_NDC and Pakistan's NDC in Nilore. The IDC obtains data from the Hagfors array (HFS) in Sweden through requests to the Auto-DRM server at NOR_NDC (in the same way requests for Spitsbergen array data are handled, see above). Fig. 4.2.6 shows the monthly number of requests for HFS data from the two IDC accounts "pipeline" and "testbed".

Current developments and future plans

NOR_NDC is continuing the efforts towards improving and hardening all critical data acquisition and data forwarding hardware and software components, so as to meet future requirements related to operation of IMS stations to the maximum extent possible.

The PrepCom has tasked its Working Group B with overseeing, coordinating, and evaluating the GSETT-3 experiment. The PrepCom has also encouraged states that operate IMS-designated stations to continue to do so on a voluntary basis and in the framework of the GSETT-experiment until such time that the stations have been certified for formal inclusion in IMS. The NOA array was formally certified by the PTS on 28 July 2000, and a contract with the PTS in Vienna currently provides partial funding for operation and maintenance of this station. The ARCES array was formally certified by the PTS on 8 November 2001. A contract has been signed with the PTS for operation and maintenance of this station, with an effective date of 1 January 2002. Provided that adequate funding continues to be made available (from the PTS and the Norwegian Ministry of Foreign Affairs), we envisage continuing the provision of data from all Norwegian IMS-designated seismic stations without interruption to the IDC in Vienna.

U. Baadshaug
S. Mykkeltveit
J. Fyen

References

Kradolfer, U. (1993): Automating the exchange of earthquake information. *EOS, Trans., AGU*, 74, 442.

Kradolfer, U. (1996): AutoDRM — The first five years, *Seism. Res. Lett.*, 67, 4, 30-33.

Mykkeltveit, S. & U. Baadshaug (1996): Norway's NDC: Experience from the first eighteen months of the full-scale phase of GSETT-3. *Semiann. Tech. Summ., 1 October 1995 - 31 March 1996*, NORSAR Sci. Rep. No. 2-95/96, Kjeller, Norway.

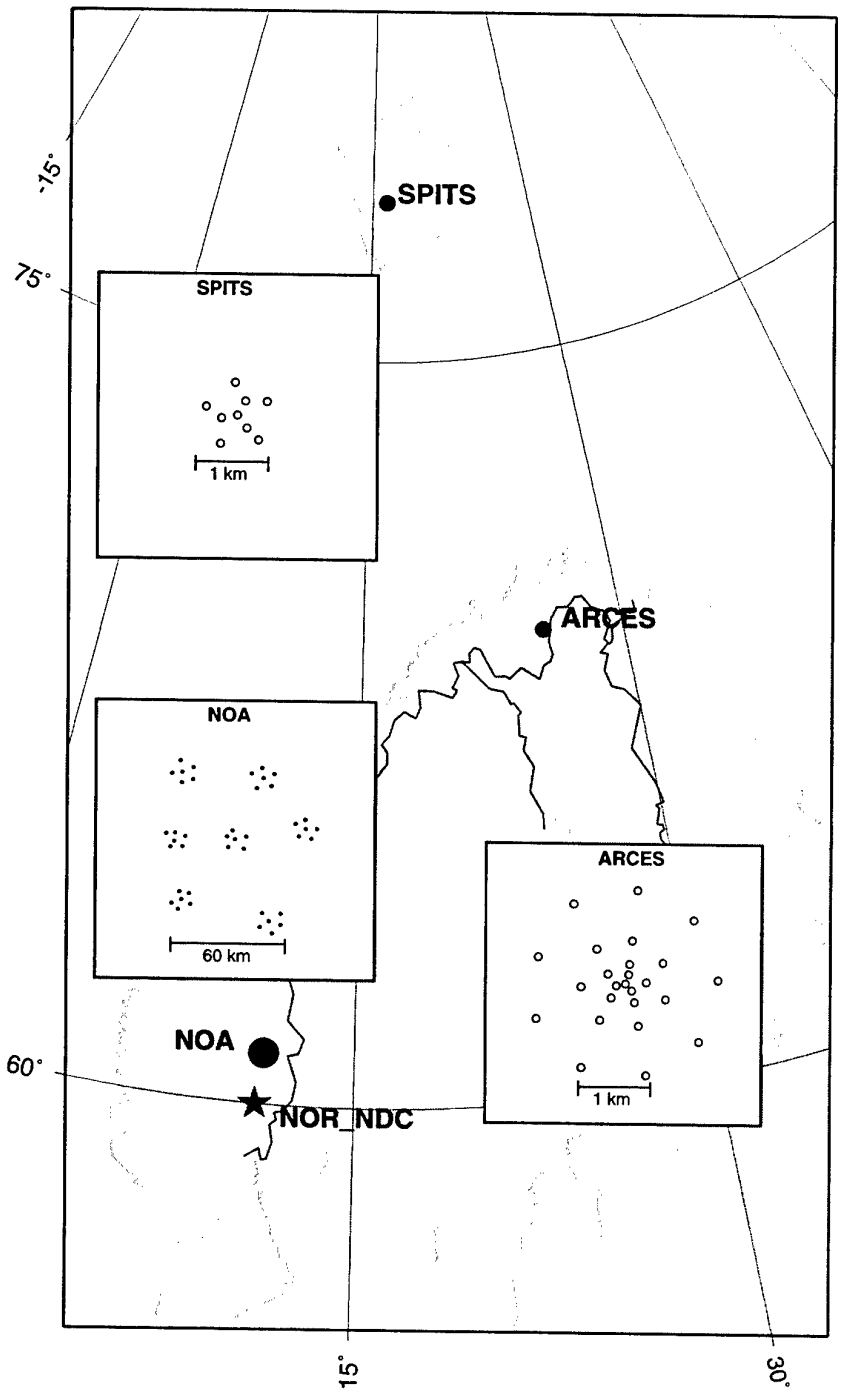

Fig. 4.2.1. The figure shows the locations and configurations of the three Norwegian seismic array stations that have provided data to the GSETT-3 experiment during the period 1 January - 30 June 2002. The data from these stations are transmitted continuously and in real time to the Norwegian NDC (NOR_NDC). The stations NOA and ARCES have participated in GSETT-3 as primary stations, whereas SPITS has contributed as an auxiliary station.

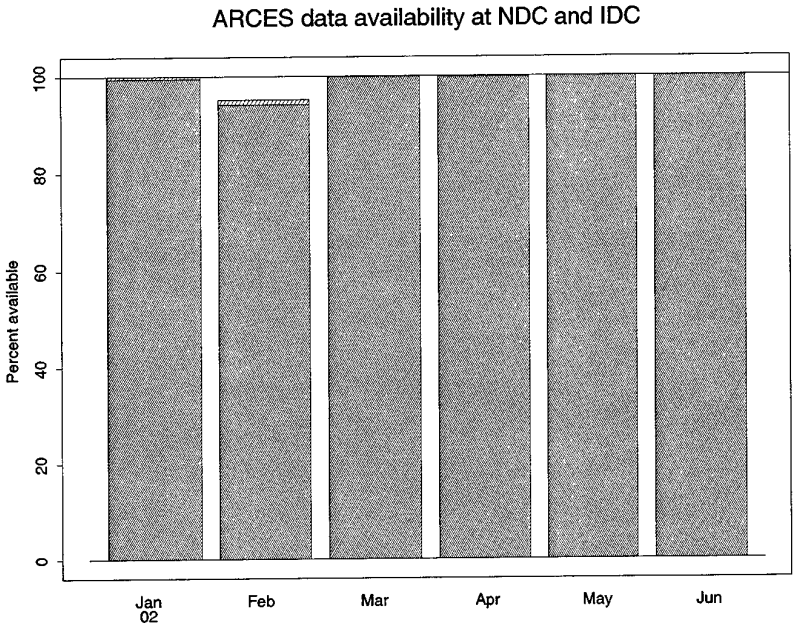

Fig. 4.2.2. The figure shows the monthly availability of ARCES array data for the period January - June 2002 at NOR_NDC and the IDC. See the text for explanation of differences in definition of the term "data availability" between the two centers. The higher values (hatched bars) represent the NOR_NDC data availability.

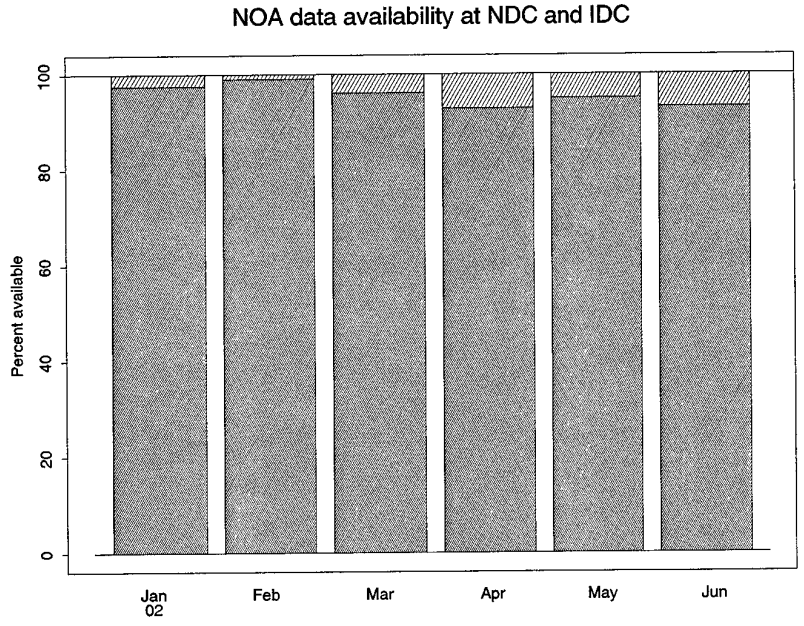

Fig. 4.2.3. The figure shows the monthly availability of NORSAR array data for the period January - June 2002 at NOR_NDC and the IDC. See the text for explanation of differences in definition of the term "data availability" between the two centers. The higher values (hatched bars) represent the NOR_NDC data availability.

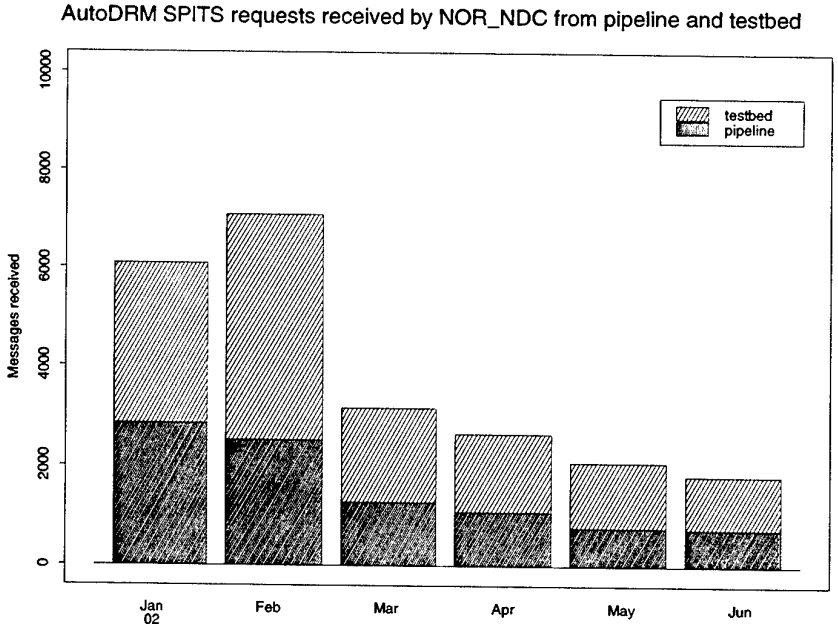

Fig. 4.2.4. The figure shows the monthly number of requests received by NOR_NDC from the IDC for SPITS waveform segments during January - June 2002.

Reviewed Supplementary events

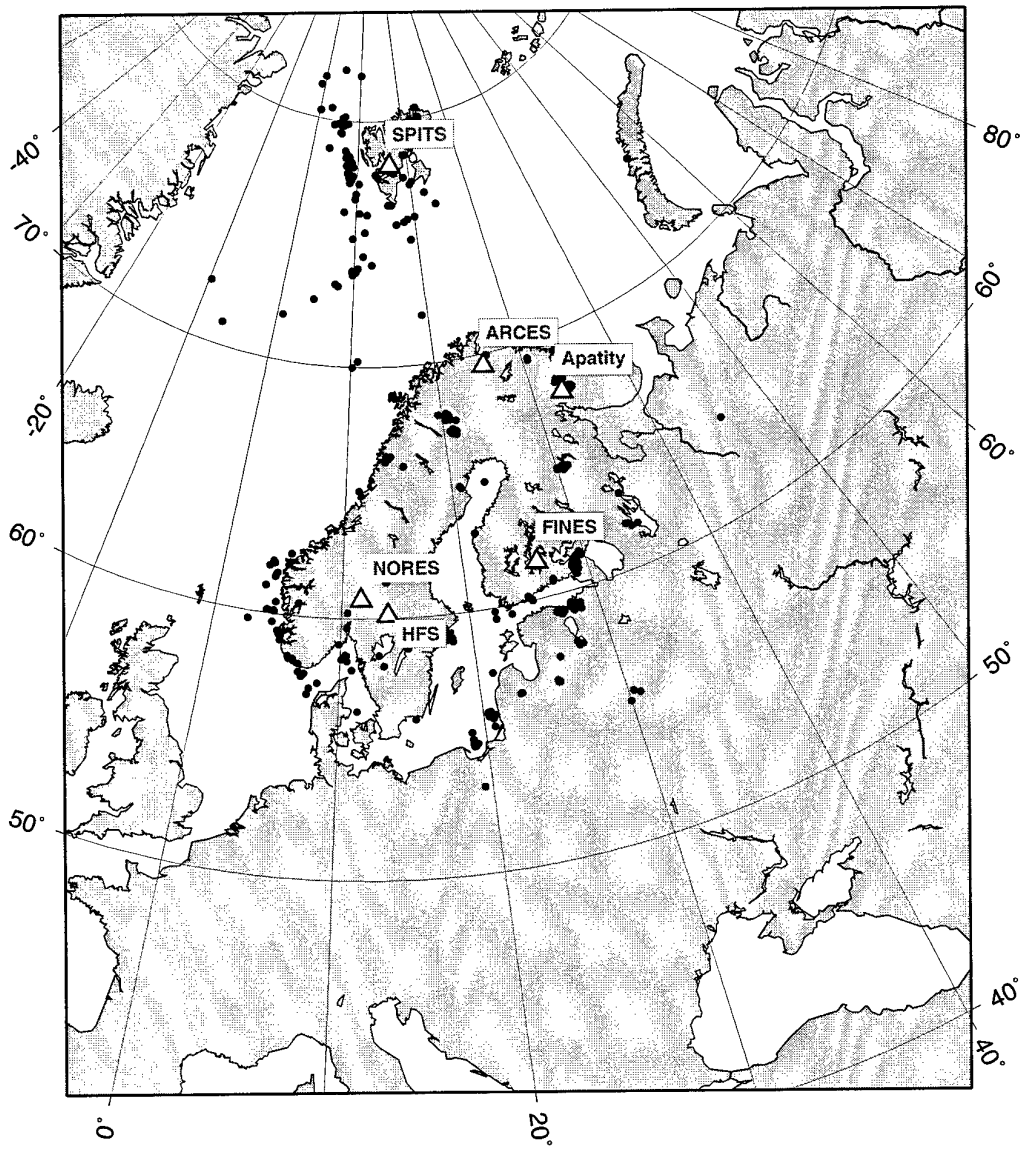

Fig. 4.2.5. The map shows the 464 events in and around Norway contributed by NOR_NDC during January - June 2002 as supplementary (Gamma) events to the IDC, as part of the Nordic supplementary data compiled by the Finnish NDC. The map also shows the seismic stations used in the data analysis to define these events.

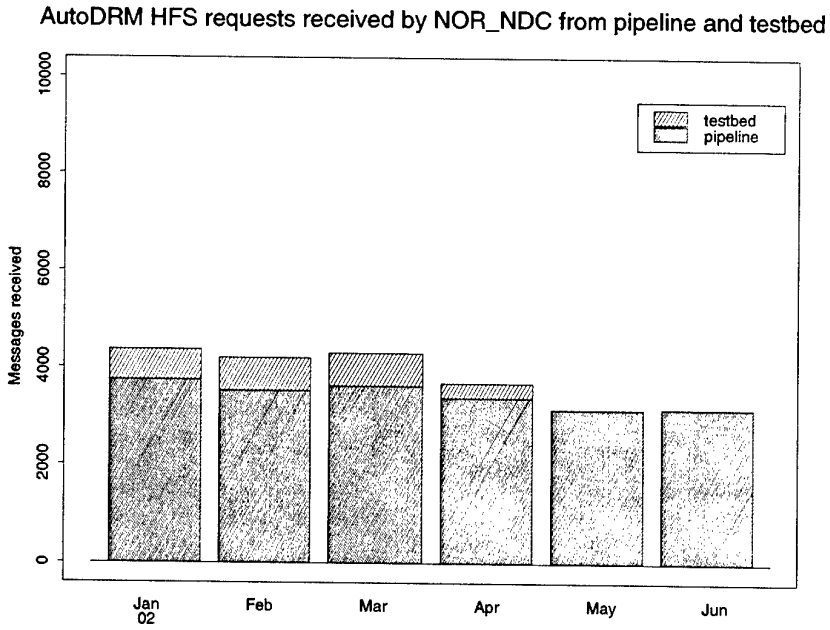

Fig. 4.2.6. The figure shows the monthly number of requests received by NOR_NDC from the IDC for HFS waveform segments during January - June 2002.

4.3 Field Activities

The activities at the NORSAR Maintenance Center (NMC) at Hamar currently include work related to operation and maintenance of the following IMS seismic stations: the NOA teleseismic array (PS27), the ARCES array (PS28) and the Spitsbergen array (AS72). Some preparatory work has also been carried out in connection with the seismic station on Jan Mayen (AS73), the infrasound station at Karasjok (IS37) and the radionuclide station at Spitsbergen (RN49). NORSAR also acts as a consultant for the operation and maintenance of the Hagfors array in Sweden (AS101).

In addition to the above activities, which are directly related to the International Monitoring System, NORSAR's field staff are continuing, within available resources, to maintain the small-aperture NORES array, which is co-located with NOA subarray 06C. These efforts are given low priority, since there is no requirement for specific uptimes at NORES.

NORSAR carries out the field activities relating to IMS stations in a manner generally consistent with the requirements specified in the appropriate IMS Operational Manuals, which are currently being developed by Working Group B of the Preparatory Commission. For seismic stations these specifications are contained in the Operational Manual for Seismological Monitoring and the International Exchange of Seismological Data (CTBT/WGB/TL-11/2), currently available in a draft version.

All regular maintenance on the NORSAR field systems is conducted on a one-shift-per-day, five-day-per-week basis. The maintenance tasks include:

- Operating and maintaining the seismic sensors and the associated digitizers, authentication devices and other electronics components.
- Maintaining the power supply to the field sites as well as backup power supplies.
- Operating and maintaining the VSATs, the data acquisition systems and the intra-array data transmission systems.
- Assisting the NDC in evaluating the data quality and making the necessary changes in gain settings, frequency response and other operating characteristics as required.
- Carrying out preventive, routine and emergency maintenance to ensure that all field systems operate properly.
- Maintaining a computerized record of the utilization, status, and maintenance history of all site equipment.
- Providing appropriate security measures to protect against incidents such as intrusion, theft and vandalism at the field installations.

Details of the daily maintenance activities are kept locally. As part of its contract with CTBTO/PTS NORSAR submits, when applicable, problem reports, outage notification reports and equipment status reports. The contents of these reports and the circumstances under which they will be submitted are specified in the draft Operational Manual.

P.W. Larsen
K.A. Løken

5 Documentation Developed

Gibbons, S., C. Lindholm, T. Kværna & F. Ringdal (2002): Analysis of cavity-decoupled chemical explosions, **In**: *NORSAR Sci. Rep. 2-2002*, 1 January - 30 June 2002, Kjeller, Norway.

Kværna, T., E. Hicks & F. Ringdal (2002): Site-Specific Generalized Beamforming (SSGBF) applied to the Lop Nor test site, **In**: *NORSAR Sci. Rep. 2-2001*, 1 July - 31 December 2001, Kjeller, Norway.

Kværna, T., E. Hicks, J. Schweitzer & F. Ringdal (2002): Regional Seismic Threshold Monitoring, **In**: *NORSAR Sci. Rep. 2-2001*, 1 July - 31 December 2001, Kjeller, Norway.

Kværna, T., F. Ringdal, J. Schweitzer & L. Taylor (2002): Optimized Seismic Threshold Monitoring — Part 1: Regional Processing, *PAGEOPH* 159, 969-987.

Kværna, T., F. Ringdal, J. Schweitzer & L. Taylor (2002): Optimized Seismic Threshold Monitoring — Part 2: Teleseismic Processing, *PAGEOPH* 159, 989-1004.

Ringdal, F. (2002): Technical Summary, *NORSAR Sci. Rep. 1-2002*, Kjeller Norway.

Ringdal, F. (2002): Seismic Event Location Calibration, **In**: *NORSAR Sci. Rep. 2-2002*, 1 January - 30 June 2002, Kjeller, Norway.

Ringdal, F., T. Kværna, E. Kremenetskaya, V. Asming, S. Mykkeltveit, C. Lindholm & J. Schweitzer (2002): Research in regional seismic monitoring, **In**: *NORSAR Sci. Rep. 2-2002*, 1 January - 30 June 2002, Kjeller, Norway.

Schweitzer, J. & T. Kværna (2002): Design study for the refurbishment of the SPITS Array (AS72), **In**: NORSAR Sci. Rep. 2-2002, 1 January - 30 June 2002, Kjeller, Norway.

6 Summary of Technical Reports / Papers Published

6.1 Seismic Event Location Calibration

Report from the IDC Technical Experts Meeting in Oslo, Norway 22-26 April 2002

6.1.1 Introduction

The International Data Centre (IDC) Technical Experts Group on Seismic Event Location held its fourth annual meeting in Oslo, Norway on 22-26 April 2002. The meeting was held jointly with the IDC Technical Experts Group on Seismoacoustic Event Screening. The purpose of the meeting was to support the ongoing calibration and screening efforts of the IDC and in particular to review progress toward developing regionalized travel times to improve the quality of location estimates of seismic events reported in the IDC bulletins.

Sixty-six technical experts, coming from twelve signatory countries and the Provisional Technical Secretariat, participated in the meeting. In accordance with previous recommendations, the focus of the discussions was on the following geographical regions: North America, Eurasia, Northern Africa and Australia. Dr. Frode Ringdal of Norway chaired the meeting.

6.1.2 Background and technical objectives

Working Group B has repeatedly encouraged States Signatories to support the location improvement efforts by supplying relevant location calibration information for their own territories as well as for other regions where they have such information available. The following types of calibration information were proposed in the document CTBT/WGB-6/CRP.26:

- Precise information on location, depth, and origin time of previous nuclear explosions or large chemical explosions
- Similar information on other seismic events that have been located by regional networks with sufficient precision
- Data as appropriate on seismic travel-time models
- Any other information (e.g., geologic or tectonic maps) that would be useful
- Ground truth data from chemical explosions.

At its first meeting in January 1999, the IDC Technical Experts Group on Seismic Event Location developed plans and recommendations for a global calibration program, and presented its report to Working Group B in February 1999 (CTBT/WGB/TL-2/18). This work was reviewed and updated during the second and third meetings of the Experts Group in March 2000 and April 2001, and the results were subsequently presented to Working Group B (CTBT/WGB/TL-2/49 and CTBT/WGB/TL-2/61). The fourth meeting of the Experts Group (22-26 April 2002) had the following objectives:

- To review new developments of common interest to location calibration and event screening, with special emphasis on event depth determination and computation of location confidence ellipses
- To report on and review progress of ongoing research work on location calibration, including calibration consortia and PTS Phase 1 calibration contracts

- To review proposals for detailed station-specific regional location corrections, with particular emphasis on IMS stations in North America, Europe, North Africa, Asia and Australia
- To recommend a set of such corrections, including appropriate model errors, for incorporation into the operational IDC software
- To develop a plan for future extensions and improvements of this regional correction data base, to be incorporated into future IDC software releases
- To review progress in the general recommendations from the first and second meetings, and make adjustments and updates to these recommendations as required.

The primary task of the meeting was to assess the status and availability of such calibration information for the regions being considered, and to plan for implementing regional location calibration at the IDC as well as discuss the need for future research and development.

6.1.3 Technical Issues

Presentations during the meeting

A number of papers relating to the collection, application and validation of calibration information were presented by participants. Models for regionalization on a global basis were presented and discussed. Specific presentations were made by several experts describing regional velocity models and calibration data for the general geographic regions being considered initially. Information was provided about the current CTBTO Calibration Programme. Progress was reported at the workshop by U.S sponsored consortia, by CTBTO sponsored contractors and by several other research groups.

It was noted that for some regions, information was incomplete or lacking, and the use of default "generic" velocity models for various tectonic regions was discussed in some detail. Valuable new data on ground truth (GT) information for seismic events was presented. These data will be organized and made available to the IDC and interested States Signatories. Countries were encouraged to continue to provide relevant calibration data for the purpose of developing accurate seismic travel-time curves for various geographical regions.

Reports were presented on a number of modelling studies, some of which showed significant improvement in location precision when applied to test sets of seismic events. Three-dimensional models were introduced for several regions and were found to provide considerable improvements in location accuracy compared to standard (IASPEI-91) models.

Techniques for improved regional processing using sparse seismic networks as well as improved azimuth determination for regional arrays were presented and discussed. The application of special location and depth estimation techniques was also addressed.

Working Group Discussions

Three Working Groups, each focusing on specific regions of the world, were established to discuss technical issues in detail during the workshop:

Working Group 1: Northern Eurasia and East Asia

Working Group 2: Southwestern Asia and the African/Mediterranean area

Working Group 3: North America, Australia, Global models

The Working Groups were given a mandate with a list of specific questions addressing the following topics:

Topic 1: Validation and Implementation of Regional Calibration Information

Topic 2: Collection of Regional Calibration Information

Topic 3: Application of Regional Calibration Information

Topic 4: Future work of the Experts Group

The results of the Working Groups were presented and discussed in a plenary session. In some cases, previous recommendations were reiterated or amplified. These presentations and discussions provided the basis for the recommendations presented below. The detailed reports of these Working Groups are available on request from the Chairman of the Experts Group, Dr. Frode Ringdal, Norway.

6.1.4 Results and recommendations

Main results

Since the 2001 workshop, participants reported considerable progress in reference event data collection, GT criteria, and regional calibration. Reference event lists have significantly increased over the last year. New GT category criteria have been proposed. Regional calibration has demonstrated reduced bias (absolute errors) and decreased uncertainty (smaller error ellipses) in accordance with the goals of the IMS calibration effort.

Regional corrections have been implemented at the IDC for IMS stations in northwestern Eurasia and northern America. Work is continuing on developing such corrections for the remaining priority regions, and encouraging results have been achieved.

For example, for much of Eastern Asia, preliminary work on source-specific station corrections (SSSCs) for Pn arrivals has given very promising results suggesting that it will be possible to achieve or exceed the uncertainty goal of 1000 km^2. For example, it was reported that relocation studies using Soviet explosions recorded by about 90 regional stations have succeeded in reducing the median 90% error ellipse to 200 km^2 for these explosions, using model-based analysis combined with an interpolation approach to provide preliminary SSSCs. More limited validation studies conducted using a sparse IMS/surrogate network have documented improvements in location accuracy to significantly better than 10 km. Some cautions needs to be exercised in extrapolating these results to smaller events, but all indications are that significant improvements in location will be obtained by applying SSSC corrections to the IMS stations in this area.

Validation data sets

During the course of the experts' work the importance of *validation* of ground truth data has become increasingly clear. Validation is a far more complex and time-consuming undertaking than initially expected. The experts recommend that a systematic development of a validation data set be undertaken. This validation set should include GT events of various categories, and should contain all relevant information (metadata) about the events in the data base. Before delivering such datasets to the IDC archive, the data should be carefully quality controlled by the organization providing the data. Information on the quality control of origins and arrival

times should be provided to the IDC along with the data. WGB should consider arrangements to make these data available from the IDC without restrictions to the research community.

The Expert Group re-emphasizes the need for a formal procedure for validation. In addition, there should be standards for implementation and periodic checking of performance. The Group recommends that global models (large-scale regional models) continue to be tested, and points out the need for a high resolution crustal model. It is also noted that there are currently no teleseismic SSSCs available, and the experts recommend that such corrections be developed.

Validation metrics

The initial set of validation metrics suggested by the 1999 Workshop (CTBT/WGB/TL-2/18) should be updated. The experts recommend that the metrics below to be used as a common ground to evaluate the performance of SSSCs:

- Average and median improvement in epicentre mislocation for all relocated events with depth fixed to the GT depth.
- Average and median reduction in the size of 90% error ellipses where these error ellipses are adjusted to GT accuracy
- Actual coverage of the 90% confidence region (adjusted to GT accuracy).
- For events where accurate origin time is available:
  - average and median improvement in origin time;
  - origin time error should provide 90% coverage
- Percentage of events improved/deteriorated with respect to GT epicentres
- Percentage of events improved/deteriorated by more than 20% w.r.t. GT epicentres; average/median improvement and deterioration in km

The experts expect that additional metrics will be developed over the next few years which may provide more robust comparisons/evaluation capability. In order to compare corrections that have overlapping geographical coverage, a central archive should be established at the IDC to encourage the international community to contribute their insights and evaluation.

It would be desirable to develop a simpler "measure of performance" that would indicate which set of models/calibrations are statistically "better". It was recognized that the problem has multiple dimensions and location performance is more complicated than what can be described by a single number, but it will be easier to communicate to non-experts if the advantages/disadvantages of multiple overlapping SSSCs can be ranked in some sense.

Implementing preliminary corrections

The experts recommend that the preliminary sets of SSSCs that are now available should be considered for testing at the IDC as soon as possible along with existing available sets of offline validation test sets. Furthermore, such testing should include computations of multiple locations of REB events for open evaluation by the expert community. Multiple models should be tested. Input and results should be available in an open and transparent database with results compared to current practice. All experts are encouraged to provide their GT events, velocity models and SSSC corrections, including supporting information (meta-data), to the IDC as soon as possible.

Transparency

The experts again expressed concern about the current restrictions on obtaining IMS data and IDC products, and recommended that the IDC make openly available to the scientists involved in the IDC location calibration effort all of the waveform data and associated IDC products that are needed in order to successfully carry out the calibration program. The experts re-emphasize concerns over lack of transparency in IDC bulletin products that reflect corrections applied to travel times, azimuths, and slownesses for location. A mechanism for access to and distribution of corrections stored in databases and flat-files should be developed.

Need for wider participation

The experts are concerned with the unfortunate low level of participation in calibration activities in under-represented areas such as Africa. The IDC and concerned states may wish to engage in programs to encourage participation in such areas. Such activities might include professional exchanges of personnel with groups actively engaged in calibration to promote exchange of data and expertise. In recognition of the importance of aftershock surveys in the generation of valuable reference events, other activities might include support of temporary aftershock recordings (instruments and personnel) and a clearing-house to collect aftershock data and maintain an open database of aftershock metadata that can be used for calibration and reference event collection.

Future work

The IDC contractors, U.S.-sponsored consortia and other research groups are expected to deliver to the IDC a variety of proposed SSSCs in the coming year. Evaluation and validation of these corrections will require substantial additional research study. The experts consider that merging SSSCs from different study groups with different methodologies in an operational system presents a significant challenge. It is recommended that the IDC begin planning for such a continuing research program.

Encouraging results were presented for depth phase detection and identification. Methods for confident detection and identification of depth phases remain an important problem, and research in this area should continue. Focused discussion of selected topics such as depth estimation in the full assembly of experts is encouraged.

The experts consider that investigation is needed into the possibility that analyst time picks (as well as automatic onset estimates) are late for low signal-to-noise ratio recordings. Such biases would result in different apparent baselines for regional and teleseismic phases. More generally, presentation and discussion of IDC analyst procedures and of the problems facing the analysts should be considered for the future.

Collection of a set of reference events will continue to be a priority with emphasis on precise hypocenters and origin times and a good geographic coverage. The reference events should be chosen so as to keep usage of surrogate (non-IMS) stations to a minimum. For clusters of events it is recommended that a few, well-constrained events be chosen (using the smallest confidence ellipse as a selection criterion). Reference events should be recorded regionally and should comprise a range of magnitudes.

These recommendations will be considered before the next meeting of the Experts Group.

F. Ringdal

6.2 Research in regional seismic monitoring

(Paper presented at the 24th Annual Seismic Research Review)

Abstract

This project represents a continuing effort aiming at three main topics: (a) to carry out research in regional monitoring of the European Arctic, (b) to apply experimental methods such as site-specific threshold monitoring to target areas of interest and assess the results and (c) to contribute to the global location calibration effort currently being undertaken by the Preparatory Commission (PrepCom) of the Comprehensive Nuclear Test-Ban-Treaty Organization's Working Group B in Vienna, Austria.

We have used data from the regional networks operated by NORSAR and the Kola Regional Seismological Centre (KRSC) to assess the seismicity and characteristics of regional phases of the European Arctic. An especially interesting recent seismic event, which has been analyzed in detail, occurred on Novaya Zemlya on 23 February 2002. This small event (magnitude about 3.0) is the first seismic event detected in or near Novaya Zemlya since the two Kara Sea events of 16 August 1997. The event was recorded with particularly high SNR by the International Monitoring System (IMS) arrays Spitsbergen and ARCES, and by the Amderma station (operated by KRSC) south of Novaya Zemlya. We have located the event at the eastern coast of Novaya Zemlya, approximately 100 km NE of the former nuclear test site. Our attempts to estimate the depth of this event proved inconclusive, and a depth of 0 could not be ruled out. We present comparisons of the recordings of this event to recordings of previous small events in the Novaya Zemlya region.

We have begun an effort to develop an optimized site-specific threshold monitoring system for the Lop Nor test site in China. Our aim is to calibrate all available high-quality seismic stations within regional distance, and supplement with the best IMS arrays at teleseismic distances. As a calibration data base, we have used several past nuclear explosions at the test site, combined with nearby, well-recorded earthquakes. Even though most events were recorded by only a few stations, this data set was sufficient to obtain a reasonable amplitude calibration for the purposes of this study.

Initial results show that, among the available stations, the IMS Makanchi array in Kazakhstan (at an epicentral distance of 6 degrees) is the most sensitive station for detecting events at Lop Nor, followed by some of the best teleseismic arrays, for example the NORES array in Norway. Combining the data by using the threshold monitoring technique, we have found that the Lop Nor site can be monitored down to a threshold close to m_b 3.2. This threshold is about 0.8 magnitude unit higher than the corresponding capability for the Novaya Zemlya test site, for which the highly sensitive arrays ARCES and Spitsbergen are both at a distance of only 10 degrees. We note that no stations inside China were selected for the Lop Nor study.

A workshop was held in Oslo, Norway, during 22-26 April 2002 in support of the global seismic event location calibration effort currently being undertaken by PrepCom's Working Group B in Vienna. The workshop, which was chaired by Dr. Frode Ringdal, was attended by 66 scientists from 12 countries and the Provisional Technical Secretariat of the CTBTO. The workshop was held jointly by the IDC Experts Groups on location calibration and event screening, and the results and recommendations were reported to Working Group B.

6.2.1 Objective

This work represents a continued effort in seismic monitoring, with emphasis on studying earthquakes and explosions in the Barents/Kara Sea region, which includes the Russian nuclear test site at Novaya Zemlya. The overall objective is to characterize the seismicity of this region, to investigate the detection and location capability of regional seismic networks and to study various methods for screening and identifying seismic events in order to improve monitoring of the Comprehensive Test Ban Treaty. Another objective is to apply advanced site-specific seismic monitoring methods to other sites of special interest, in particular known nuclear test sites. A third objective is to support the international effort to provide regional location calibration of the International Monitoring System.

6.2.2 Research Accomplished

Introduction

NORSAR and Kola Regional Seismological Centre (KRSC) of the Russian Academy of Sciences have for many years cooperated in the continuous monitoring of seismic events in North-West Russia and adjacent sea areas. The research has been based on data from a network of sensitive regional arrays which has been installed in northern Europe during the last decade in preparation for the CTBT monitoring network. This regional network, which comprises stations in Fennoscandia, Spitsbergen and NW Russia provides a detection capability for the Barents/Kara Sea region that is close to $m_b = 2.5$ (Ringdal, 1997).

The research carried out during this effort is documented in detail in several contributions contained in the NORSAR Semiannual Technical Summaries. In the present paper we will limit the discussions to some recent results of interest in the general context of regional monitoring of seismic events in the European Arctic, a presentation of an initial threshold monitoring study for the Lop Nor test site in China and a brief review the location calibration effort currently underway for the International Monitoring System (IMS).

Low-magnitude seismic events in or near Novaya Zemlya

We have updated our previous studies of low-magnitude events in the Novaya Zemlya region recorded by the NORSAR regional seismic network. Table 6.2.1 and Fig. 6.2.1 summarize the information on such events detected since 1980. In spite of the low threshold for detection, only 8 seismic events with estimated location outside the test site have been recorded during these more than 20 years. Furthermore, we have since 1992 applied the site-specific threshold monitoring network to the test site, and have thereby been able to confirm that no other seismic event of magnitude 2.5 or greater has occurred in this region since then.

An especially interesting recent seismic event, which has been analyzed in detail, occurred on Novaya Zemlya on 23 February 2002. This small event (magnitude about 3.0) is the first seismic event detected in or near Novaya Zemlya since the two Kara Sea events of 16 August 1997. The event was recorded with particularly high SNR by the International Monitoring System (IMS) arrays Spitsbergen (SPITS) and ARCES, and by the Amderma station (AMD), operated by KRSC, south of Novaya Zemlya. We have located the event at the eastern coast of Novaya Zemlya, approximately 100 km NE of the former nuclear test site.

For this recent event, as well as other events recorded by the regional network, we have frequently noted uncertainties in onset measurements amounting to 1-2 seconds. This is in fact a general problem, and is due partly to the low SNR for some phases, partly to the emergent nature of some signal recordings. We have conducted a study to assess the effects of such uncertainty on location and depth estimates, using a number of seismic events in the European Arctic (Novaya Zemlya, Kara Sea, Northern Norway, Kola Peninsula). For each event, and each detected phase, we selected up to three onset time picks, spanning the estimated uncertainty (typically +/- 1-2 seconds). We then relocated each event using all possible combinations of such time picks, and compiled all solutions except those which showed clear inconsistencies. In this way, we obtained a large number of locations and depths for each event, and made plots to indicate the distribution of both the epicenters and the estimated depths.

The results for the 23 February 2002 event near Novaya Zemlya are illustrated in Fig. 6.2.2. We note that the epicentral error area is similar to the 90% confidence ellipse in Fig. 6.2.1. The depth distribution is inconclusive, although most solutions have an estimated depth near 0. From the general study, we note that for all the analyzed events, except for one known earthquake in Northern Norway, a depth of zero cannot be ruled out. We consider that this should serve as a caution against using estimated depth as a screening criterion in this region. In particular, we note that depth estimation using regional velocity models depend very strongly on the assumed Vp/Vs ratio.

Waveforms for the 23 February 2002 event from a number of seismic stations at regional distances from Novaya Zemlya are shown in Fig. 6.2.3. The high signal-to-noise ratios indicates that this event is well above the detection threshold, especially for the Amderma, SPITS and ARCES stations. Note that by array beamforming, the SNR at ARCES and SPITS could be improved by more than 0.5 magnitude units. This again reconfirms the capability of this regional network to monitor seismic events at Novaya Zemlya down to a magnitude level of 2.0-2.5, depending on the actual background noise levels.

In the context of event screening, which is an important topic for the CTBT International Data Center, it is clear from these results that no screening should take place for a region with as low seismic activity as Novaya Zemlya. In fact, any seismic event in this region is of potential monitoring interest, and with a frquency of occurrence of magnitude 2.5 or larger at less than one event per year, the actual analysis work would be quite modest. Similarly, as noted by Ringdal et. al. (2000), the much larger geographical area of western Russia and the Barents Sea is also characterized by modest natural seismic activity, and could be exempted from event screening, at least at the current magnitude threshold of 3.5 for screening purposes.

Table 6.2.1. Seismic events in or near Novaya Zemlya (1980-2002) located outside the test site.

Date/time	Location	m_b	Comment
01.08.86/ 13.56.38	72.945 N, 56.549 E	4.3	Located by Marshall et.al. (1989)
31.12.92/ 09.29.24	73.600 N 55.200 E	2.7	Located by NORSAR
23.02.95/ 21.50.00	71.856 N, 55.685 E	2.5	Located by NORSAR
13.06.95/ 19.22.38	75.170 N, 56.740 E	3.5	Located by NORSAR
13.01.96/ 17.17.23	75.240 N, 56.660 E	2.4	Approximately co-located with preceding event
16.08.97/ 02.11.00	72.510 N, 57.550 E	3.5	Located by NORSAR
16.08.97/ 06.19.10	72.510 N, 57.550 E	2.6	Co-located with preceding event
23.02.02/ 01.21.14	74.047 N, 57.671 E	3.0	Located by NORSAR

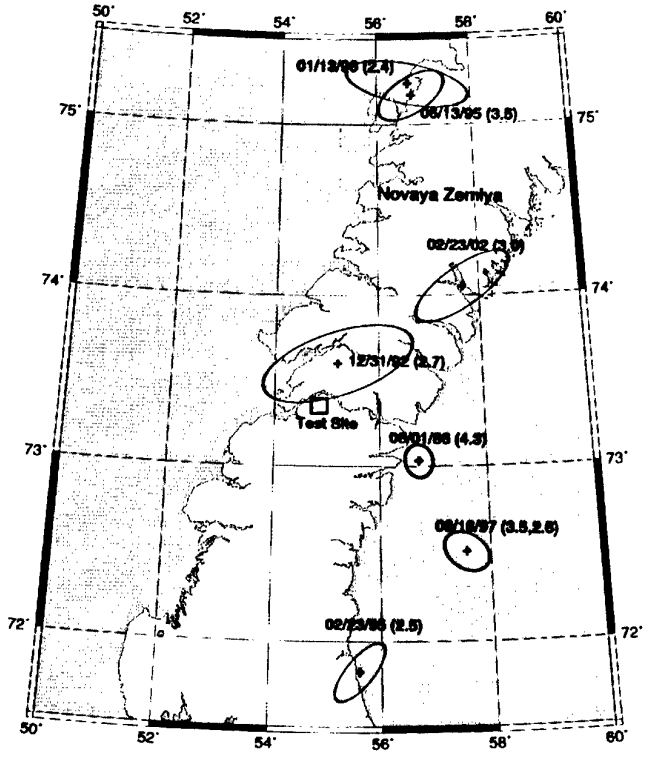

Fig. 6.2.1. Seismic events detected by the NORSAR regional array system in or near Novaya Zemlya during 1980-2002. Only events with estimated location outside the former nuclear test site are included. Estimated 90% error ellipses are indicated.

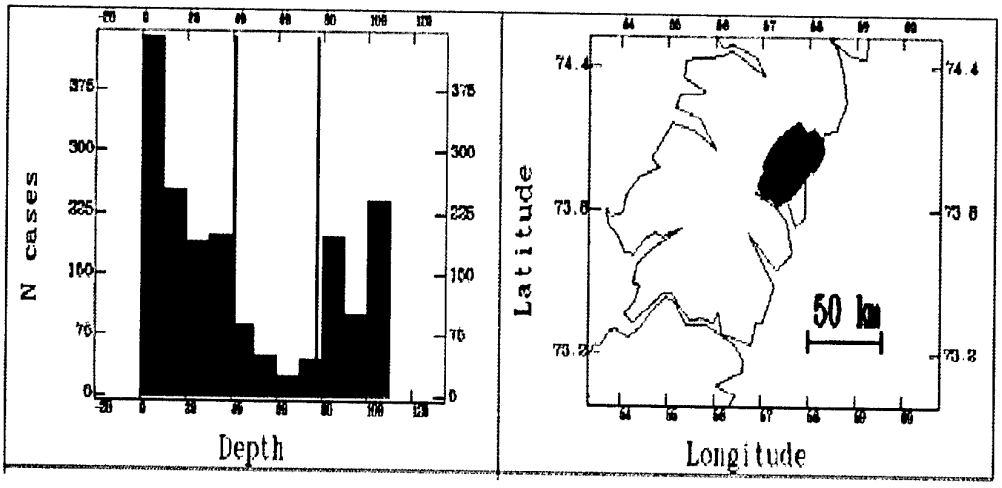

Fig. 6.2.2. Estimates of the location of the 23.02.2002 seismic event, as explained in the text. Note that the epicenters correspond well with the estimated uncertainty ellipse of Fig. 6.2.1, and that the depth of the event cannot be conclusively determined.

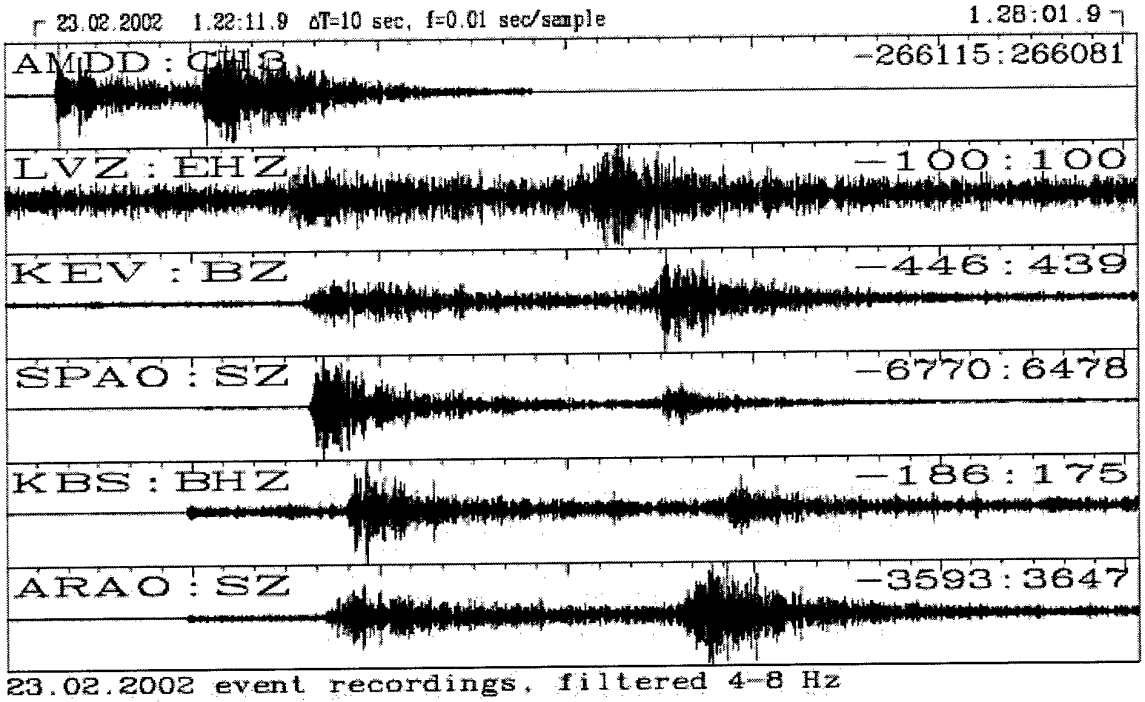

Fig. 6.2.3. Recorded SPZ waveforms for the 23.02.2002 seismic event. The data are filtered in the 4-8 Hz band. Note the high P-phase SNR in paricular at the Spitsbergen array (sensor SPA0) and the Amderma station (AMDD). Note also the relatively weak S-phase for the two stations at Spitsbergen (SPA0 and KBS).

Khibiny mines

We have continued our research on rockbursts and mining explosions in the mining areas of NW Russia, in particular the Khibiny Massif. Recently, seismic instrumentation has been installed inside the mines in the Khibiny Massif of the Kola peninsula in order to provide origin times of the seismic events as well as to contribute to additional validation of the location accuracy. Fig. 6.2.4 shows an example of recordings for a mining explosion of about magnitude 2.0.

We are also cooperating with Lawrence Livermore National Laboratory in a DOE-funded project to carry out more detailed studies of the characteristics of recordings from mining events in nothern Fennoscandia and Western Russia. That project includes the installation of additional seismometers along profiles in Norway, Finland and the Kola Peninsula, for recording over a period of one year.

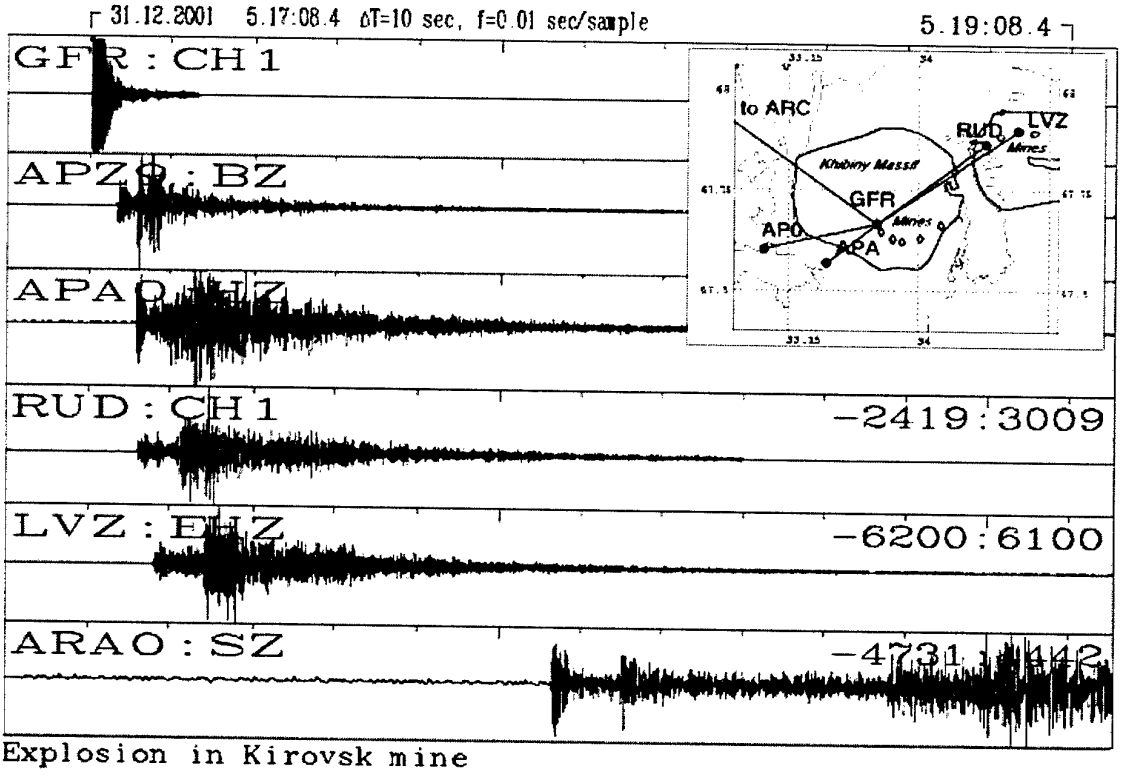

Fig. 6.2.4. Example of recordings of a mining explosion in the Khibiny Massif, Kola Peninsula, using a network of recently installed local stations as well as stations at regional distances.

Threshold monitoring of the Lop Nor, China test site

As part of the DoD Advanced Concept Demonstration, we have applied the Site-Specific Threshold Monitoring (SSTM) technique to the Lop Nor test site in China (Lindholm et. al., 2002). The emphasis has been on detection (and location) of small seismic events with mb < 4.0, and the purpose is to evaluate the SSTM method as a potential monitoring tool for this site. In contrast to most previous case studies, which have been based on recordings by seismic arrays at regional distances, we have in this study applied a combination of 3-component stations and arrays, at both regional and teleseismic ranges.

Our efforts so far, as reported in this contribution, comprises mainly a study of available seismic stations, selection of those stations which are most sensitive to seismic events in the Lop Nor general area, and tuning of the signal parameters of these stations so as to prepare processing recipes for the application of the threshold monitoring tool.

Development of processing recipes

For the successful implementation of SSTM, beams filtered in optimal frequency bands must be steered from the individual arrays towards the Lop Nor test site, and amplitude calibration constants developed from older events are applied to facilitate the calculation of continuous

magnitude thresholds for the site. For single (or 3-component) stations, the vertical component is filtered in the optimal frequency band.

For the purposes of this study, 23 single stations and arrays were initially chosen as shown in Fig. 6.2.5. For each of the stations data were collected from known nuclear tests at Lop Nor, and supplemented with data for low-magnitude earhquakes near the test site. We note that for most stations only a few data sets with explosions were available for the calibration.

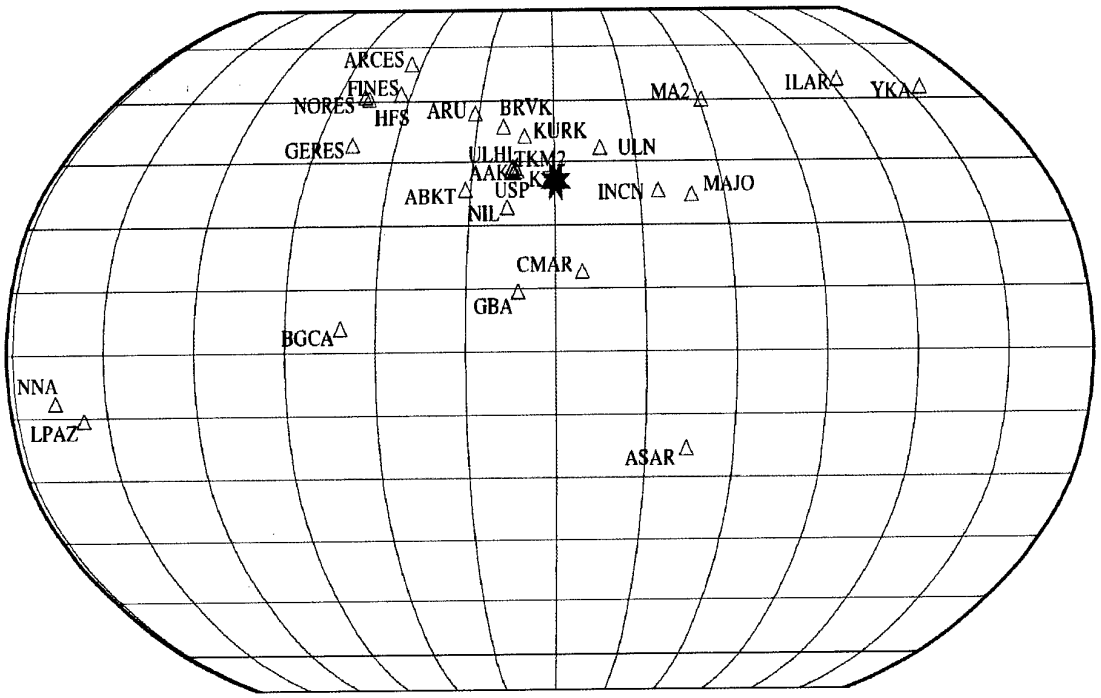

Fig. 6.2.5. Network selected for threshold monitoring of the Lop Nor, China test site. The test site is marked with a star symbol.

6.2.3 Preliminary Results

Two performance tests were carried out. First, data for one day (September 10, 2001) was collected, and in these data the recordings of 4 explosions were scaled and embedded at some (but not all of the) stations. The explosions were scaled to magnitude 3.5 and 3.0, so that a total of 8 embedded explosions were included. Secondly, a 10 day test period with data from August 2 through 11, 2001 was selected and data were collected for all available stations in our network. Fig. 6.2.6 shows examples of network results of these two performance tests.

From these tests the following preliminary observations can be stated:

- Out of the eight embedded explosions on day 253 six were detected automatically on the threshold trace, and the remaining two could be clearly seen on the trace, even if the automatic detector did not trigger.
- The quiet day (214) did not have any events flagged.

- On day 217 the SSTM method triggered on two large teleseismic events.
- The network threshold is close to or better than 3.0 (based on both arrays and single stations). The "trigger level" (shown as a continuous, smooth line in Fig. 6.2.6) is at magnitude 3.2 or lower.
- In a monitoring situation, all peaks exceeding the threshold could be analyzed. The maximum number of such peaks during one day was 10-15 for the days processed. If such peaks were analyzed, all of the scaled events on day 2001-253 would have been found.

The above observations should be evaluated under the perspective that the calibration is a preliminary one, where the majority of the stations could only be calibrated with one or two events/explosions, and where only some of the calibrated stations were included in the performance test. Furthermore, the day with embedded events did not include embedded data for all the stations, and this did reduce the performance of the threshold monitoring.

In the paper by Lindholm et. al. (2002), there is also some discussion of the relative performance of individual stations in the network. The SSTM threshold traces for single stations and arrays can in fact be used to assess this performance. We have observed that the arrays generally have thresholds between magnitude 3.2 and 3.8, and that the single stations vary considerably, from about 3.5 for the best (closest) stations to almost 4.5 for some of the lower performing stations. Some stations in the data set feature frequent data problems.

As the IMS system is further developed, there is a clear potential for imrovement in the performance illustrated above. For example, the sensitive array in Makanchi, Kazakhstan, was not available to us for the test period in August/September 2001. Studies of the performance of this array has indicated that it has a superior capability for detecting events at Lop Nor compared to the other stations in the network, and therefore would contribute to significantly improved thresholds, once included.

We also note that the current study has been done without including any Chinese IMS stations in our experimental network. Including such stations would no doubt contribute to improved thresholds, but there are other considerations that may make it useful to evaluate how the test site can be monitored using only station outside the country.

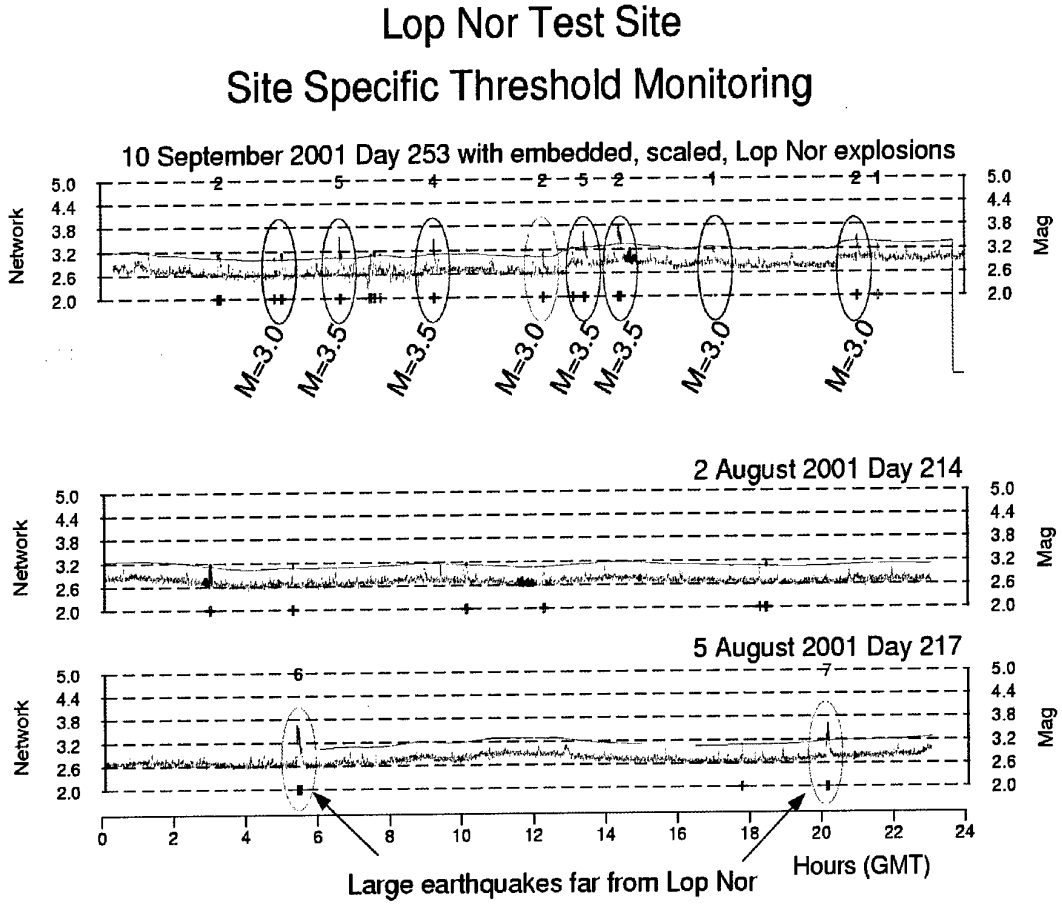

Fig. 6.2.6. Threshold monitoring network traces from three different days. The upper trace is from day 253 with eight embedded Lop Nor explosion recordings scaled to magnitudes 3.0 and 3.5. The ellipses indicate the times of the embedded explosions. For six of the eight embedded explosions the SSTM automatic analysis picked the events, while two events (No. 1 and No. 7) were not picked. The lower traces are from days 214 and 217. Day 214 is quiet with no detections, while day 217 show two detections resulting from "interference" by large earthquakes (located far from Lop Nor). The continuous, smooth line above each threshold trace is an estimated "trigger level" for identifying significant peaks on the threshold trace.

6.2.4 Location Calibration

Oslo Workshop on location calibration

A workshop was held in Oslo, Norway during 22-26 April 2002 in support of the global seismic event location calibration effort currently being undertaken by Working Group B of the CTBTO Preparatory Commission in Vienna, Austria. Dr. Frode Ringdal chaired the meeting, which was attended by 66 experts from 12 countries and the Provisional Technical Secretariat of the CTBTO The recommendations from this workshop have been provided in the paper CTBT/WGB/TL-2/70, issued by Working Group B of the CTBTO Preparatory Commission.

6.2.5 Conclusions and Recommendations

The analysis of the 23 February 2002 Novaya Zemlya seismic event has reconfirmed our previous estimates of the detection and location capability of the regional network in northern Europe. This experimental network operation will continue, and will be used to evaluate and supplement the IMS network in this region. Further research is required in regional event identification criteria, especially depth estimation. In the case of depth estimates, a detailed study of the Vp/Vs ratio as well as its uncertainty limits should be undertaken.

Our initial performance tests of Site-Specific Threshold Monitoring for the Lop Nor test site were successful. We recommend that these initial tests be followed by more detailed studies, where in particular the calibration parameters should be more firmly established. It is also of interest to include additional sensitive IMS arrays in the monitoring network, and evaluate the ensuing improvement in capability.

The location calibration effort will continue to be an important part of our work. The recommendations provided in the paper CTBT/WGB/TL-2/70 should be followed up by the international community, and the progress of this work will be reviewed in a planned workshop in Oslo during 4-9 May 2003.

F. Ringdal
T. Kværna
E. Kremenetskaya
V. Asming
S. Mykkeltveit
C. Lindholm
J. Schweitzer

References

Lindholm, C., T. Kvœrna and J. Schweitzer (2002): Site-Specific Threshold Monitoring (SSTM) applied to the Lop Nor test site, *Semiannual Technical Summary, 1 July 2001 - 31 December 2001*, NORSAR Sci. Rep. 1-2002, Norway.

Marshall, P.D., R.C. Stewart and R.C. Lilwall (1989). The seismic disturbance on 1986 August 1 near Novaya Zemlya: a source of concern? *Geophys. J.* 98, 565-573.

Ringdal, F. (1997): Study of low-magnitude seismic events near the Novaya Zemlya nuclear test site, *Bull. Seism. Soc. Am. 87 No. 6,* 1563-1575.

Ringdal, F., E.O. Kremenetskaya, V.E. Asming, T. Kvœrna and J. Schweitzer (2000): Research in Regional Seismic Monitoring, *Paper presented at the 22nd Annual Sesimic Reseach Symposium,* New Orleans.

6.3 Design Study for the Refurbishment of the SPITS Array (AS 72)

6.3.1 Introduction

The SPITS array is located on Jansonhaugen in Adventdalen on Spitsbergen, Svalbard, approximately 15 km east-southeast of Longyearbyen. Jansonhaugen is a hill in the middle of a valley (Adventdalen), and the largest part of the array is deployed on the plateau of this hill. The rocks at the site are of Cretaceous age, partly covered by thin top soil or by moraine deposits of variable depth. The twelve sensors of the array are placed at the bottom of nine 6 m deep cased boreholes. The bottom of the boreholes are either in Cretaceous rock or in moraine material in stable permafrost conditions (temperature approximately -5°C all year around at a depth of 6 m), such that there is no melting/freezing taking place at this depth. The 9 array sites are deployed in two rings around a center element (see Fig. 6.3.1). The radii of the rings are approximately 250 m for the A-ring and 500 m for the B-ring. More detailed descriptions of the array and an initial data processing were presented by Mykkeltveit et al. (1992) and Fyen and Ringdal (1993).

As of summer 2002 the SPITS array consists of the following equipment:

- 9 vertical component short-period seismometers, Guralp CMG-3V-borehole, placed at the bottom of 6 m deep cased boreholes.
- 1 three component broad-band seismometer of type Guralp CMG-3T-borehole, also placed at the bottom of the borehole at array site SPB4. This instrument has, however, been out of operation since March 2001.
- 2 Nanometrics RD-6 digitizers, 16-bit resolution, 40 Hz sampling rate.

The transfer function of the SPITS array is shown in Fig. 6.3.2. The yellow dashed circle indicates the highest wavenumber that is likely to be considered for any signals at SPITS, i.e., high frequency Rg-phases (apparent velocity: 1.3 km/s, dominant frequency: 6 Hz). As seen from Fig. 6.3.2, the array exhibits significant sidelobes that are likely to influence the data processing of Rg-phases due to aliasing.

6.3.2 Problematic Signals

We will in this section show some typical examples of signals that are difficult to process properly with the current SPITS configuration. The problems are related to both signal detection, and the estimation of the slowness vector (i.e., apparent velocity and backazimuth) of the detected phases.

The Spitsbergen array (SPITS) often reports a large number of detections (Schweitzer, 1998), which can reach thousands per day. A detailed analysis shows that the majority of these detections are real seismic signals caused by small sources located at close distances. The numerous local events (see e.g., Fig. 6.3.3) typically show P onsets, no well defined S onsets, and dominant Rg onsets. Investigating the mean backazimuths of these Rg phases one can see a strong correlation with the direction to the coal-mine area at about 8 km distance and directions to nearby glaciers (shortest distance about 3 km), for more details see Schweitzer (1998).

At the SPITS array we also observe a relatively large number of high SNR P detections from regional events without any corresponding detection of an S phase. Fig. 6.3.4 shows seismograms observed at the three-component site SPB4 from an earthquake located at the Knipovich

Ridge west of Svalbard at an epicentral distance of about 3°. In addition to the original horizontal components, the rotated radial and transverse components are shown (at the bottom). The S phase has a low SNR and the signal is particularly weak in SV energy, which should be visible on the radial and vertical components. The S phase can, however, be observed on the transverse component SPB4_bt.

Due to the presence of low-velocity materials in the uppermost crust, Sn arrivals from regional events at larger distances also show the largest amplitudes and SNR on the radial or transverse components. As an example, we show in Fig. 6.3.5 SPITS recordings of the Kara Sea event on 16 August 1997. The epicentral distance to this event was 11.6°. The upper trace shows the vertical-component array beam steered with the S-phase apparent velocity of 4.0 km/s. The three lower traces show the vertical, radial and transverse components for the three-component sensor SPB4. All traces of Fig. 6.3.5 are bandpass filtered between 4 and 8 Hz. Notice the improved SNR on the radial and transverse components as compared to the vertical-component S-beam.

6.3.3 Spatial aliasing of high frequency Rg-phases

As seen from Fig. 6.3.2, the transfer function of the SPITS array exhibits significant side lobes that are likely to influence the data processing of the numerous Rg-phases, all having low apparent velocities. The low apparent velocities of the Rg phases are caused by the low seismic velocities of the Cretaceous sediments.

Schweitzer (1998) has introduced a rather complex signal processing scheme to reduce aliasing problems when processing the Rg onsets. There are, however, still cases when Rg phases are mis-identified as P-onsets, and vice versa. In such cases the F-K analysis picks the energy maximum on a sidelobe, in particular for onsets with low SNR.

The numerous local events often contain a mixture of Pg, Sg, and Rg within a time window of 2-5 seconds (see Fig. 6.3.3). In order to estimate the slowness and backazimuth of such onsets, short time windows are needed for the F-K analysis. With the current SPITS configuration we will need at least a 2 s long time window for processing of the low-velocity Rg-phases. For these local events an automatically positioned 2 s long time window often contains all types of phases (Pg, Sg, Rg).

In order to remove the side lobes of the array transfer function and to give us the possibility to analyze the low-velocity onsets in shorter time windows, we propose to install three additional sensors close to the center element SPA0. The geometry of an array cannot be inverted from a given transfer function. It must be found by a trial-and-error search trough different geometries. Therefore, to find a position for the three new sensors, which gives the best suppression of the side lobes in Fig. 6.3.2, we applied a systematic search by adding one station after the other at different locations and calculating the array-transfer function (see e.g., Schweitzer et al., 2002). The searched area was a square of 600*600 m centered at the central site SPA0. In this area all possible site locations on a 5*5 m grid were tested as locations for the new array sensors; the criterion for optimizing the transfer function was to minimize this function in the slowness range between the main lobe and the yellow broken line of Fig. 6.3.2. The best solution found is shown in Fig. 6.3.6 and the location of the three newly proposed sensors SPE1, SPE2, and SPE3 to reach this solution is seen on Fig. 6.3.7. Notice the reduction of the side lobes as compared to Fig. 6.3.2.

6.3.4 Low resolution of the F-K estimates

As seen from Fig. 6.3.6, the transfer function of the SPITS array, including the three new sites in the center, has a relatively wide main lobe. This feature limits the resolution capability of the array, which is critical for classifying signals as local, regional or teleseismic based on the apparent velocity estimates from the F-K analysis. In addition, the backazimuth estimates from the F-K analysis have large uncertainties.

In order to narrow the main lobe we have to extend the aperture of the array. Based on experience with other regional arrays in Fennoscandia (FINES, ARCES and NORES) we propose to install new instruments in a C-ring like configuration. The plateau on the hill on which SPITS is located is surrounded by steep slopes and rivers both to the north and south, and the array can therefore not be extended in these directions. From analysis of topography maps, satellite photos, and from inspections during visits to the SPITS array we propose a new configuration as shown in Fig. 6.3.7: three C-ring sites towards east (SPC1, SPC2, SPC3) and three C-ring sites towards west-southwest (SPC4, SPC5, SPC6). The exact positions of these additional six new C-ring sites were also found by a systematic trial-and-error search on a 10*10 m grid. The array-transfer function, for which the main lobe became the smallest, was chosen as the best one.

The transfer function of the new configuration of the SPITS array, i.e. the original nine sites extended by three sites in the center (SPE1, SPE2, SPE3) and six sites in the C-ring (SPC1, SPC2, SPC3,SPC4, SPC5, SPC6) is shown in Fig. 6.3.8. Notice that the main lobe has become narrower as compared to Figs. 6.6 and 6.2, and that it is elongated in the north-south direction due to the non-circular array geometry. The relative coordinates of all sites with respect to the center site SPA0 are listed in 6.4.1.

6.3.5 Detection and F-K analysis of S-phases

As shown in Figs. 6.4 and 6.5, regional S-phases at SPITS in general have the largest amplitudes and SNR on the horizontal components. The current SPITS configuration has only one three-component instrument at site SPB4. This instrument has, however, been quite unstable in operation. In order to detect S-phases more efficiently, more three component instruments are needed. While one three-component instrument already improves the detection capability of S-phases (see Figs. 6.4 and 6.5), the subsequent F-K analysis would suffer from low SNR as the vertical component sensors have to be used for this purpose.

With more three-component sites, the detection capability of S-phases can be further improved by creating S-velocity beams from the rotated radial and transverse components, as now done for ARCES and NORES (Kværna et al., 1999). In addition, the F-K analysis can now be run on the horizontal components, as e.g., demonstrated by Schweitzer (1994).

As a first attempt, we calculate the array response of 4 three-component sensors, which is a minimum number of traces for running an F-K analysis. After testing several combinations of the SPITS geometry, our best result was obtained by using SPA1, SPC3, SPC4 and the already existing three-component sensor SPB4 (see Fig. 6.3.7). With only four sensors we were unable to remove all side lobes from the S-phase wavenumber range, but we can obtain a relatively narrow main lobe. However, with four sensors only, we will lose the capability to run an F-K analysis on the horizontal components in the case that one of the horizontal sensors is down. The best "realistic" three-component configuration was obtained by having three-component

instruments at all five B-ring sites and at SPA0 in the center. Such a configuration can improve the SNR for S onsets by a factor of about 2.5; the corresponding transfer function of Fig. 6.3.9 shows no side lobes within the wavenumber range for regional Sn phases (i.e., between the red and the yellow rings).

6.3.6 Sampling rate, high-frequency spectra, and 24 bits digitizers

With the current sampling rate of 40 Hz at SPITS, we can conduct array processing for signal frequencies up to 16-20 Hz. For higher frequencies the coherency among the signals at the different sensors is heavily reduced such that beamforming and F-K analysis have little effect. Therefore, we see no need to increase the general sampling rate for SPITS.

However, it is well known that we at SPITS observe high signal frequencies (e.g., Bowers et al., 2001). Therefore we suggest that one of the three-component sensors (e.g., SPA0) is sampled at 120 Hz, or alternatively 80 Hz.

In order to meet the standard of the CTBT International Monitoring System an upgrade of the digitizers to 24 bit words is needed.

6.3.7 Conclusion

In conclusion, the following extensions are suggested for the SPITS array to increase its detection and monitoring capabilities:

- Three new sites in the center of the array (SPE1, SPE2, SPE3) equipped with vertical component instruments.
- Six new sites in a C-ring equipped with vertical component instruments.
- Add 5 three-component instruments to SPA1, SPB1, SPB2, SPB3 and SPB5. The existing broad-band three-component instrument at SPB4 can be used for array processing after digitally reshaping the response.
- Install 24 bits digitizer for all channels.
- Sample one of the three-component sensors at 120 Hz, e.g., SPA0.

Johannes Schweitzer
Tormod Kværna

References

Bowers, D., P. D. Marshall and A. Douglas (2001): The level of deterrence provided by data from the SPITS seismometer array to possible violations of the Comprehensive Test Ban in the Novaya Zemlya region. *Geophys. J. Int.*, 146, 425-438.

Fyen, J and F. Ringdal (1993): Initial processing results for the Spitsbergen small-aperture array. Semiannual Technical Summary, 1 October 1992 - 31 March 1993, NORSAR Scientific Report 2-92/93, 119-131.

Kværna, T., J. Schweitzer, L. Taylor and F. Ringdal (1999): Monitoring of the European Arctic Using Regional Generalized Beamforming. Semiannual Technical Summary, 1 October 1998 - 31 March 1999, NORSAR Scientific Report 2-98/99, 78-94.

Mykkeltveit, S., A. Dahle, J. Fyen, T. Kværna, P.W. Larsen, R. Paulsen, F. Ringdal and I. Kuzmin (1992): Extensions of the northern Europe regional array network -- new small-aperture arrays at Apatity, Russia, and on the Arctic Island of Spitsbergen. Semiannual Technical Summary, 1 April - 30 September 1992, NORSAR Scientific Report 1-92/93, 58-71.

Schweitzer J. (1994): Some improvements of the detector / SigPro-system at NORSAR. Semiannual Technical Summary, 1 October 1993 - 31 March 1994, NORSAR Scientific Report 2-93/94, 128-139.

Schweitzer J. (1998): Tuning the automatic data processing for the Spitsbergen array (SPITS). Semiannual Technical Summary, 1 April - 30 September 1998, NORSAR Scientific Report 1-98/99, 110-125.

Schweitzer, J., J. Fyen, S. Mykkeltveit and T. Kværna (2002): Seismic Arrays. **In**: P. Bormann (ed.), 2002: *New Manual of Seismological Observatory Practice*, Chapter 9, 52 pp. (in press).

Table 6.3.1. The relative coordinates of the old and newly proposed sites of the SPITS array with respect to the central element SPA0, which is located at 78.1777° N and 16.36998° E.

Site	X (E-W) [m]	Y (N-S) [m]
SPA0	0	0
SPA1	125	227
SPA2	150	-202
SPA3	-255	-44
SPB1	470	228
SPB2	333	-381
SPB3	-255	-451
SPB4	-501	123
SPB5	-49	513
SPE1	150	-30
SPE2	-30	-160
SPE3	-230	-240
SPC1	1030	500
SPC2	1100	-200
SPC3	745	-240
SPC4	-800	-835
SPC5	-710	-460
SPC6	-1140	-40

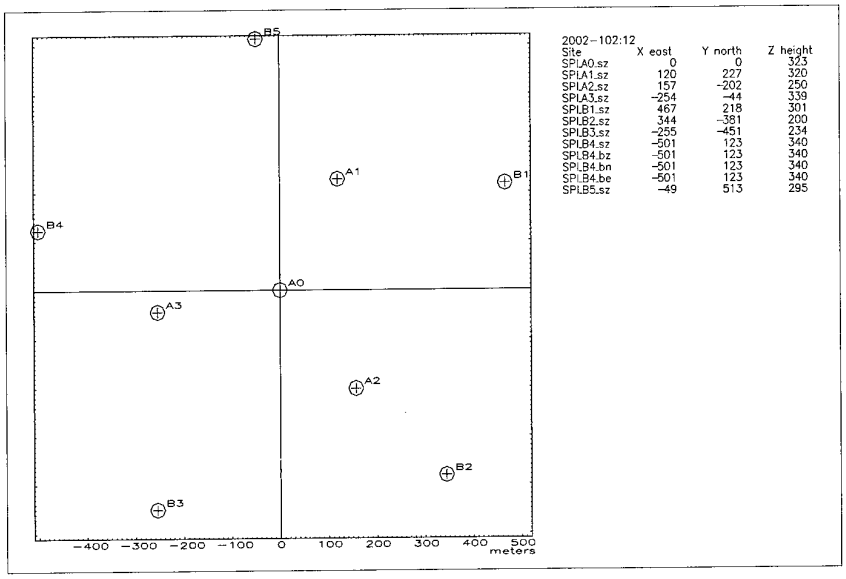

Fig. 6.3.1. Current geometry of the SPITS array.

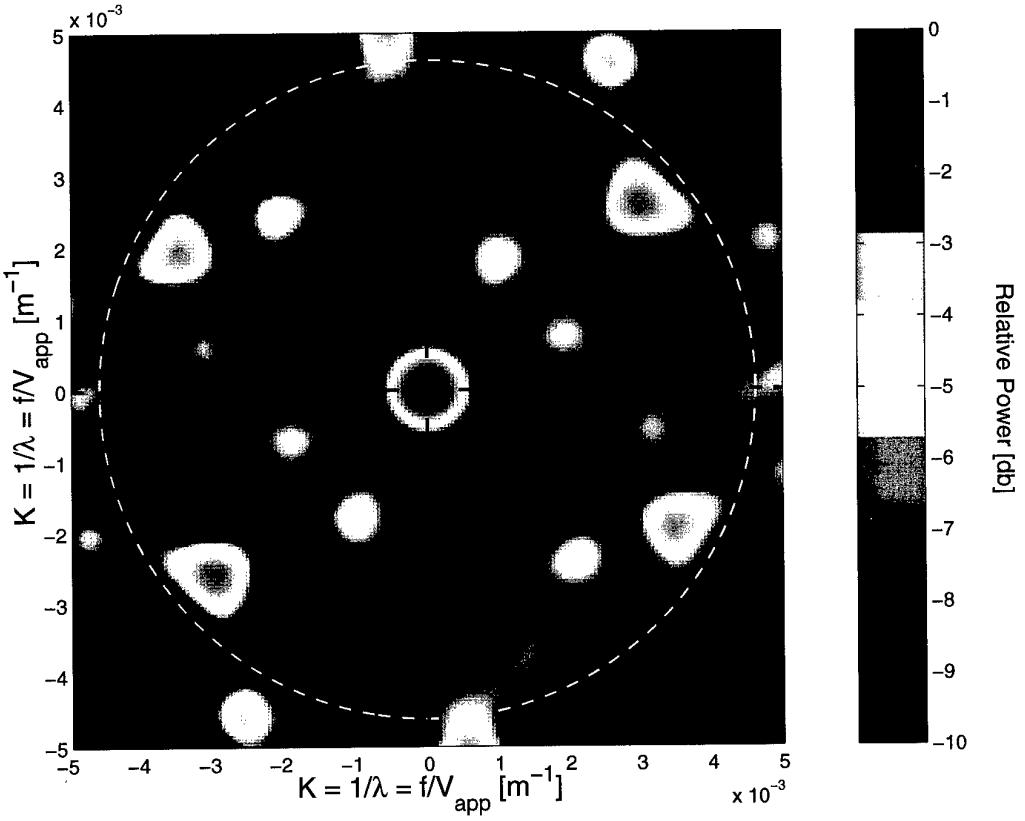

Fig. 6.3.2. The transfer function of the current SPITS array (vertical components).

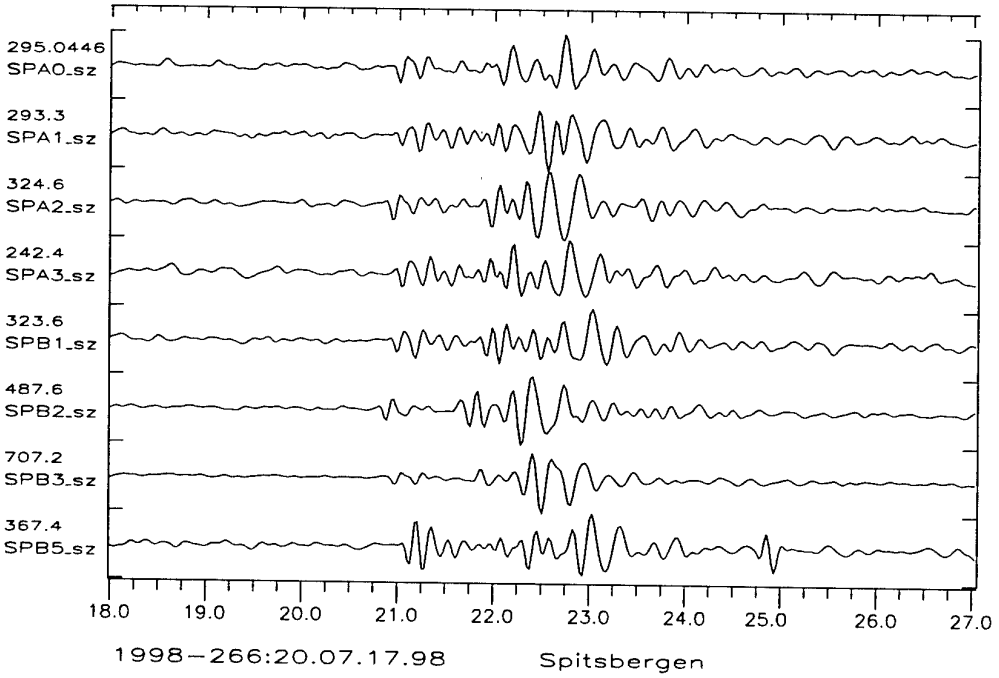

Fig. 6.3.3. *Example of a local event observed at SPITS, located in the glacier Gløttfjellbreen (backazimuth = 141°, D = 4 km). The traces are the band pass filtered (3-8 Hz) vertical-component seismograms.*

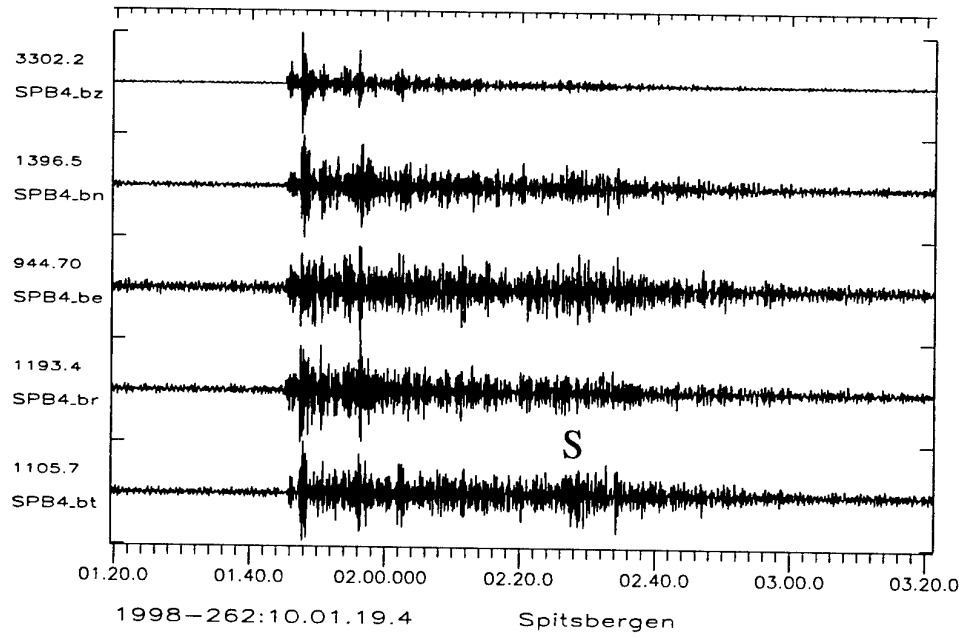

Fig. 6.3.4. *Filtered seismograms (3-6 Hz) at the three-component site SPB4 from an earthquake located at the Knipovich Ridge northwest of Svalbard at an epicentral distance of about 3°. The rotated radial and transverse components are shown (at the bottom).*

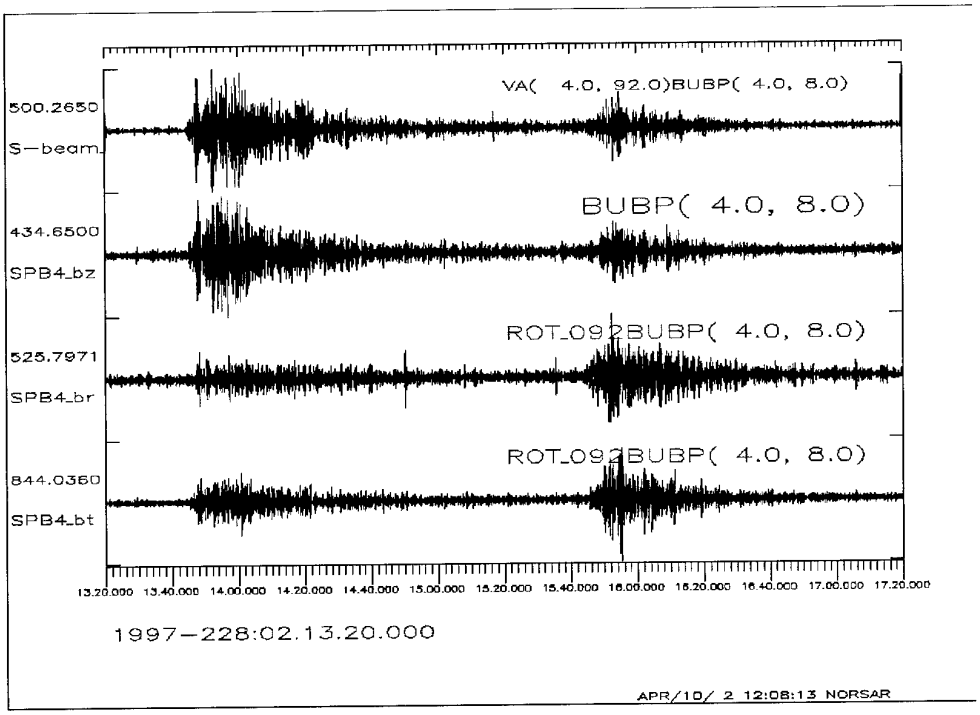

Fig. 6.3.5. SPITS observations of the Kara Sea event on 16. August 1997. The upper trace shows the vertical-component array beam steered with the S-phase apparent velocity of 4.0 km/s. The three lower traces show the vertical, radial and transverse components for the three-component sensor SPB4. All traces are bandpass filtered between 4 and 8 Hz.

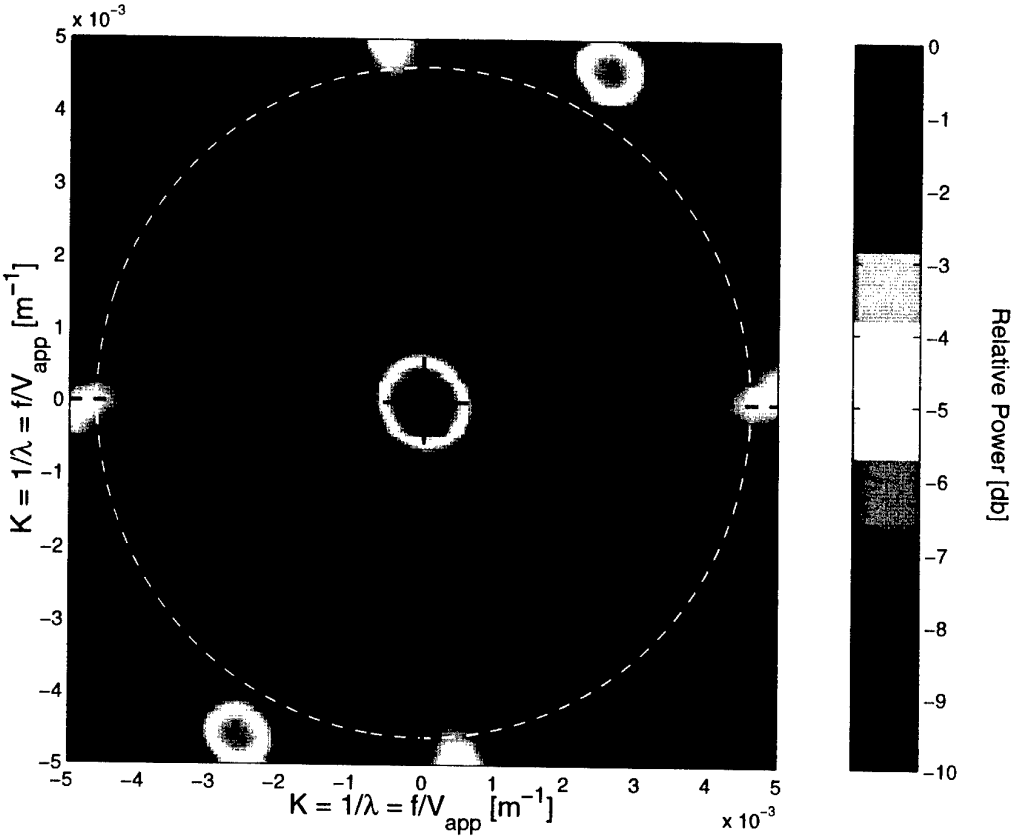

Fig. 6.3.6. *The transfer function of the SPITS array extended by three sites (SPE1, SPE2, SPE3) in the center, note the side-lobe reduction inside the yellow ring with respect to Fig. 6.3.2.*

Fig. 6.3.7. The suggested extended configuration of the SPITS array plotted on a satellite photo of Jansonhaugen. The original configuration is extended by three sites (E1, E2, E3) in the center and six sites in the C-ring (C1, C2, C3, C4, C5, C6). Green symbols: sites unchanged from the old configuration. White circles: new sites equipped with vertical component sensors. Green triangles: Sites of the old configuration upgraded to three-component sensors. High-frequency sensor: the three-component instrument at A0 should be sampled at e.g., 120 Hz.

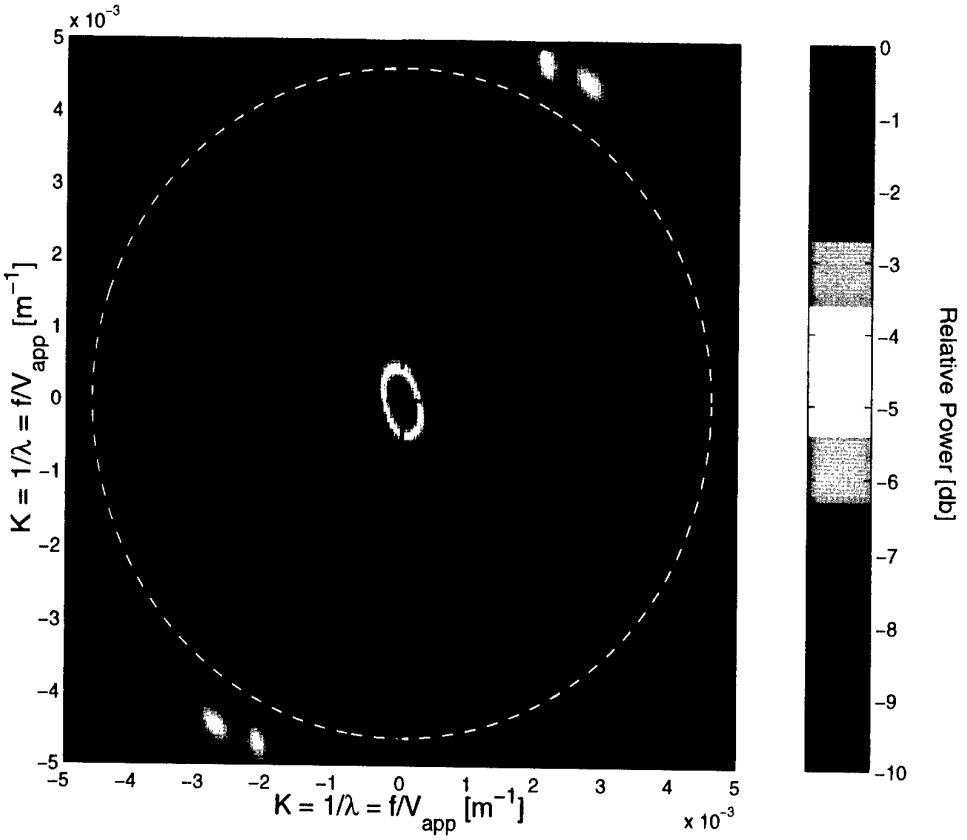

Fig. 6.3.8. *The transfer function of the new SPITS array configuration for vertical sensors at all sites as shown on satellite picture in Fig. 6.3.7.*

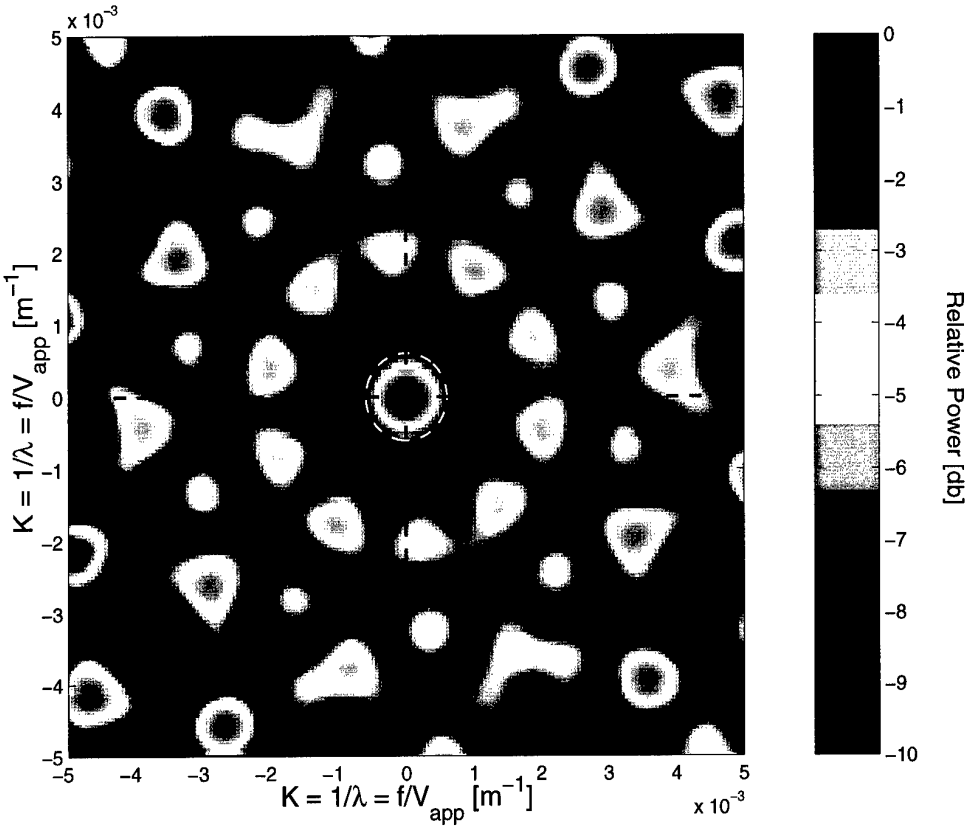

Fig. 6.3.9. *The transfer function of the 6 SPITS array sites SPA0, SPB1, SPB2, SPB3, SPB4 and SPB5. The yellow and red circles represent the wavenumber range for regional Sn phases.*

6.4 Analysis of cavity-decoupled chemical explosions

This research is conducted under Defense Threat Reduction Agency contract no. 01-01-C-0069

Introduction

Cavity decoupling has long been acknowledged to be the most effective means of evading detection of an underground nuclear test, and is thus one of the most probable scenarios for a violation of the Comprehensive Nuclear Test Ban Treaty (CTBT). NORSAR has recorded and analysed seismic data from a series of underground cavity explosions in the Kopparberg region of Sweden, with the aim of quantitatively predicting the decoupling effect of underground cavities of known dimensions and shape.

A database of seismic waveform data has been compiled for seven such cavity explosions. A series of four explosions has taken place between December 2000 and June 2002 using varying quantities and compositions of explosives within a chamber of size 1000m^3 with an overburden of rock of approximately 100m. In addition, NORSAR also recorded a series of explosions between 1987 and 1989 which took place within smaller chambers on the same site. Only three factors differentiate these events; the quantity of explosive, the composition and arrangement of the explosives, and the size and configuration of the explosion chamber.

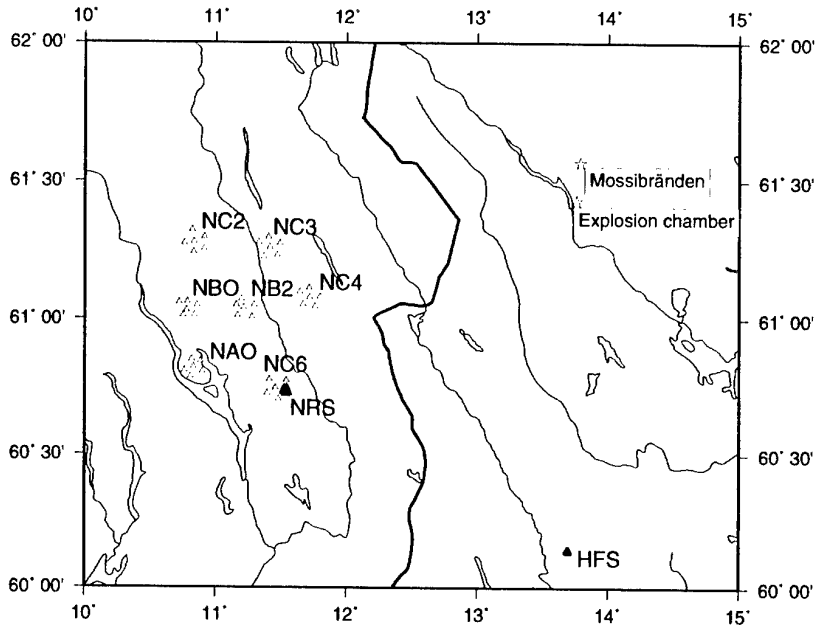

Fig. 6.4.1. The location of the explosion sites relative to the HFS and NRS arrays and the NORSAR sub-arrays. The red line is the Norway-Sweden national boundary.

The cavity explosion data has been complemented by records from a series of surface explosions at Mossibränden, a site approximately 15 km from the underground cavities. The distance between the surface and cavity explosions is small compared with the distance between the explosion sites and the NORSAR, NORES and Hagfors seismic arrays (see Fig. 6.4.1). This will largely eliminate path effects and allow a comparison of source properties.

Cavity decoupled explosions

The cavity explosions, which comprise two separate series of experiments, are listed in Table 6.4.1. The first six of these were recorded by the NORES array, which was unfortunately put out of action by lightning shortly before the June 2002 event; waveforms from the NRA0 instrument are displayed in Fig. 6.4.2. The signals resulting from the three events from 1987 and 1989 have far higher amplitudes than the later events, which probably reflects the differences in charge/cavity volume as displayed in Table 6.4.1. The signal from event 2001C150 (2500kg TNT in the 1000m^3 chamber) is indistinguishable from the noise without filtering of the data. The explosions were set off in chambers open to the access tunnels (unsealed explosions).

Table 6.4.1. Cavity decoupled explosions at the Älvdalen site. Origin times of the 1987-1989 events were estimated from arrival times at NORES. Origin times of the 2000-2002 events were determined from a station at the explosion site.

Origin ID	Explosion origin time	Explosion charge (kg)	Explosive	Chamber volume (m^3)[a]	Charge/ Chamber volume (kg/m^3)
1987C146	1987-146:10.47.38.2	5000	ANFO[b]	300	16.7
1987C259	1987-259:10.36.13.0	5000	ANFO	200	25.0
1989C263	1989-263:10.06.03.5	5000	ANFO	300	16.7
2000C348	2000-348:10.03.02.0	10000	TNT	1000	10.0
2001C150	2001-150:10.03.56.2	2500	TNT	1000	2.5
2001C186	2001-186:10.41.23.5	10000	TNT and ammunition shells	1000	10.0
2002C164	2002-164:08.59.25.1	10000	TNT / powder	1000	10.0

a. Not including access tunnel.
b. The ANFO explosive used in the 1987 and 1989 events had an explosion equivalent of 0.82 of TNT

In order to quantify the differences between these six events, we examine the power density spectra (PDS). For each component, three time windows were defined corresponding to the P arrival, the S arrival and pre-event noise. The P-window was defined beginning at the P-wave onset and ending 5 seconds later. The S-window consists of the 10 seconds immediately following the S-wave onset. A third 10 second window, ending 2 seconds before the P-wave onset, was defined to measure the background noise level.

For each event, the PDS was calculated for the three time windows for each vertical component trace. The PDS, averaged over all vertical component traces for the NORES array, is shown for the first six decoupled explosions in Fig. 6.4.3. In order to provide a common basis for compar-

ison, we have converted all spectra to the characteristics of the HFS response which, unlike the NORES array response, is flat to velocity over the bandpass.

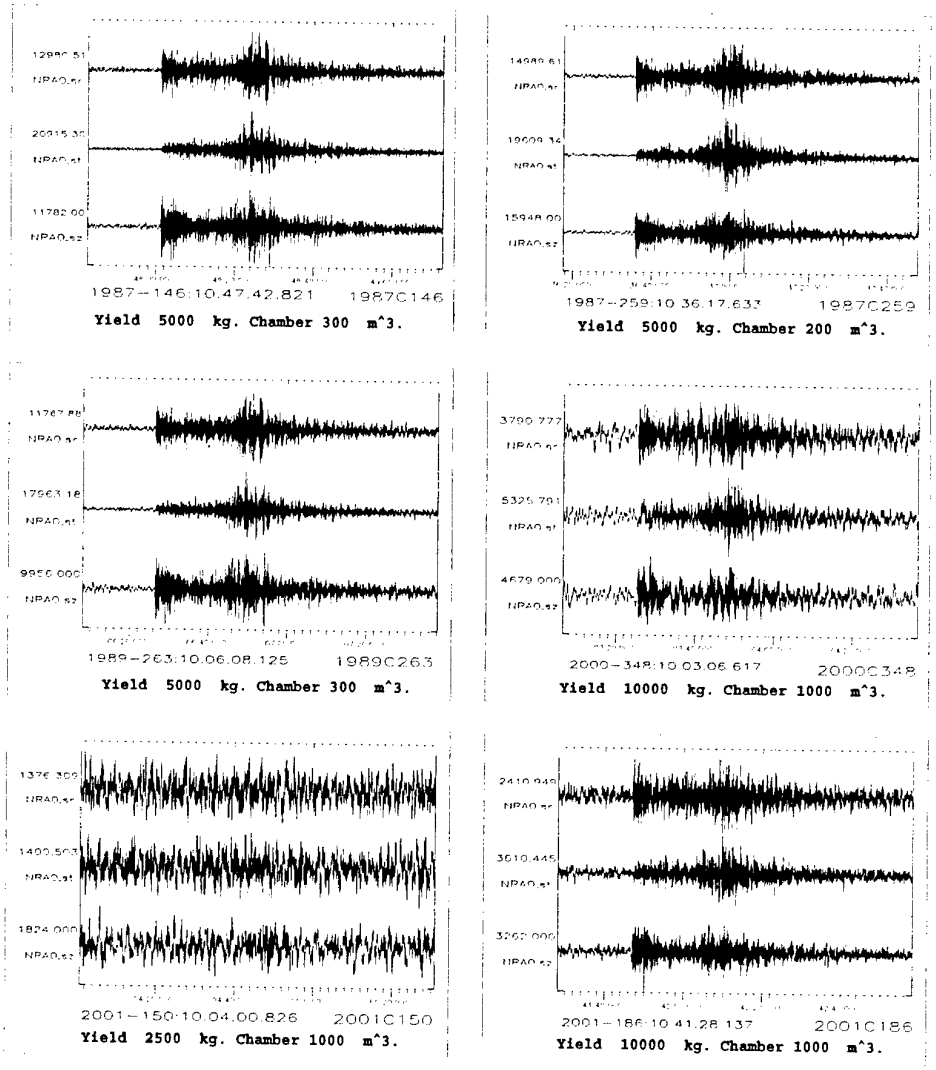

Fig. 6.4.2. *Unfiltered waveforms for the 6 decoupled explosions prior to June 2002 from the 3-component NRA0 instrument of the NORES array. North and East waveforms have been rotated into radial and transverse components. Maximum values of traces (counts) are indicated in red.*

The results shown in Fig. 6.4.3 clearly show the effect of substantially greater decoupling for the larger chamber. The spectra for events 1987C146 and 1987C263 show great similarity, which is to be expected given that both occured in the same chamber using the same quantity and type of explosives. Event 1987C259, which occured in the 200m^3 rather than the 300m^3 chamber, has a spectrum which is similar to the 1987C146 and 1987C263 spectra at high frequencies but which differs significantly in the 3 to 8 Hz frequency band. Events 2000C348 and 2001C186 both took place within the 1000m^3 chamber using the same yield of explosives. However, the PDS for event 2000C348 is greater than that for 2001C186 by an approximate

factor of 2 for all frequencies. The only difference between these two events was that pure TNT was used as the explosive for 2000C348 whereas TNT mixed with ammunition shells was used for event 2001C186.

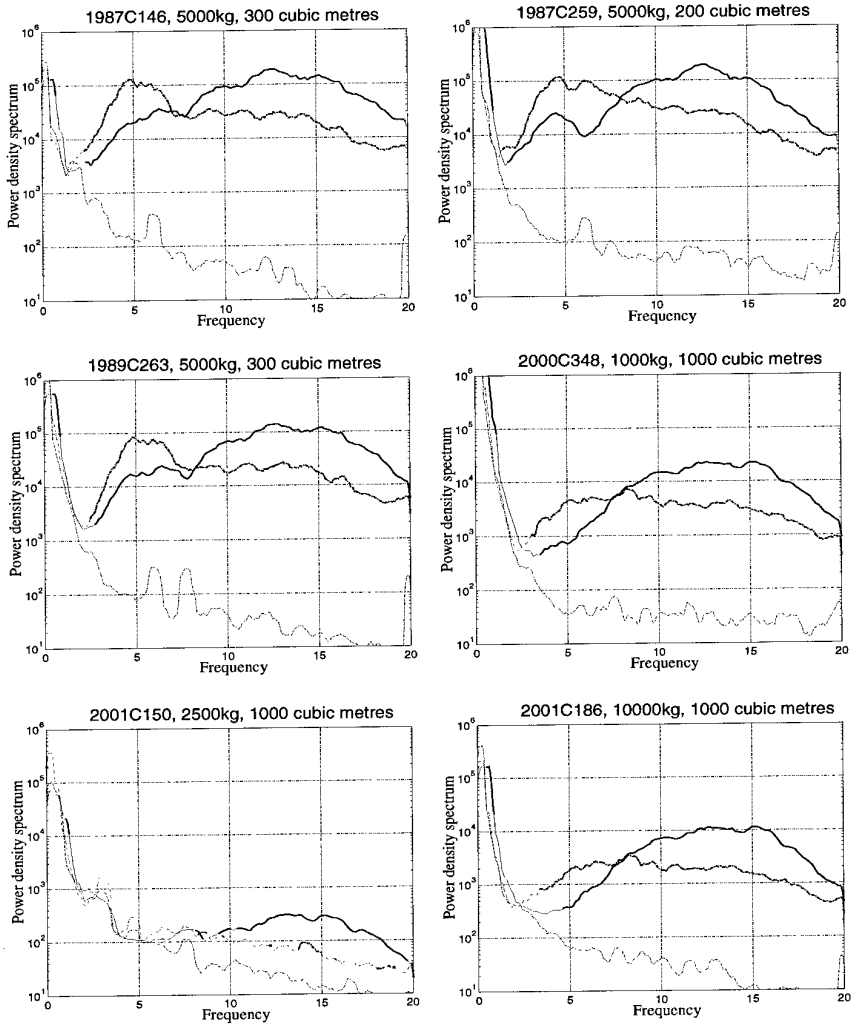

Fig. 6.4.3. *Power density spectra, averaged over all vertical component traces from the NORES array for six cavity explosions as indicated. Solid red lines indicate PDS for P-window (5 seconds following P), dashed blue lines indicate PDS for the S-window (10 seconds following S) and the dotted black line indicates PDS for the noise window (12 to 2 seconds before P). At frequencies for which the PDS for P or S window is less than 4.0 times that for the noise window, the signal spectrum is shown as a thin line.*

Using the average of vertical component traces from the NRS, NOA and HFS arrays, we compare the power density spectra from the P-arrival windows from all of the seven cavity explosions listed in 6.4.1. Performing a simple arithmetic mean on these spectra recorded at different locations is justified by the comparable source-receiver distances between the explosion sites and seismic arrays (see Fig. 6.4.1). Figure 6.4.4 demonstrates the greater PDS in the signal

resulting from explosions in the smaller chambers. The 10000 kg of explosives used for the 2002C164 event consisted of 6600 kg powder and 3400 kg TNT in shells.

All of the spectra in Fig. 6.4.4 exhibit low power at low frequencies, although the ratio of low-frequency power density to high-frequency power density is lower for the events within the 1000m^3 chamber, indicating a higher degree of decoupling. The signal to noise ratio for event 2001C150 was very low for frequencies below 10 Hz and a low-frequency power to high-frequency power ratio cannot be estimated.

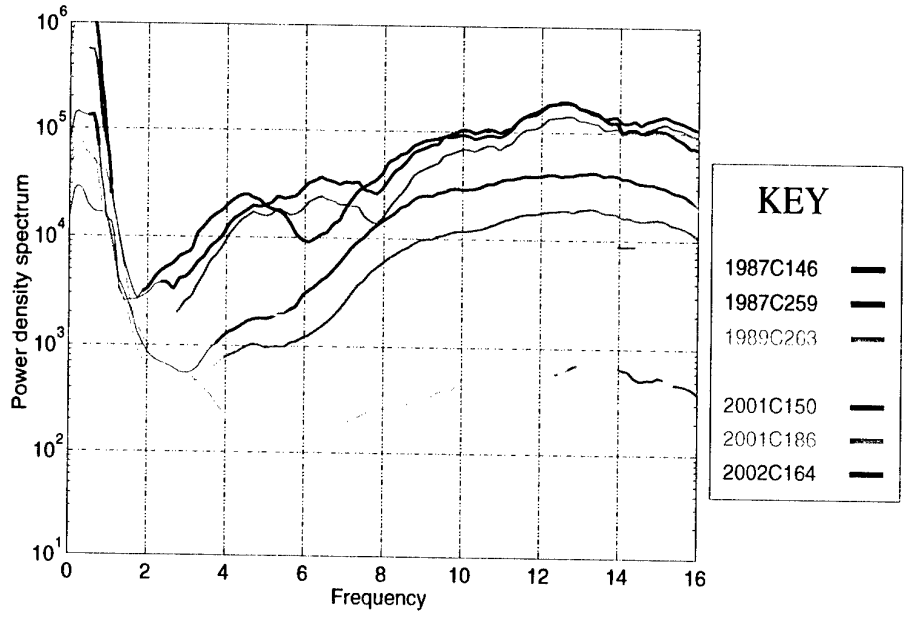

Fig. 6.4.4. *Power density spectra for the P time window averaged over all vertical component instruments for the arrays NOA, NRS and HFS. Thin lines indicate that the ratio PDS(signal)/PDS(noise) was below 4.0 for a given frequency. Events 1987C146, 1987C259 and 1989C263 only include instruments from the NORES array. Event 2002C164 only includes instruments from the HFS and NOA arrays.*

A comparison between the underground cavity explosions and surface explosions at Mossibränden

The Swedish Armed Forces regularly detonate outdated ammunition at ground level at a site approximately 15 km from the underground chambers (see Fig. 6.4.1). Seismic waveforms from 12 such events were added to the database to provide a comparison between underground explosions (where the explosive is completely surrounded by air) and detonations at the surface in the open air. The surface explosions at the Mossibränden site are listed in Table 6.4.2.

Table 6.4.2. Explosions at the Mossibränden site in Älvdalen, June and July 2001. Charges are TNT weights.

Origin ID	Date	Charge/ kg	Origin time as determined by NDC, NORSAR
2001S176	25 June 2001	18831	2001-176:13.46.17.7
2001S177a	26 June 2001	20327	2001-177:07.15.31.2
2001S177b	26 June 2001	20408	2001-177:13.00.11.1
2001S178a	27 June 2001	20101	2001-178:09.16.04.5
2001S178b	27 June 2001	20432	2001-178:13.40.12.4
2001S179a	28 June 2001	20793	2001-179:09.40.55.4
2001S179b	28 June 2001	20242	2001-179:13.50.31.6
2001S183	2 July 2001	21024	2001-183:11.36.00.6
2001S184a	3 July 2001	19044	2001-184:07.31.01.9
2001S184b	3 July 2001	20540	2001-184:13.01.00.0
2001S185	4 July 2001	19118	2001-185:09.36.05.6
2001S186	5 July 2001	20102	2001-186:08.46.05.1

In Fig. 6.4.5 we compare the waveforms resulting from one of the underground cavity explosions (2002C164) and one of the surface explosions (2001S186) filtered through several different frequency bands. The amplitudes resulting from the surface explosion are somewhat greater than those resulting from the decoupled explosion. This is particularly pronounced for low frequencies; in the 1.5-3.0 Hz frequency band, the signal from 2002C164 barely exceeds the background noise level whereas there is a clear signal at these low frequencies from the surface explosion. In the 3-6 Hz band there is a weak S-wave signal from the cavity explosion but no discernible P-wave arrival. In the higher frequency bands, the cavity explosion has a strong P-signal which is comparable to that from the surface explosion.

The spectral properties of the energy resulting from these two events is seen more clearly in the power density spectra: see Fig. 6.4.6. The clear distinction between the two events is the energy in the P spectrum at low frequencies. The underground cavity explosion on the left has a peak of P-energy between 8 Hz and 16 Hz, with approximately an order of magnitude less energy below 8 Hz. By contrast, the surface explosion on the right has slightly more P-wave energy between 3 Hz and 8 Hz than at higher frequencies. There is less difference between the S-wave spectra for the two events.

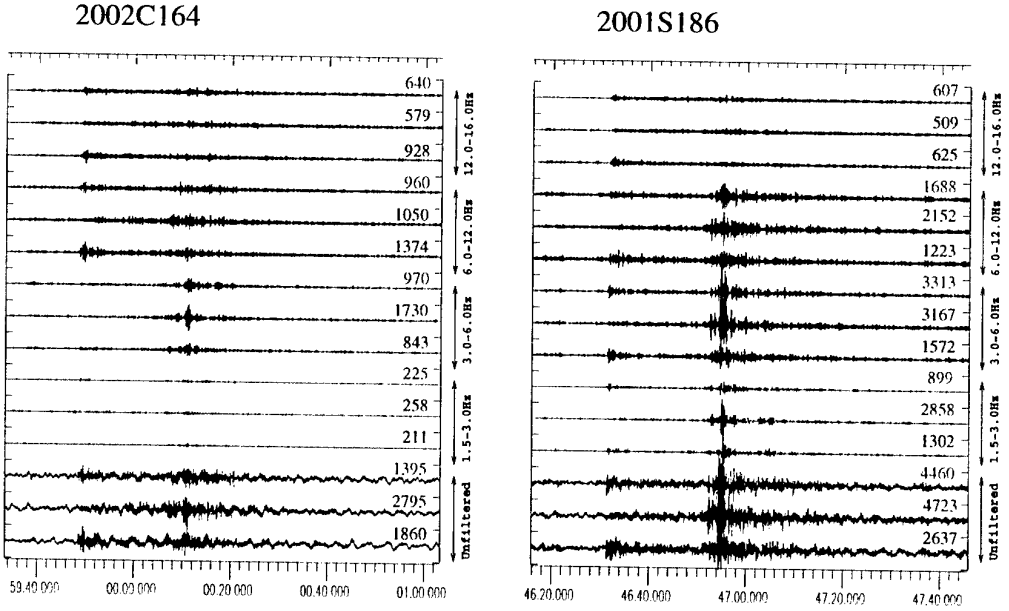

Fig. 6.4.5. *Waveform data from the 3-component HFSC2 instrument for events 2002C164 (cavity explosion: 10000kg powder and TNT in shells in a 1000m^3 cavity) and 2001S186 (surface explosion of 20102kg out-of-date ammunition). Vertical component traces are in black; rotated radial and transverse components are in red and blue respectively. All traces are scaled identically with the largest amplitude as indicated. Frequency bands for filtering are shown on the right hand side.*

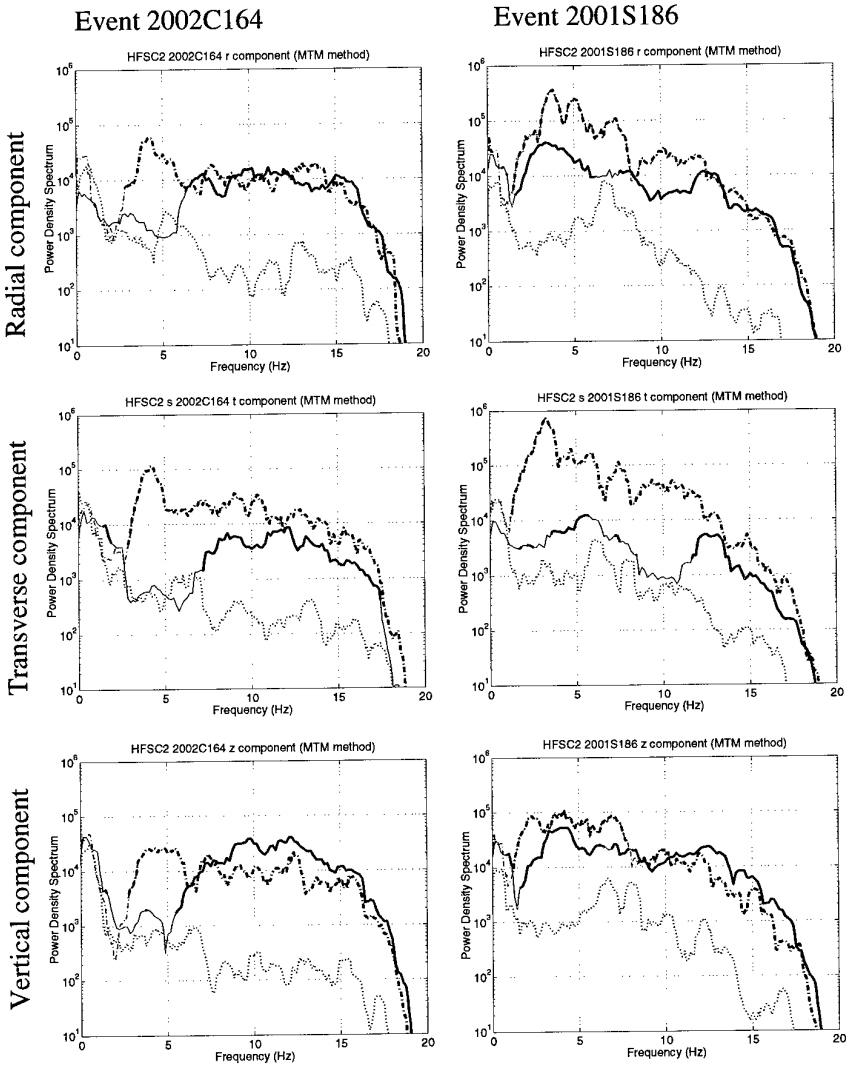

Fig. 6.4.6. *Power density spectra (PDS) of the radial (top), transverse (center) and vertical (bottom) components of the signals from events 2002C164 (decoupled, left) and 2001S186 (Mossibränden, right) from the HFSC2 instrument. The solid red line is the PDS for a 5 second interval starting at the P arrival, the dashed blue line is the PDS for a 10 second interval starting at the S arrival and the dotted line is the PDS for a 10 second interval ending 2 seconds before the P arrival (noise window). The dashed and solid lines are displayed with double thickness for frequencies where the signal to noise ratio is greater than 4.0 .*

A discriminant for cavity-decoupled explosions

The comparison between events 2002C164 and 2001S186 (Fig. 6.4.5 and Fig. 6.4.6) indicates that the primary difference between the underground cavity explosions and the surface explosions is relatively low P energy at low frequencies for the decoupled explosions. We applied the following step-wise procedure to find a quantity which summarises the visual discriminant in the vertical component spectra of Fig. 6.4.6, which can then be applied to all of the events in the database in order to find a systematic difference between the cavity (C) events and the surface (S) events.

For each event in the data-base, the following steps were carried out:

- Waveform data was obtained for every available vertical component station in the HFS, NRS and NOA arrays.
- For each trace, a P-window (5 seconds following the P-arrival), an S-window (10 seconds following the S-arrival) and a noise window, N (10 seconds ending 2 seconds before the P-wave arrival), were defined.
- Power density spectra were calculated over all time windows for all traces.
- Two frequency bands were defined: band 1 (3 - 8 Hz) and band 2 (8 - 14 Hz). Median values of the P, S and noise power density spectra were calculated for frequencies within these bands. For a given trace, we denote the median value of the power density spectra between frequencies f1 and f2 P(f1-f2), S(f1-f2) and N(f1-f2) for the P time window, S time window and noise time window respectively.
- For each trace, the ratios P(8-14):N(8-14), S(8-14):N(8-14), P(3-8):N(3-8) and S(3-8):N(3-8) were calculated. If one or more of these ratios was below 2.0, then the trace was excluded. For the remaining traces, the ratios P(8-14):P(3-8) and S(8-14):S(3-8) were evaluated and the mean and standard deviations calculated. The results are displayed in Fig. 6.4.7.

Fig. 6.4.7(a) shows a clear distinction between the decoupled explosions (blue bars) and the surface detonations (green bars) with the former having far higher ratios of P energy in the higher frequencies to P energy in the lower frequencies. This ratio is highest for three 10000kg explosions suggesting that they were the most effectively decoupled. The 2500 kg explosion (2001C150) was probably even more effectively decoupled, but was excluded from this analysis on the grounds of poor signal to noise ratio. This ratio is approximately an order of magnitude greater for the decoupled explosions than for the surface explosions.

Fig. 6.4.7(b) shows a similar pattern for the S waves but with a much smaller difference in the ratios. The P(high):P(low) ratio appears therefore to be a far better discriminant than the S(high):S(low) ratio. This is in accordance with expectations, since only P-energy is transmitted through the air surrounding an explosion and all shear energy is generated by conversion from P-energy. Given that S and P exhibit similar trends (i.e. decoupling produces both less P and less S at low frequencies), the P(high):P(low) ratio is probably a better discriminant than the S:P ratio.

The simplicity of this single ratio discriminant may lead to spurious conclusions being drawn and it therefore provides no substitute for a thorough examination of the spectra. For example, on the basis of the P(8-14):P(3-8) discriminant (Fig. 6.4.7a), event 1987C259 would appear to be more effectively coupled than events 1987C146 and 1989C263: two events which involved equal quantities of explosives but in a larger chamber. The low P(3-8) value for event 1987C259 is the result of a decrease in power between 5 and 8 Hz (Fig. 6.4.4) which is not shown by events 1987C146 and 1989C263. Below 5 Hz, event 1987C259 displays more P energy than the other two events.

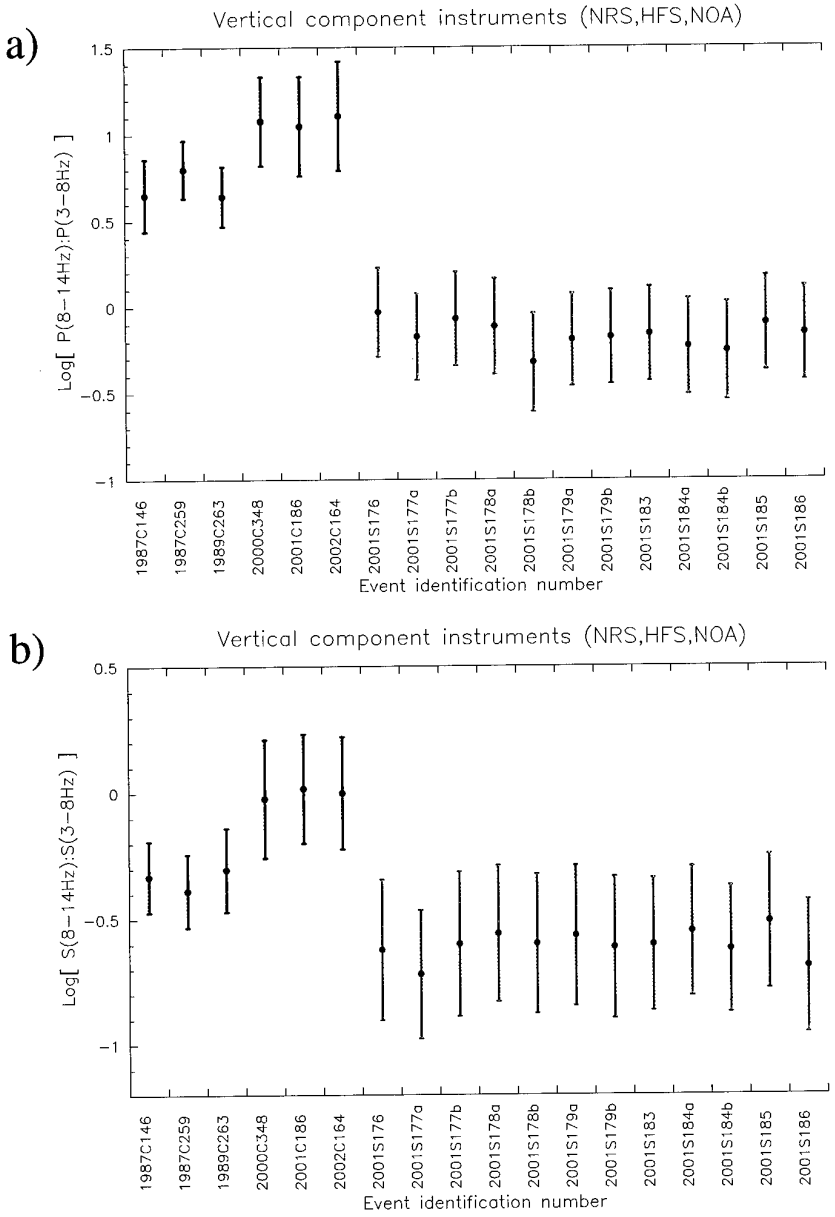

Fig. 6.4.7. *Mean values of (a) log(P(8-14)/P(3-8)) and (b) log(S(8-14)/S(3-8)) for all vertical component stations in the three arrays HFS, NRS and NOA for which the ratios P:N and S:N were greater than 2.0 in both frequency intervals. Error bars surrounding the mean values are standard deviations. Decoupled cavity explosions are denoted with blue bars and surface explosions from Mossibränden with green bars.*

Conclusions

Throughout the analysis, local site effects have been reduced as a result of averaging of values from many array stations. The synthesis below and the main conclusions of Fig. 6.4.7 are based on different wavepaths and distances, and it is therefore reasonable to assume that the findings are largely source related.

- The recordings from explosions in the cavities at Älvdalen are characterized by a large amount of high-frequency energy (8-16 Hz) compared with the energy at lower frequencies (2-5 Hz). Such spectral characteristics are not observed for any of the other events included in the database. The effect is more pronounced for P than for S waves.
- The three 10000kg explosions in a 1000m^3 chamber appear to have been more efficiently decoupled than the 5000kg explosions in chambers of 200m^3 and 300m^3. The signals from the explosions in the smaller chambers were far stronger, in spite of significantly lower yields, and displayed a less pronounced high-to-low frequency energy ratio than the explosions in the larger chambers.
- The 2500kg explosion in the 1000m^3 chamber appeared to be very effectively decoupled, and was visible on our recordings only at frequencies above 8 Hz.

The Office of Technology Assessment report (OTA, 1988) estimates that a one kiloton explosion in granite at a depth of 828 meters would be decoupled by a spherical cavity with a radius of approximately 20 metres. It might be possible to scale this to a yield of 10 tons at a depth of 100 metres, as in Älvdalen, to obtain the cavity volume required for full decoupling. There are, however, large uncertainties associated with such scaling, in particular when it comes to the use of high-explosive materials and non-spherical cavities. The 10 ton explosions in Älvdalen were detonated in a cavity 5 meters high by 25 meters long, by 10 meters wide (~1000 m^3), and the explosive charge was made up of 10 simultaneous one ton charges detonated on the floor of the cavity (lifted from the floor on styropor 'mattresses'). It is therefore uncertain whether the 10 ton shots were fully or only partially decoupled. As a qualitative indicator for the degree of decoupling it can be noted that the damages to the cavity are minor and limited to 'surface scratches', and the repeated use of the same cavity is warranted. On the other hand, both the 200m^3 and 300m^3 cavities have been closed for further use due to structural damage caused by the explosions. From the P-wave spectra shown in Figure 6.4.4 we make the following observations:

- The power spectral levels of the 2000C348 and 2001C186 10 ton explosions detonated in the 1000 m^3 cavity differ by a factor 2 ($\sqrt{2}$ in amplitude) over the entire observable frequency band. At high frequencies, the 2002C164 10 ton explosion has a similar spectral level to the (stronger) 2000C348 event, although it shows slightly lower power at lower frequencies.
- Between 8 and 16 Hz we find a factor 6 amplitude difference between the 2.5 ton and the weakest 10 ton explosion, both detonated in the 1000 m^3 cavity. Below 8 Hz, the 2.5 ton explosion had too low SNR to enable a comparison.

- The two 5 ton charges detonated in the 300 m^3 cavity had very similar spectra. Below 5 Hz, the 5 ton charge detonated in the 200 m^3 cavity had higher spectral levels than the 300 m^3 cavity shots. Between 5 and 8 Hz, the 200 m^3 cavity shot displays a reduction in power spectrum whereas the 300m^3 shots display an increase. Above 8 Hz the spectral levels were all similar.
- When comparing the spectral levels of the "smallest" 10 ton explosion detonated in the 1000 m^3 cavity with the 5 ton explosions detonated in the 300 m^3 cavity, we find the amplitudes of the 5 ton explosion exceeds the amplitudes of the 10 ton explosion by a factor 3-3.5 in the band 10-16 Hz. At 5 Hz, the amplitude difference is increased to a factor 7.

The spectral characteristics found for the decoupled explosions as shown in Fig. 6.4.7 may be influenced by the open tunnel during the explosions. This entails that it is presently unknown if these characteristics are reproducible in a sealed decoupled explosion.

These observations of the cavity explosions provide information that can be used to assess the full and partial decoupling effects. This is a topic that we plan to look into in the continuation of this project. For the newer events we have also collected high-frequency data that we will investigate in more detail. The high-frequency data was obtained using portable stations which were placed both alongside fixed instruments within the arrays and at selected sites closer to the source locations.

We also plan to assemble NOA, HFS and NRS recordings of earthquakes located at distances similar to Älvdalen and Mossibränden, but at different azimuths, in order to make comparative studies of their spectral characteristics.

Comparisons between records from decoupled explosions and ripple fired mining explosions are recognized as an important future target.

References

Office of Technology Assessment (OTA, 1988), "Seismic Verification of Nuclear Testing Treaties", Congress of the United States Office of Technology Assessment, OTA-ISC-361, May 1988.

S. J. Gibbons
C. Lindholm
T. Kværna
F. Ringdal

6.5 Site-Specific Generalized Beamforming (SSGBF) applied to the Lop Nor test site

Introduction

In the preceding NORSAR Semiannual Technical Summary we reported on our initial efforts to develop an optimized site-specific threshold monitoring (SSTM) system for the Lop Nor test site in China (Lindholm et. al., 2002). Our aim was to calibrate all available high-quality seismic stations within regional distance, and supplement with the best IMS arrays at teleseismic distances. As a calibration data base, we used several past nuclear explosions at the test site, combined with nearby, well-recorded earthquakes.

We have now developed a site-specific Generalized Beamforming (SSGBF) approach to supplement the SSTM system for monitoring the Lop Nor test site. This paper describes the methodology and initial results using the SSGBF approach. We also comment briefly on the relative merits of the two approaches (SSTM and SSGBF), and the extent to which they complement each other in this particular case study.

Development of site-specific GBF

The Generalized Beamforming (GBF) technique, originally developed by Ringdal and Kværna (1989), is now widely accepted as the most efficient method for associating seismic phases from a global or regional network. In a typical implementation, a large number of generalized "beams" are steered to the points in a global or regional grid. An automatic detector is applied to each station or array in the network, and a set of "box-car" functions is generated for each station, so that the non-zero parts of these functions correspond to a time interval around a detection. By adding these functions with appropriate weights and with time delays corresponding to the particular phase-station-grid point combination, one obtains a "beam" that may then be subjected to a detector algorithm.

A common feature of such implementations is the need to group the large number of individual beam "detections" so as to eliminate side-lobes and associate the detection group with an event at the correct hypocenter. This grouping, which can become quite complex, is clearly unavoidable when a large geographical region is to be monitored. However, if one is monitoring a particular site, such as a suspected nuclear test site, it is possible to simplify this procedure considerably, and at the same time optimize the parameter settings to ensure the best possible detection probability for the target site. This idea was first tested by Ringdal and Kværna (1993) to monitor the aftershocks of a large earthquake sequence occurring in Western Caucasus during the GSETT-2 experiment. They concluded that the approach showed a superior performance compared to the association procedures being employed at the four experimental international data centers operating during GSETT-2. In the present paper we elaborate further on this site-specific GBF (SSGBF) approach to monitor the Lop Nor test site.

Data base and analysis procedure

The data base for this study has consisted of recordings by an experimental seismic network composed of stations and arrays at teleseismic as well as regional distances from the Lop Nor test site. We develop and test a parameter set calibrated towards the test site, and discuss the

SSGBF results in conjunction with the results from the site-specific threshold monitoring (SSTM) technique applied to the same site.

For the purposes of this study, 18 seismic stations (including 9 arrays) were initially chosen as shown in Fig. 6.5.1. These stations are a subset of the 23 stations used in the study by Lindholm et. al. (2002). Table 6.5.1 summarizes the station information and also lists the range of the azimuth and slowness parameters used for forming the beam towards the test site. Only P-phases are used in this study. We note that the slowness restriction is only defined for the array stations, whereas for the 3-component stations we do not impose any restriction on the slowness value. The azimuth restrictions are defined for all stations, and have been set to +/- 30 degrees of true azimuth.

The limits on arrival time tolerances are not defined in Table 6.5.1, since these tolerances are to a large extent dependent on the desired sharpness of the generalized beam. We have used the formula:

dT=S*R/111.13

where dT is the time tolerance in seconds, R is the desired beam radius in km and S is the P-phase slowness (in s/km) corresponding to the distance from the target site to the station being processed. If a beam radius of e.g. 50 km is desired, and the expected P-wave phase velocity at a given station is 8 km/s, then the assumed range of the time tolerance is approximately +/- 6 seconds.

In general, there is a trade-off between the sharpness of the generalized beam and the size of the tolerance intervals of the parameters. We have chosen to use fairly large tolerances, to ensure that there is only a small probability of missing real detections corresponding to an event at the site. In future studies, these parameters may be fine tuned to take advantage of those arrays and 3-component stations that are particularly well calibrated. For example, for well-calibrated stations the azimuth tolerances may be greatly narrowed, resulting in a reduced false association rate at no loss in detectability for real on-site events.

The beamforming procedure follows the GBF standard, except that only one generalized beam is formed in the site-specific case. The main steps are:

- Applying an automatic detector at each of the stations/arrays in the network
- Adding together weighted "box-car functions" representing the detector outputs with the appropriate restrictions on travel time, azimuth and slowness
- Applying a thresholding procedure on the resulting generalized beam

We have used 0-1 weights for the beamforming in our initial analysis, with standard (rectangular) box-car functions. In addition, we have made some experiment with using alternative functions (e.g. triangular functions centered at the expected arrival time). We will return to the results of these experiments in a later paper. For now, we proceed to present preliminary results using the standard approach.

Table 6.5.1. The stations used for Site-Specific Generalized Beamforming processing of the Lop Nor test site. In order for a signal detection to be used as a candidates an event at the Lop Nor test site, its azimuth and slowness estimates has to be within the ranges given in the table. Notice that for three-component stations only the azimuth range is used.

Station	Type	Delta	P travel time	Azimuth Range (deg)	Slowness Range (sec/deg)
ARCES	Array	42.47	478.2	60 - 124	5.5 - 12.5
ASAR	Array	77.16	719.2	300 - 359	3.0 - 9.0
CMAR	Array	24.64	326.8	305 - 359	6.3 - 12.3
FINES	Array	41.75	472.4	58 - 118	5.2 - 11.2
GERES	Array	51.41	548.6	42 - 102	6.3 - 12.3
HFS	Array	47.93	521.0	45 - 105	3.2 - 9.2
ILAR	Array	65.57	645.9	283 - 343	2.1 - 8.1
NORES	Array	48.84	528.5	50 - 110	4.9 - 10.9
MKAR	3C/Array	6.88	103.3	120 - 170	10.1 - 16.1
ARU	3C	24.43	322.8	84 - 144	NA
BRVK	3C	16.87	239.6	95 - 155	NA
KURK	3C	11.47	165.7	109 - 169	NA
KZA	3C	9.92	149.8	58 - 118	NA
NIL	3C	14.38	209.0	22 - 82	NA
TKM2	3C	9.68	146.0	63 - 123	NA
ULHL	3C	9.18	139.8	60 - 120	NA
ULN	3C	14.64	216.4	221 - 281	NA
USP	3C	10.51	156.6	65 - 125	NA

Preliminary results

We present below some preliminary results in applying site-specific generalized beamforming to the Lop Nor test site in China.Two data sets for performance testing were compiled. The first data set covered one day (10 September 2001), and in these data the recordings of 4 explosions were scaled and embedded at some (but not all of) the stations (see Lindholm et. al., 2002). Secondly, a 10 day test period with data from August 2 through 11, 2001 was selected and data were collected for the stations.

Example 1: 10 August 2001

Our first example is the day 10 August 2001. Figs. 6.5.2 and 6.5.3 show the SSGBF traces for arrays and single stations respectively for that day. In Fig. 6.5.2, the peaks of the panels for each array represent detections that fall within the Lop Nor azimuth and slowness ranges given in Table 6.5.1. To align the detections we have subtracted the P travel-time from Lop Nor to the respective arrays. The network trace on top is calculated by adding boxcar functions surrounding each detection, using both the arrays of this figure and the three-component stations of Figure 6.5.3. In Fig. 6.5.3, the same type of display is shown, but only for the 3-component

stations. Furthermore, in Fig. 6.5.3, the top trace uses only detector information from the 3-component stations in the network.

Alerts (red diamonds) are declared when the network trace (the full network) has at least three matching detections, where at least one detections has to be at an array. The red diamonds at the individual arrays or 3-component stations on the two figures show detections that fall within the alert interval defined on the network trace. The event at 03:15 is located in northern Xinjang, about 200 km north of the Lop Nor test site. It is interesting to note that this event triggers a clear detection on the generalized beam steered towards Lop Nor, even if the distance to the test site exceeds the beam coverage radius of 50 km. In practice, it is difficult to avoid such side lobe detections at nearby sites, and in any case, it may be useful to have indications on the beam trace that such nearby events may have occurred. The two alerts between 19:00 and 21:00 are caused by signals of unknown origin. Most likely these alerts are false alarms caused by coinciding detections at the different stations.

Example 2: 5 August 2001

As another example, Fig. 6.5.4 shows (in the top panels) SSGBF processing results for 5 August 2001. Only the arrays and the full network trace are shown. Two alerts are declared, and we note that several detections fall within the alert interval. However, these detections do not add constructively to the network trace, indicating that they were associated with an event *outside* the source region. At the bottom panel of Fig. 6.5.4 we show the corresponding SSTM results (presented by Lindholm et. al., 2002), having threshold peaks at the same times as the SSGBF network trace. These peaks are verified to be caused by events far from the Lop Nor test site, (Andaman Islands and Afghanistan, respectively).

Example 3: 2 August 2001

Our third example is similar to Example 2, but covers a "quiet" day (2 August 2001) during which there were no large seismic events globally, and no significant event near Lop Nor. The top panels of Fig. 6.5.5 show the SSGBF processing results. No alerts are declared. The corresponding SSTM, shown below the red line, has no significant peaks and a background level varying between 2.6 and 3.0.

Example 4: 10 September 2001

Our final example (Figs. 6.5.6 and 6.5.7) is the one day (10 September 2001) which contained the scaled, embedded events, and the combined network SSGBF trace (using all stations) is shown on top of each figure. In Fig. 6.5.6, which gives the standard display of the arrays and the combined network SSGBF traces, we note the large number of alerts declared automatically. A total of 11 alerts are declared for that day by the SSGBF method. These alerts correspond to the eight embedded explosions (scaled magnitudes 3.0 to 3.5), one additional trigger that turned out to be a real event near Lop Nor, and two alerts of unknown origin.

Fig. 6.5.7 shows a combination of SSGBF and SSTM results for the same day (10 September 2001) with scaled, embedded events. The top panel shows the SSGBF network trace for 10 September 2001. Below is shown the SSTM network trace for the same day. Red circles indicate events for which the SSTM processing issued an alert, whereas blue circles indicate events

for which an alert was not issued. Notice the good correspondence between the SSGBF alerts (red diamonds) and the SSTM alerts.

Conclusions

From these tests the following preliminary observations can be stated:

- Out of the eight embedded explosions on 10 September 2001, six were flagged by the automatic SSTM detector, whereas all eight were flagged by the automatic SSGBF detector.
- The quiet day (2 August 2001) did not have any events flagged, neither by the SSTM nor the SSGBF detector.
- On 5 August 2001 the SSGBF as well as the SSTM method triggered on two large teleseismic events.

The above observations should be evaluated under the perspective that the study is of a very preliminary nature, and that further optimization and tuning of the SSGBF method is clearly possible. Furthermore, the addition of newly developed and planned IMS stations would contribute to a significant improvement in detector performance.

The false association problem of the SSGBF approach has not yet been evaluated in detail, but preliminary indication are that the likelihood of spurious associations is low, even with the fairly relaxed set of parameter tolerances used in this study. A more extensive study of this topic is being planned.

The combination of the SSTM and the SSGBF techniques appears to be a very promising new development. Each of these two approaches has its specific strengths. The SSTM technique has as its main strength the ability to display the real seismic field, without regard to "station detector performance". On the other hand, the SSGBF technique takes advantage of the individual station detector outputs, and uses this combined information to narrow down the number of possible candidates for events in the target area.

From the above we conclude that the Site-Specific Generalized Beamforming performance tests for the Lop Nor test site were successful. It is expected that these initial tests will be followed by more detailed studies, where in particular the calibration parameters will be more firmly established and the combined benefits of the SSTM and the SSGBF methods will be further explored.

Tormod Kværna
Erik Hicks
Frode Ringdal

References:

Lindholm, C., T. Kværna and J. Schweitzer (2002): Site-Specific Threshold Monitoring (SSTM) applied to the Lop Nor test site, *Semiannual Technical Summary, 1 July - 31 December 2001*, NORSAR Sci. Rep. 1-2002, Norway.

Ringdal, F. and T. Kværna (1989): A multichannel processing approach to real time network detection, phase association and threshold monitoring, *Bull. Seism. Soc. Am.*, 79, 1927-1940.

Ringdal, F. and T. Kværna (1993): Generalized Beamforming as a tool in IDC processing of large earthquake sequences, *Semiannual Technical Summary, 1 April - 30 September 1993*, NORSAR Sci. Rep. 1-93/94, Norway.

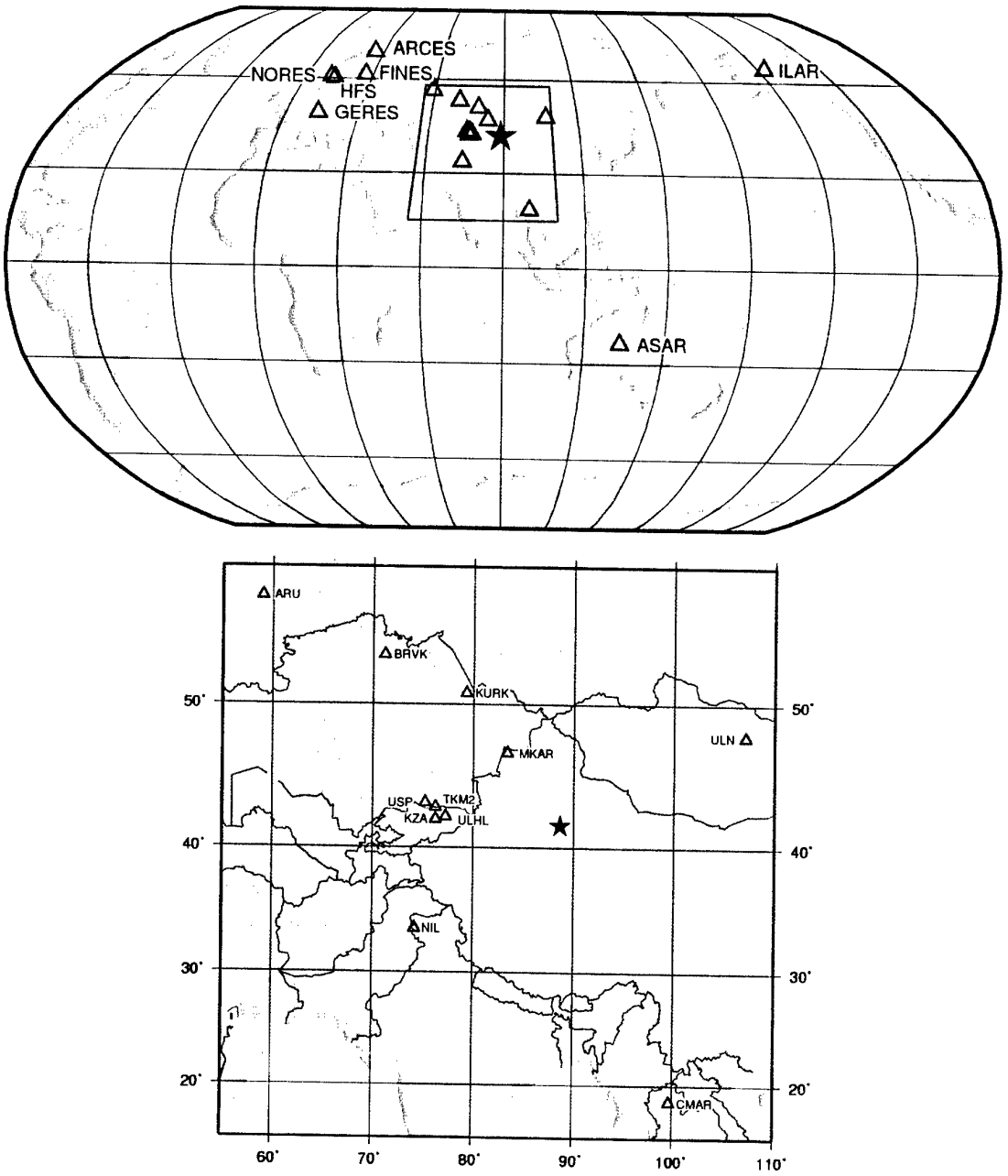

Fig. 6.5.1. Maps showing arrays and stations used for Site-Specific GBF processing of the Lop Nor Test Site (indicated with red star).

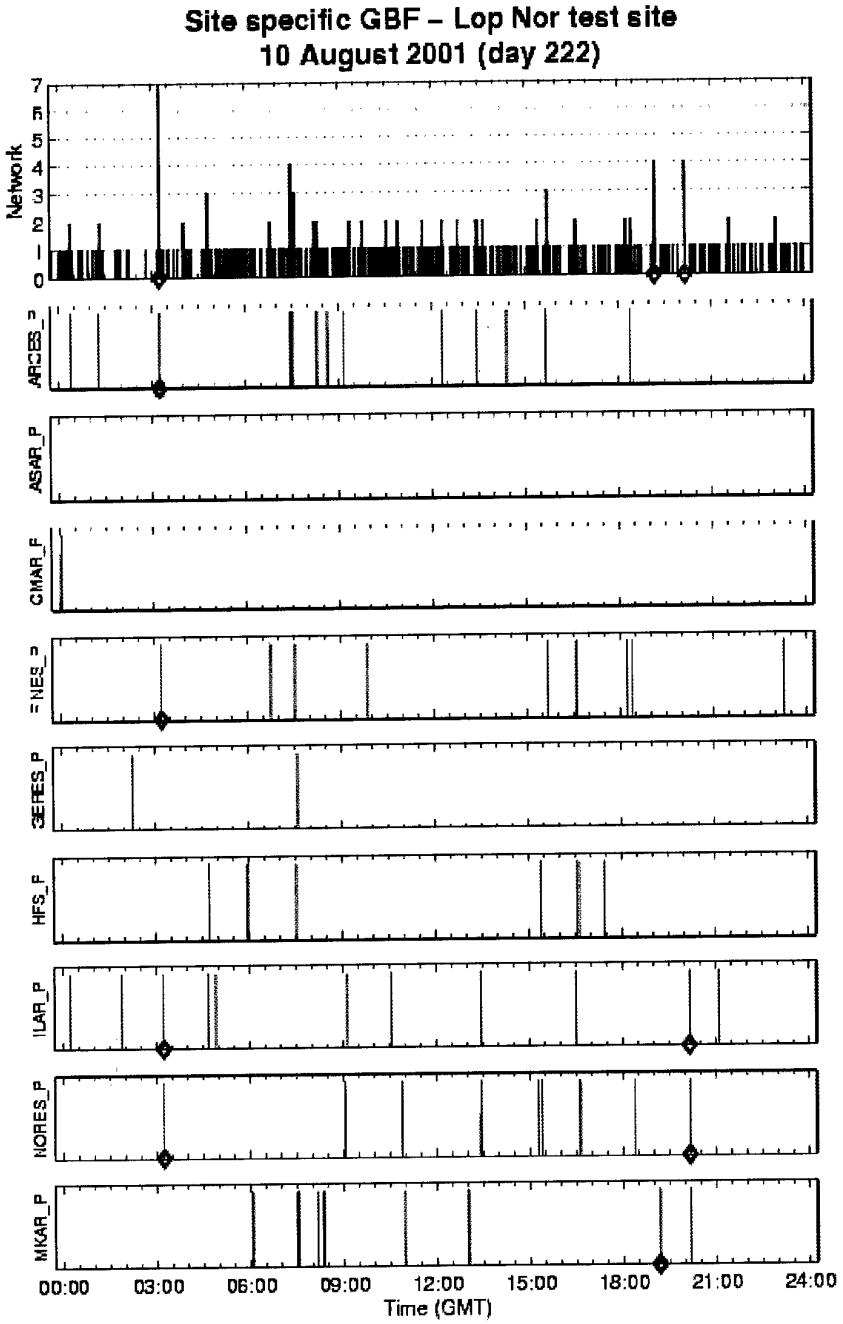

Fig. 6.5.2. The peaks of the panels for each array represent detections that fall within the Lop Nor azimuth and slowness ranges given in Table 6.5.1. To align the detections we have subtracted the P travel-time from Lop Nor to the respective arrays. The network trace on top is calculated by adding boxcar functions surrounding each detection, using both the arrays of this figure and the three-component stations of Figure 6.5.3. Alerts (red diamonds) are declared when the network trace has at least three matching detections, where at least one detections has to be at an array. The red diamonds at the individual arrays show detections that fall within the alert interval defined on the network trace.
The event at 03:15 is located in northern Xinjang, about 200 km north of the Lop Nor test site. The two alerts between 19:00 and 21:00 are caused by signals of unknown origin.

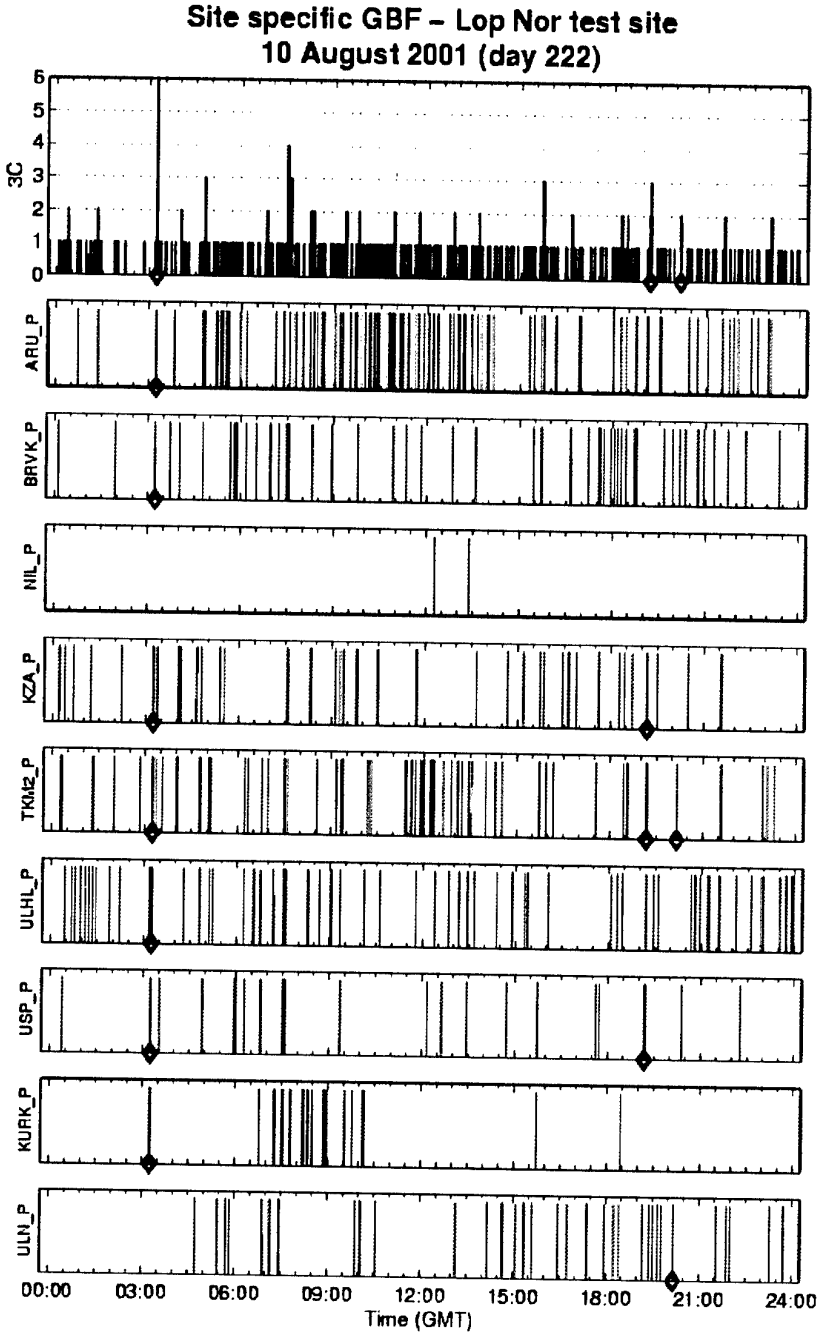

Fig. 6.5.3. The peaks of the panels for each 3C station represent detections that fall within the Lop Nor azimuth ranges given in Table 6.5.1. To align the detections we have subtracted the P travel-time from Lop Nor to the respective stations. The 3C network trace on top is calculated by adding boxcar functions surrounding each detection, using the three-component stations only. The red diamonds at the 3C network trace and the individual stations show peaks that fall within the alert interval defined on the full network trace shown in Figure 6.5.2.

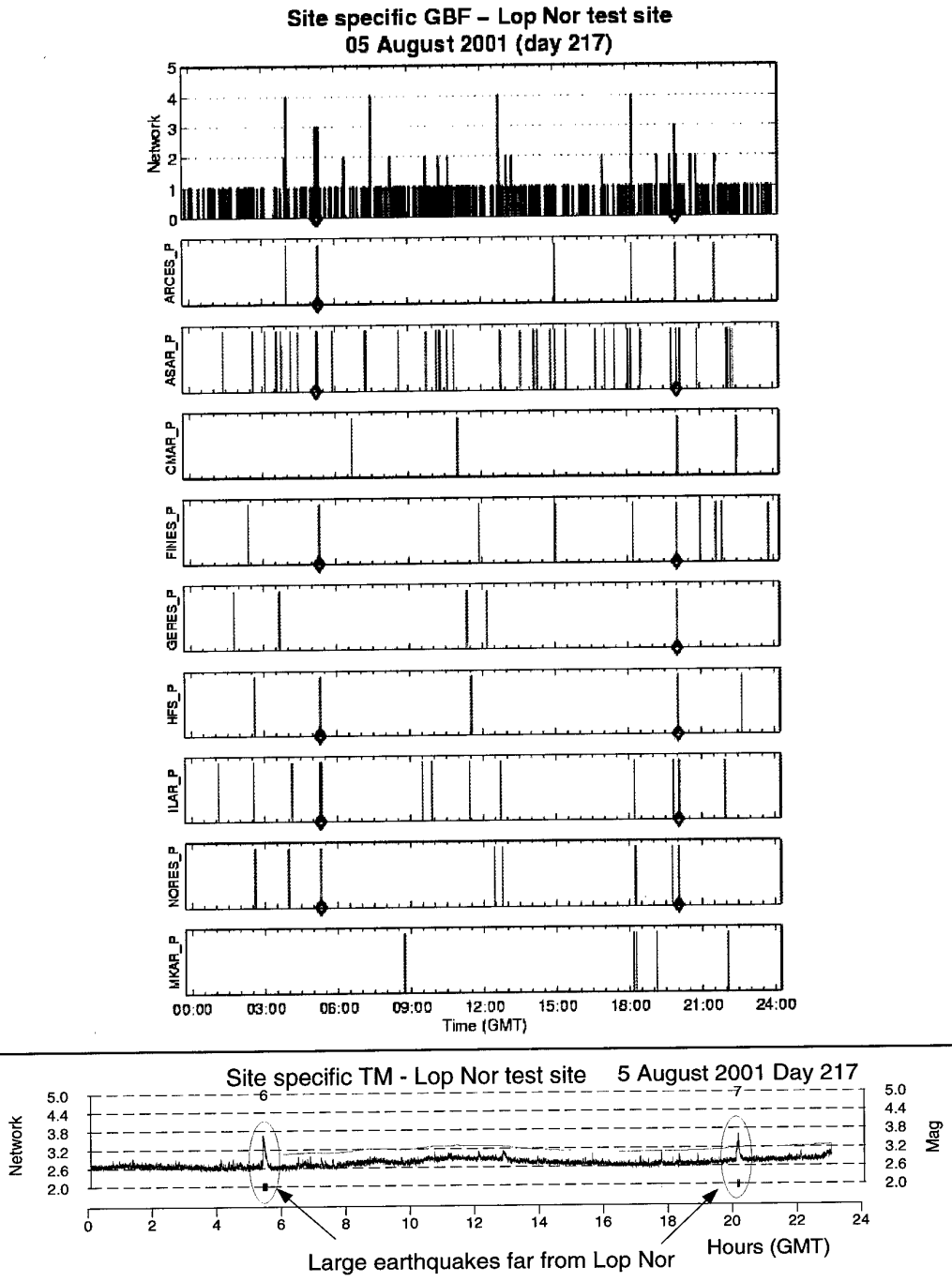

Fig. 6.5.4. The top panels show SSGBF processing results for 5 August 2001. Two alerts are declared, and we find that several detections fall within the alert interval. However, these detections do not add constructively to the network trace, indicating an event outside the source region. Below the red line we show the corresponding SSTM results (presented in the previous NORSAR Semiannual Report), having threshold peaks at the same time as the SSGBF network trace. These peaks are verified to be caused by events far from the Lop Nor test site, respectively, Andaman Islands and Afghanistan.

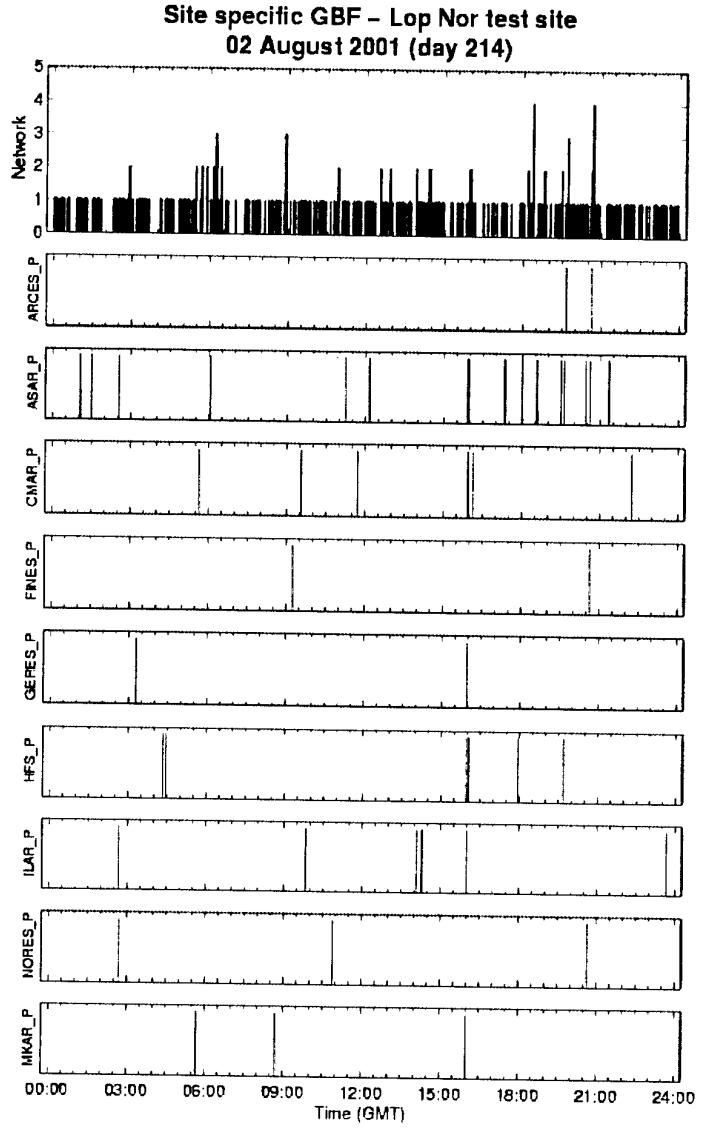

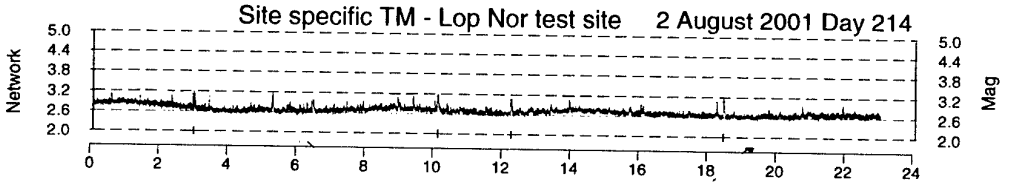

Fig. 6.5.5. The top panels show SSGBF processing results for2 August 2001. No alerts are declared. The corresponding SSTM, shown below the red line, has no significant peaks and a background level varying between 2.6 and 3.0.

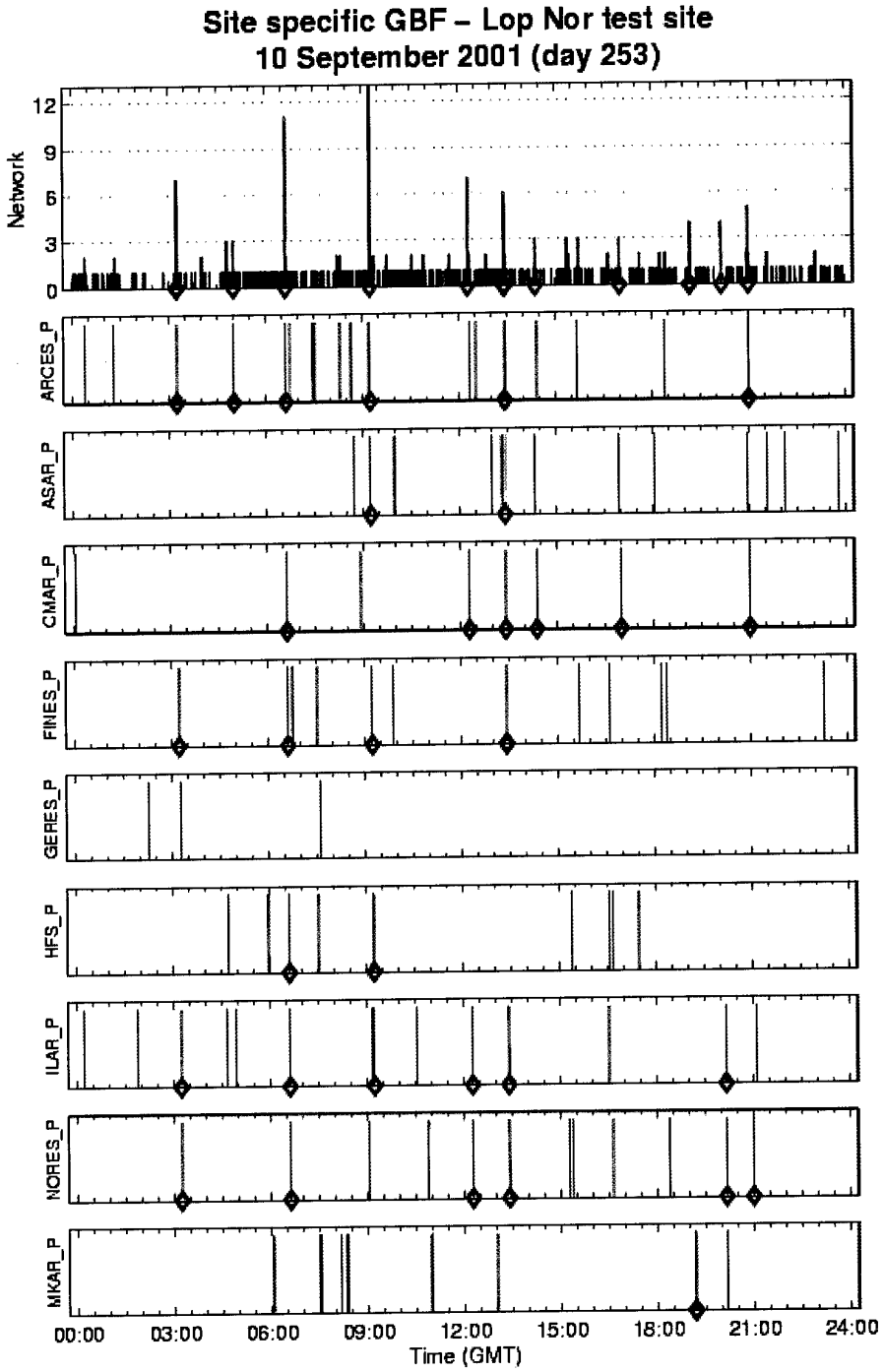

Fig. 6.5.6. The top panels show SSGBF processing results for10 September 2001, with several embedded Lop Nor event recordings scaled to magnitudes 3.0 and 3.5. Notice the large number of alerts declared.

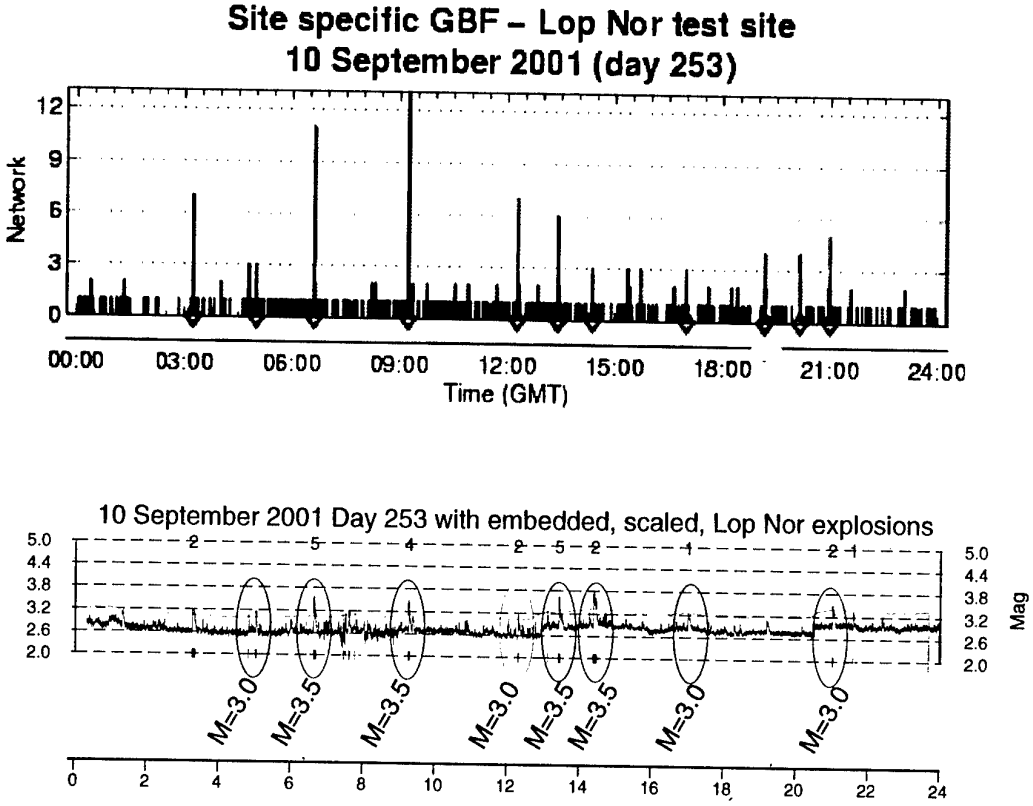

Fig. 6.5.7. The top panels show SSGBF network trace for 10 September 2001. Below is shown the Network SSTM trace for the same day. Red circles indicate events for which the SSTM processing issued an alert, whereas blue circles indicate events for which an alert was not issued.
Notice the good correspondence between the SSGBF alerts (red diamonds) and the SSTM alerts. The event at 03:15 is located in northern Xinjang, about 200 km north of the Lop Nor test site.

6.6 Regional Seismic Threshold Monitoring

Sponsored by Defense Threat Reduction Agency, Contract No. DTRA01-00-C-0107

Abstract

A database comprising a total of 45 events, selected to provide the best possible ray path coverage of the Barents Sea and adjacent areas, was compiled and reanalyzed in a consistent manner. This resulted in new regional attenuation relations for Pn and Sn, together with a preferred average velocity model to be used for predicting the travel times of regional phases. We have now applied these attenuation relations to investigate a regional threshold monitoring scheme for the Barents Sea area.

A grid system with an approximately 100-km grid spacing was deployed for the Barents Sea region, and the observations at the arrays ARCES, SPITS, FINES and NORES were then used for calculating threshold magnitudes for each of the grid points. During an interval without seismic signals, the threshold magnitudes showed large variations over the region, and, in particular, in the vicinity of each array. However, for the region around the island of Novaya Zemlya the variations are modest, varying around a mean of magnitude 2.1-2.2.

In order to investigate in more detail the variations in threshold magnitudes for the Novaya Zemlya region, we deployed a dense grid with an areal extent of about 500 x 500 km around the former Novaya Zemlya nuclear test site. For each of the grid nodes, we calculated magnitude thresholds for the two-hour time interval 00:00 - 02:00 on 23. February 2002. At 01:21:12.1 there was an event with a magnitude of about 3, located about 100 km northeast of the former nuclear test site.

Regions of different sizes were constructed by selecting grid points within different radii from the former nuclear test site. Average, minimum and maximum threshold magnitudes were calculated for circular regions with radii of 20, 50, 100 and 200 km respectively.

The most important result is that even for a target region with radius as large as 100 km, the variations in threshold magnitudes are all within 0.2 magnitude units. This applies both for the time interval with the event and for background noise conditions. For the investigated station geometry, it will therefore be meaningful to represent the monitoring threshold of the entire Novaya Zemlya region with the values of a single target point, together with the *á priori* determined uncertainty bounds.

We can therefore conclude that the experimental site-specific threshold monitoring which has been run daily by NORSAR for the past 5 years, aiming at the Novaya Zemlya test site, can be used with only minor adjustments to assess the threshold within 100 km of the site. This monitoring has shown that between 16 August 1997 and 23 February 2002, the threshold level has been consistently below 2.5, except during "interfering" large regional or teleseismic events located well outside the target region.

For areas with larger variations in threshold magnitudes, like in the vicinity of the arrays, a 100-km radius target region will obviously show larger differences between the maximum and minimum values. Examples illustrating this point will be shown.

Objective

The main objective of this research is to develop and test a new, advanced method for applying regional seismic array technology to the field of nuclear test ban monitoring. To that end, we address the development and testing of a method for optimized seismic monitoring of an extended geographical region, using a sparse network of regional arrays and three-component stations. Our earlier work on optimized site-specific threshold monitoring serves as a basis for the development of this new method. Emphasis of the research is on algorithms that can be efficiently applied in a real-time monitoring environment, which are using primarily automated processing, and which can be readily implemented in an operational CTBT monitoring system.

Research Accomplished

Travel-times and attenuation relations for regional phases in the Barents Sea region

A database containing 45 events in the Barents Sea region (Fig. 6.6.1) has been compiled and analyzed with the aim of evaluating crustal models, travel-times and attenuation relations in the context of performing regional detection threshold monitoring of this region. The 45 events are mostly located around the circumference of the study area due to the virtually aseismic nature of the Barents Sea itself. Regional Pn and Sn phases were observable for most events in the database, while Pg and Lg phases were only observable for events with ray paths that do not cross the tectonic structures in the Barents Sea. This corroborates a number of previous observations of Lg-wave blockage within the Barents Sea.

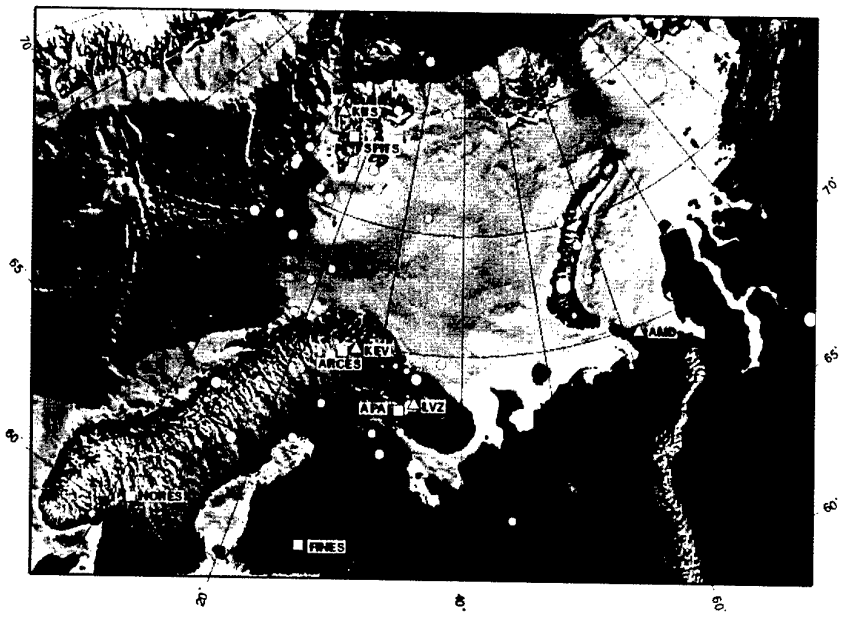

Fig. 6.6.1. *Events (circles) and seismic stations used for deriving wave propagations characteristics of the Barents Sea and surrounding areas. Array stations are shown as squares, while 3C stations are shown as triangles. The symbol size for the events are proportional to the network magnitudes.*

In order to estimate magnitudes, short term average (STA) and spectral amplitude values were calculated in several frequency bands for all phase arrivals in the data base. There were no significant differences between spectral and STA amplitudes, so the latter were used as this parameter is more efficient to calculate in real-time processing. A joint inversion of the regional phases Pn, Pg, Sn and Lg was performed in order to determine attenuation relations specific for this region according to the relation given in equation 1.

$$M_L = \log A - \log e \cdot \alpha_i^0 \cdot f + (a_i f + b_i)\log\left(\frac{200}{\Delta}\right) + \delta_{ik} + 1.66 \qquad (1)$$

where A is observed STA amplitude within a frequency band with logarithmic center frequency f, Δ is epicentral distance, the α^0_i term represents the total attenuation for phase i out to the reference distance of 200 km, and a_i and b_i are phase-dependent attenuation constants. The inversion results for the parameters α^0, a and b are given in Table 6.6.1.

Table 6.6.1. The inversion results for the a, b and α^0 coefficients (1s) for Pn, Sn, Pg and Lg phases used in the attenuation relation (equation 1).

Phase	a	b	α^0
P_n	-0.002 ± 0.023	2.340 ± 0.099	0.584 ± 0.030
S_n	0.141 ± 0.028	2.021 ± 0.110	0.419 ± 0.037
P_g	0.091 ± 0.084	0.851 ± 0.366	-0.538 ± 0.035
L_g	0.534 ± 0.062	-0.186 ± 0.123	-0.609 ± 0.063

Fig. 6.6.2 shows a comparison between the phase magnitude residuals calculated using the relations and parameters of Jenkins et al. (1998) and our inversion results. Our results using the relations and parameters of Jenkins et al. (1998) revealed a relatively high scatter between individual station and phase magnitudes, and also some systematic inconsistencies, most notably magnitudes calculated from different frequency bands at the same station. Magnitudes calculated from STA values in the 2-4 Hz passband are mostly higher than magnitudes calculated in the 3-6 Hz passband, which again are generally higher than magnitudes calculated from the 4-8 Hz passband. The coefficients used in this case were determined using data from eastern North America, central Asia and Australia. However, this relation is not primarily intended for local magnitude calculation, and some of the scatter in the magnitudes from Pg and Lg arrivals in particular may be due to the small distance for some of these observations, below the lower distance limit of 1.8° used by Jenkins et al. (1998).

Phase magnitudes calculated using equation 1 and the parameters of Table 6.6.1 are shown to the right of Fig. 6.6.2. These results show that the scatter (expressed as standard deviation) was significantly reduced compared to the original calculations. There is also no apparent frequency dependency in the magnitude residuals.

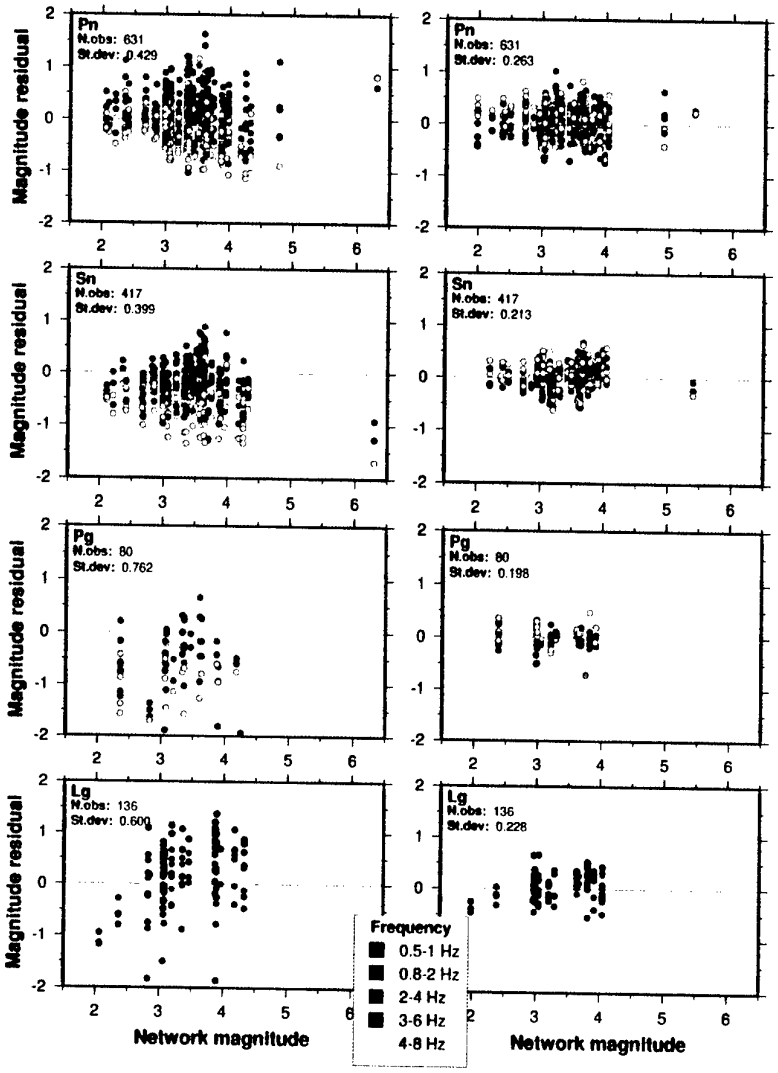

Fig. 6.6.2. Magnitudes calculated using the relation from Jenkins et al. (1998) (left) and this study (right) from individual amplitude readings, plotted vs. network magnitudes for the 45 events. Note the significant reduction in scatter (St. dev.) and also the absence of frequency-dependent effects when the relation from this study is used.

As an example we show in Table 6.6.2 the individual phase magnitude estimates of the 23 February 2002 event located on the northeastern coast of Novaya Zemlya. The consistency of these phase magnitudes is remarkably high.

Table 6.6.2. Phase magnitudes and network magnitudes for the 23 February 2002 event located on the northeastern coast of Novaya Zemlya, using the attenuation relations developed in this study.

Station	Phase	Distance	Magnitude
AMD	Pn	509	3.19
AMD	Sn	509	3.15
LVZ	Pn	1055	3.22
LVZ	Sn	1055	3.01
SPITS	Pn	1095	3.44
SPITS	Sn	1095	3.11
ARCES	Pn	1144	2.97
ARCES	Sn	1144	3.08
KBS	Pn	1197	3.16
KBS	Sn	1197	3.19
FINES	Pn	1850	3.17

Magnitude Type	Magnitude
Network Pn	3.19
Network Sn	3.11
Network All	3.15

Fig. 6.6.3 shows comparisons of corrected network magnitudes compared to magnitudes calculated from individual phases. Although relative P and S magnitudes could be used as an aid in discriminating between earthquakes and explosions, Fig. 6.6.3 shows that regional path effects in this area also give rise to substantial differences in magnitude. This is particularly visible for Pn and Sn magnitudes, as they are available for events covering the entire region. Events that predominantly have ray paths within Fennoscandia have larger Sn magnitudes, while the opposite is true for events that have ray paths crossing the sediment basins of the Barents Sea (Novaya Zemlya/Kara Sea and the western Barents Sea/Mid-Atlantic ridge areas).

From this study, it is clear that Pn and Sn are the most useful phases for calculating magnitudes for events in the Barents Sea. In fact, Fig. 6.6.3 shows that Pg and Lg are mainly observed at close epicentral distances (< 300 km). This situation is quite different from what we have previously found for the Scandinavian Peninsula and the Baltic Shield, where Lg is the dominant phase on the seismogram out to at least 1000 km. Thus, even for a stable continental region, one may expect quite significant regional variations in the magnitude correction factors.

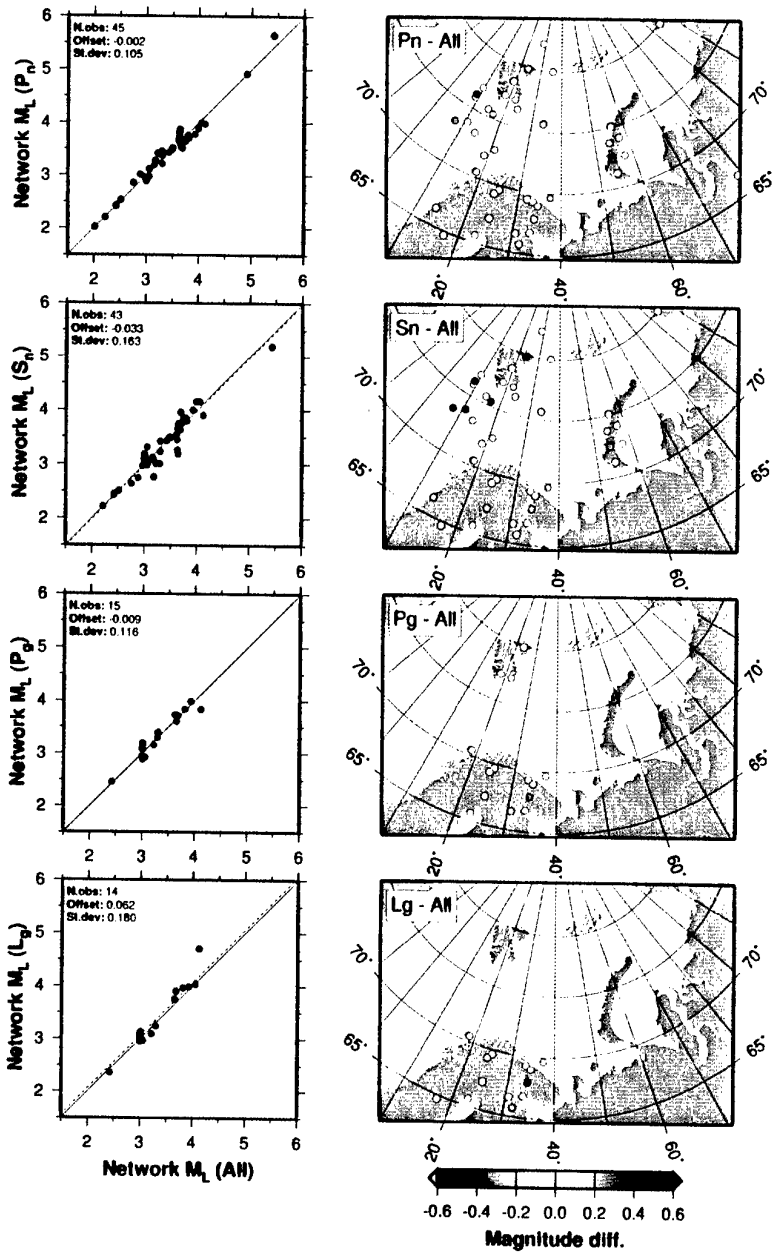

Fig. 6.6.3. Network event magnitude comparisons and maps of the geographical distribution of the magnitude differences for individual phase magnitudes compared to network magnitudes. Note that Sn magnitudes are overestimated for events that have paths predominantly within the Baltic shield, while events with paths that cross the Barents Sea have lower Sn magnitudes. Pg and Lg magnitudes appear to be quite stable within the limited distance range from which readings are available.

Regional Threshold Magnitudes

Using the developed attenuation relations described above, observations at the arrays ARCES, SPITS, FINES and NORES were used for calculating threshold magnitudes for a grid system covering the entire Barents Sea region. The grid spacing was approximately 100 km. Fig. 6.6.4 shows the threshold magnitudes during a time instant without seismic signals. We find large variations over the region, and in particular when approaching each of the arrays. However, for the region around the island of Novaya Zemlya, the variations are modest, varying around a mean of magnitude 2.2.

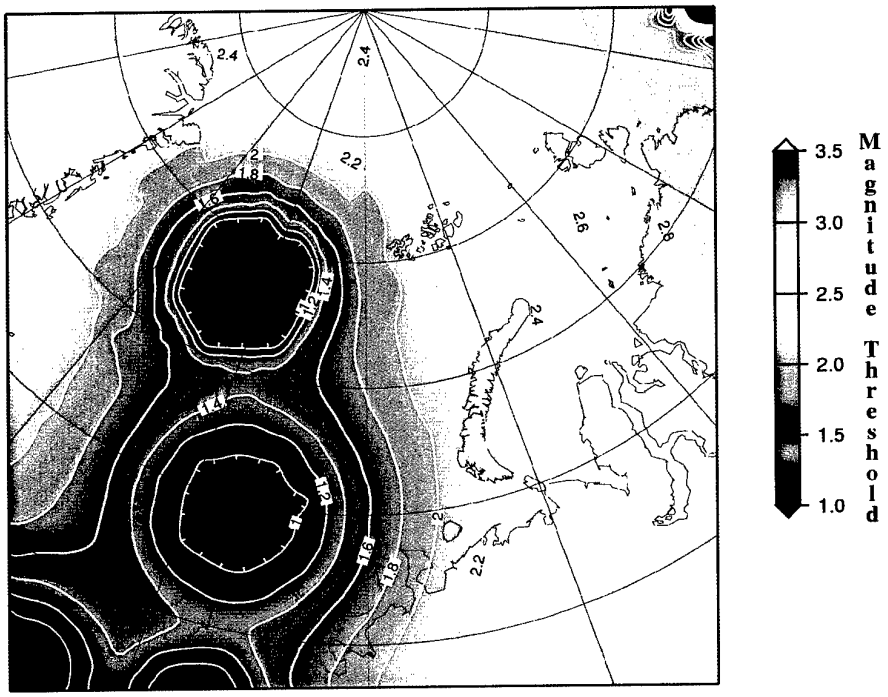

Fig. 6.6.4. *Threshold magnitudes for the time instant 2002-054:01.11.20.0. Notice the improved monitoring capability in the vicinity of each station. For distances above 1.5 degrees of each station we have considered the Pn and Sn phases, whereas Pg and Lg have been used for distances less than 1.5 degrees.*

In order to investigate in more detail the variations in threshold magnitudes for the Novaya Zemlya region, we deployed a dense grid with an areal extent of about 500 x 500 km as shown in Fig. 6.6.5. For each of the grid nodes we calculated magnitude thresholds for the 2 hour time interval 00:00 - 02:00 on 23 February 2002. At 01:21:12.1 there was an event with a magnitude of about 3.2 (see Table 2), located about 100 km north-east of the former nuclear test site.

Regions of different sizes were constructed by selecting grid points within different radii from the former nuclear test site. Fig. 6.6.6 (left) shows the variations in threshold magnitudes for a circular region with a radius of 20 km around the test site. The blue line shows the average

threshold, whereas the red lines represent the minimum and maximum values. Fig. 6.6.6 (right) show similar curves for a region with radius 100 km.

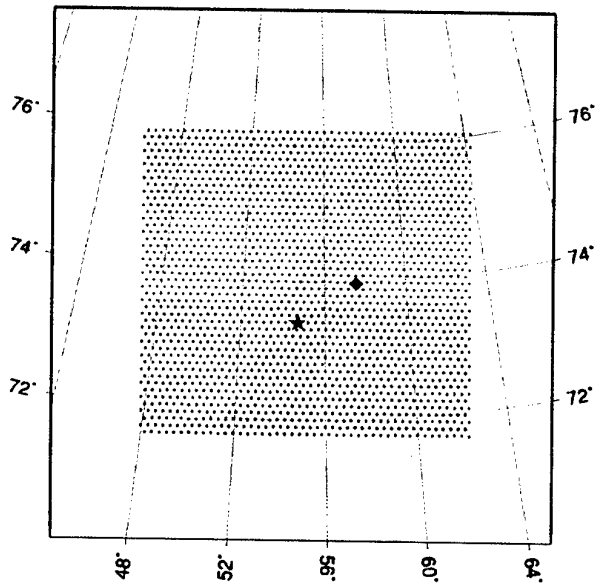

Fig. 6.6.5. *Dense grid deployment around Novaya Zemlya (grid spacing 11 km). The red star shows the location of the former nuclear test site, whereas the red diamond shows the location of the event on 23. February 2002 with origin time 01:21:12.1.*

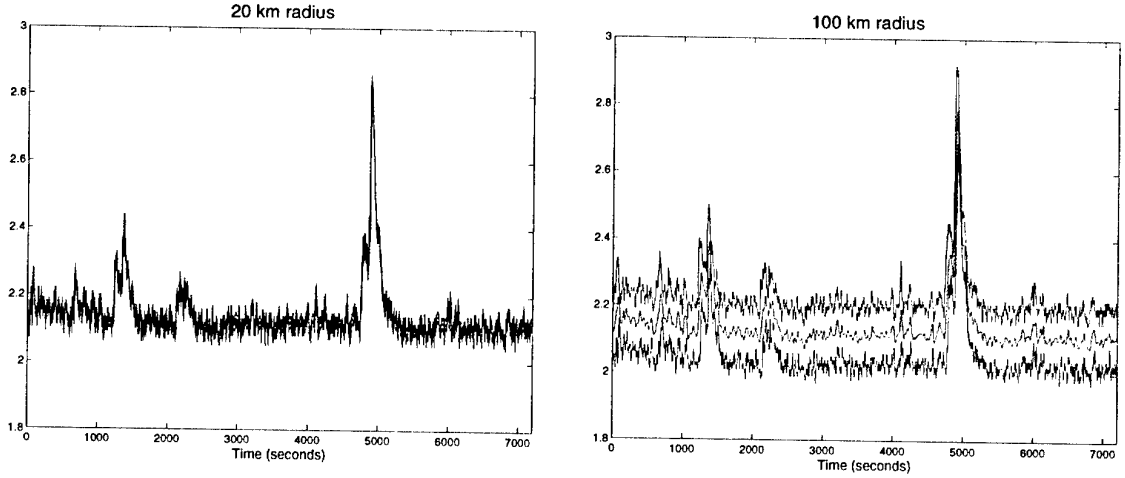

Fig. 6.6.6. *Threshold magnitudes for the time interval 00:00 - 02:00 on 23. February 2002 for 20km (left) and 100 km (right) radius target regions centered around the former nuclear test site. The peak at about 5000 seconds corresponds to signals for the 3.2 event located about 100 km north-east of the test site.The blue line shows the average threshold, whereas the red lines represent the minimum and maximum values.*

It is interesting to notice that even for a region with 100 km radius, the variations in threshold magnitudes are all within 0.2 magnitude units. For this particular configuration of the monitoring network relative to the target area, it will therefore be meaningful to represent the monitoring threshold of the entire region with the values of a single target point, together with uncertainty bounds as shown in Fig. 6.6.6. For areas with larger variations in threshold magnitudes, like in the vicinity of the arrays, a 100 km radius target region will obviously show larger differences between the maximum and minimum values.

We would like to comment on the threshold magnitude of the peak corresponding to the event located north-east of the test site. In cases where an event actually occur in the target region, the magnitude thresholds will often be biased slightly low. In Fig. 6.6.6, we find a maximum value of about 2.9, whereas the event magnitude is estimated to 3.15. In such cases, a maximum-likelihood magnitude estimation algorithm should be activated. However, for small events with a size close to the threshold magnitudes, this bias will not be significant.

Regional Threshold Monitoring including the Amderma station

The KRSC group in Apatity, Russia has provided us with about 3 days of continuous data from the station in Amderma, located on mainland Russia, just south of the island of Novaya Zemlya. The data interval is centered around the origin time of the 23 February 2002 event located on the northeastern coast of Novaya Zemlya. In addition, data from the array in Apatity on the Kola Peninsula were included.

Fig. 6.6.7 shows the threshold magnitudes during an instant without seismic signals, using the developed attenuation relations for Pn, Pg, Sn and Lg. We find large variations over the region, and in particular when approaching each of the arrays. With the Amderma station included, we also find significant variations for the island of Novaya Zemlya, ranging from 1.4 at the southern tip to 2.2 at the northern tip. This implies that a regional threshold monitoring scheme for the NZ region has to be divided into geographical sub-regions having similar threshold magnitudes during background noise conditions.

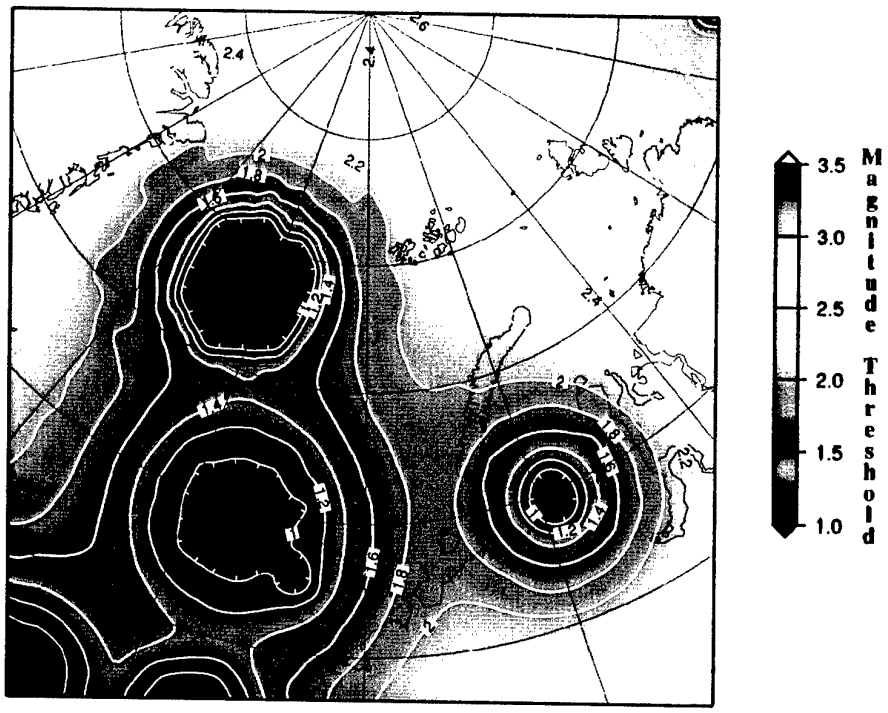

Fig. 6.6.7. Threshold magnitudes for the time instant 2002-054:01.11.20.0, including data from the Amderma station and the Apatity array. Notice the improved monitoring capability in the vicinity of the Amderma station as compared to the thresholds shown in Fig. 6.6.4.

Conclusions and Recommendations

The pattern of Lg arrivals and associated amplitudes supports the previously published indications that the deep sediment basins and Moho topography under the Barents Sea efficiently block Lg wave energy from crossing. From this, it is clear that Pn and Sn are the most useful phases for calculating stable and consistent magnitudes for events in the Barents Sea.

The 'BAREY' model from Schweitzer and Kennett (2002), based on a model for the Barents Sea area from Kremenetskaya et al. (2001), provides the smallest overall travel-time residuals when locating events within the vicinity of the Barents- and Kara Seas.

The attenuation in the Barents Sea region differs somewhat from that observed in other stable tectonic regions, as evidenced by the fact that the coefficients given by Jenkins et al. (1998) for such regions do not give consistent magnitudes across frequencies, phases and stations for our amplitude observations from the events in the Barents Sea region.

Amplitude inversion has been used in this study to resolve new attenuation coefficients and station corrections for estimating magnitudes from STA amplitude observations for Pn, Pg, Sn and Lg phases in the Barents Sea region. The distance range of observations on which the Pg and Lg relations are based is limited; a future study using a greater number of continental

events could most likely provide a relation for STA based Lg magnitudes that is applicable at larger distances, albeit limited to paths within Fennoscandia.

The seismic station in Amderma can be incorporated into the regional network in Fennoscandia and on the Svalbard archipelago using an appropriate crustal model, and is able to provide important information regarding the location of events in the eastern parts of the Barents Sea and the Kara Sea (Schweitzer and Kennett, 2002). Magnitudes calculated at this station are on the whole consistent with the other observations.

For the time interval under study, the seismic arrays ARCES, SPITS, FINES and NORES provide an average monitoring capability of about magnitude 2.2 for the island of Novaya Zemlya. For a region with a 100 km radius around the former nuclear test site the variations in threshold magnitudes are all within 0.2 magnitude units. It will therefore be meaningful to represent the monitoring threshold of the entire region with the values of a single target point, together with uncertainty bounds as shown in Fig. 6.6.6.

In cases when data from the Amderma station can be retrieved, we find significant variations in threshold magnitudes over the island of Novaya Zemlya, ranging from 1.4 at the southern tip to 2.2 at the northern tip. For the actual time interval, the monitoring capability for the former nuclear test site is lowered by about 0.3 magnitude units to about 1.9. This implies that a regional threshold monitoring scheme for the NZ region has to be divided into geographical sub-regions having similar threshold magnitudes during background noise conditions.

T. Kværna
E. Hicks
J. Schweitzer
F. Ringdal

References

Jenkins, R.D., T.J. Sereno, and D.A. Brumbaugh (1998), Regional attenuation at PIDC stations and the transportability of the S/P discriminant. AFRL-VS-HA-TR-98-0046, Science Applications International Corporation, San Diego, CA, USA.

Kremenetskaya, E., Asming, V., and Ringdal, F. (2001). Seismic location calibration of the European Arctic, *Pure Appl. Geophys.* 158, 117-128.

Schweitzer, J., and Kennett, B.L.N. (2002), Comparison of location procedures - the Kara Sea event 16 August 1997, *Semiannual Technical Summary, 1 July - 31 December 2001*, NORSAR Sci. Rep. 2-2001/2002, Kjeller, Norway, 97-114.